PHYTOPLANKTON COMPOSITION OF THE CENTRAL ARCTIC OCEAN IN SUMMER 2011

WITH SPECIAL EMPHASIS ON PICO- AND NANOPLANKTON

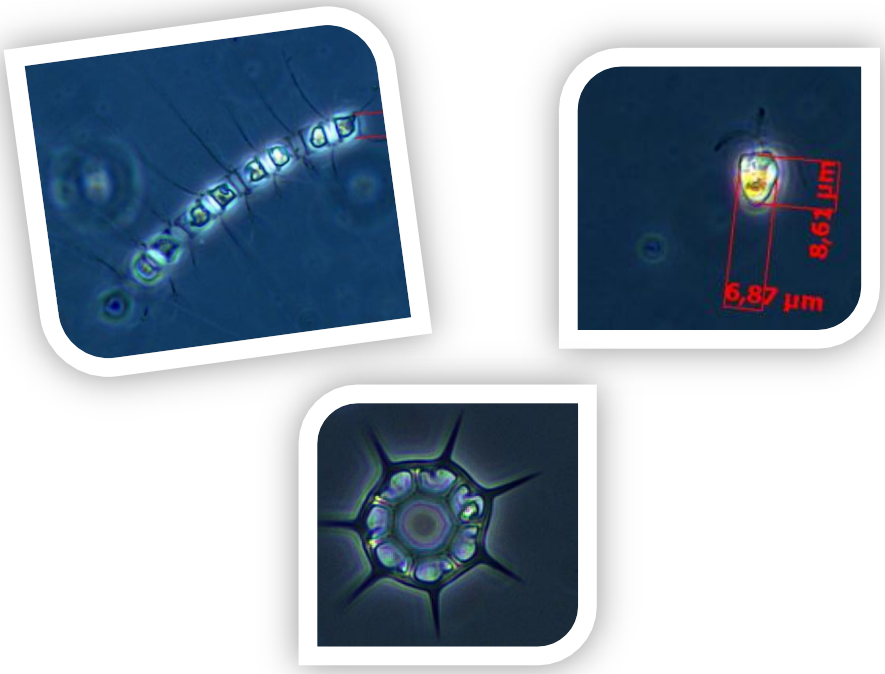

H. TONKES
JULY 2012

WAGENINGEN UNIVERSITY

PHYTOPLANKTON COMPOSITION OF THE CENTRAL ARCTIC OCEAN IN SUMMER 2011

WITH SPECIAL EMPHASIS ON PICO- AND NANOPLANKTON

Student: Henrieke Tonkes (840419838050)

Degree: Master of Aquaculture and Marine Resources Management
Wageningen University and Research

Supervisors: Dr. Peeken (AWI)
Dr. Roijackers (Wageningen University and Research – AEW)

Document: Major thesis

Document nr: 013/2012

Version: Final

Date: 12 July 2012

Photos on the cover: H. Tonkes (*Chaetoceros* sp., *Pyramimonas* sp., and unidentified flagellate)

Summary

This thesis aimed to quantify and describe the phytoplankton community of the central Arctic Ocean in summer 2011 and to correlate this community to the different water masses and other constrains of their environment. This was important since studies concerning this community are scarce. Furthermore, climate induced changes are expected to alter the current marine ecosystem. A *Polarstern* cruise (ARK-XXVI/3) conducted between half August and half September 2011 gave me the opportunity to investigate the phytoplankton community of the central Arctic Ocean, which was covered by sea ice for 80-100%. The transect of the cruise crossed four water masses: waters of mainly Atlantic origin (Adw), waters influenced by both Atlantic and Pacific water (MwI and MwII) and waters of mainly Pacific origin (Pdw). The Adw and MwI were relatively nutrient rich and cold while the Pdw and MwII were relatively warm, stratified and nutrient depleted. The aims of this thesis were addressed by making use of three methods: HPLC, inverted light microscopy and flow cytometry and together they showed the following picture:

The central Arctic Ocean contained a phytoplankton biomass characteristic for an oligotrophic ocean. It was a flagellate and picoplankton based ecosystem in terms of abundance and a flagellate and dinoflagellate based system in terms of biomass. Nanoplankton or microplankton contributed mostly to biomass and picoplankton biomass was less important. Diatoms contributed only slightly to total biomass and this contribution was higher in the Adw and the MwI than in the Pdw and MwII. The phytoplankton community was concentrated in the upper 50 – 60 m of the water column. This community comprised a total phytoplankton biomass between 1 and 18 µg C L^{-1}. The Adw and MwI showed a significantly higher biomass than the Pdw and the MwII. The biomass at station 203 in the Adw was unusually high: > 40 µg C L^{-1} and not included in the before mentioned range. Sea ice, as a proxy for light availability, showed to be of significant importance. The higher the sea ice cover was, the lower was the phytoplankton biomass. The phytoplankton community was also influenced by the nutrient concentrations. The MwII showed not only the highest biomass, the highest nutrient concentrations of nitrate, phosphate and silicate, and the lowest sea ice concentration. Temperature also seemed to influence the phytoplankton community and especially microplankton: the lower the temperature, the higher was the biomass. It was however hypothesized that the temperature was only a proxy for other patterns and not so much the reason for the high biomass of the Adw and MwI. The water temperature seemed to be especially important in determining the amount of stratification of the water column. As such, the water masses where of pivotal importance in determining the phytoplankton biomass. They not only transport the nutrients, but also the warm and fresh waters that stratify the Pdw and together resulted in a low biomass. The ice cover of 100% was of course also responsible for the low phytoplankton biomass at these waters. But despite the low nutrients, and the warm, fresh and stratified waters of the Pdw, this water mass contained a significantly lower picoplankton biomass compared the Adw and the MwI. This contradicted with findings in the literature. A lot of speculation exists about the consequences of a decreasing ice cover and an increase in warm water for the phytoplankton composition. Based on the results of this thesis it might be hypothesized that especially the phytoplankton community at the Adw and MwI will change the most.

Acknowledgements

A special thanks goes to the “Alfred-Wegener-Institut für Polar- und Meeresforschung’ and the division ‘Polare Biologische Ozeanographie’ who kindly provided me this thesis project and the lab space including the appropriate equipment to work on this project.

I would like to thank: Dr. I. Peeken (AWI) (my supervisor) and Dr. E.M. Nöthig (AWI) (who supervised during proposal writing). Thank you very much for introducing me to the different methods, for sharing your expertise with me, for answering my many questions and for introduce me to the world of Arctic phytoplankton. A special thanks goes also to: Dr. R. Roijackers (Wageningen UR) (my supervisor from the Wageningen University) who was always available to answer questions and to give feedback.

A special thanks goes to the following scientists for kindly provided me with data: Kattner et al. (AWI) for providing the nutrient data, Dr. Damm (AWI) for providing me the scheme of the different water masses, Dr. Nicolaus (AW) for providing the map of the different water masses, and Schauer et al. (AWI) for providing the hydrography data. Furthermore, I would like to thank Dr. Ir. Aarts (Imares) who kindly helped me with parts of my statistics, and Dr. Flores (AWI) who also assisted with the statistics and was so kind to provide me with some additional feedback.

Contents

1. Introduction

Quantifying the community and biomass of phytoplankton and other unicellular protists is essential to understand the structure of marine ecosystems and the importance of phytoplankton biomass in the ocean carbon cycles. This quantification is especially important for the central Arctic Ocean since only a few studies regarding the standing stock of microbial plankton for this ocean exist (Poulin et al. 2011). Furthermore, climate induced changes like the thinning ice cover and warmer water temperatures are expected to alter the current marine ecosystem structure (Johannessen & Miles 2011, Wassmann 2011). Therefore, in this thesis I aim to describe and to quantify the unicellular plankton community of the ice covered central Arctic Ocean and to investigate the correlation with water masses and other environmental and chemical constrains of their environment. This thesis will focus on phytoplankton, and autotrophic picoplankton and nanoplankton in particular.

Autotrophic phytoplankton are small and passively drifting photo-autotrophic organisms which are responsible for the bulk of the primary production in marine systems. They support directly or indirectly the entire animal population of the oceans (Sakshaug et al. 2009). Although phytoplankton is to a minor degree able to change depths by movement or change in buoyancy, the distribution of phytoplankton depends on the ocean currents (Hays et al. 2005). Being microscopically small, phytoplankton varies substantially in size. Picoplankton cells vary between 0.2 and 2 µm, whereas microplankton cells are > 20 µm. The cells between 2 and 20 µm are considered to be nanoplankton (Sieburth et al. 1978). Survival of phytoplankton population depends on a delicate equilibrium of success in maintaining floating and unavoidable sinking of which the movement of water has a crucial influence. Light, nutrients, water column stability, grazing, sedimentation, all these ecosystem characteristics influence the phytoplankton species composition of the ocean (Margalef 1978).

The Arctic Ocean (box I), dominated by an extreme climate for several million years, accommodates an unique marine ecosystem (box II). This ecosystem is characterized by organisms that are adapted to low temperatures (between -1.8 and 6°C), low sun elevations (< 40-50°), an alternation between midnight sun and polar night, and a permanent sea ice cover on top of stratified oceanic surface waters (Sakshaug & Slagstad 1991, Darnis et al. 2012). As a result, phytoplankton growth rates are small (Sakshaug & Slagstad 1991). In early June, when ice and snow starts to melt, phytoplankton biomass increases strongly due to an increase of available light. The increasing phytoplankton biomass is being seed by pennate diatoms and flagellates that are released from the sea ice into the water column (Gradinger et al. 1999), resulting in the first spring bloom in late June / early July (Sherr et al. 2003). As reviewed by von Quillfeldt (1997), pennate diatoms are the first to bloom, followed by the centric diatoms. Flagellates like *Micromonas* spp. are also important in this spring bloom. A second bloom, mainly comprising of *Phaeocystis* spp. follows at the end of July (von Quillfeldt 1997, Sherr et al. 2003). Simultaneously with phytoplankton growth, the stock of heterotrophic protists increases as well and remains relatively high in the upper 60 m of the water column during the summer, even when phytoplankton stocks decline (Sherr et al. 2003). At the end of the season, the ocean freezes again, the sun disappears and primary production diminishes.

During the winter, biomass of heterotrophic protists is higher than biomass of bacteria and autotrophs, and the protist biomass include almost all taxa that are present in spring and summer, serving as food for zooplankton (Sherr et al. 2003, Darnis et al. 2012). This description of the Arctic Ocean protist composition is applicable to the ice edge regions and the Arctic shelf regions and less to the permanently ice covered central Arctic Ocean.

Box I: The Arctic Ocean. The Arctic Ocean and adjacent seas are enclosed by land. The Fram Strait and the Barents Sea connect the ocean to the Atlantic Ocean and the Bering Strait constitutes the connection to the Pacific Ocean. The Arctic Ocean comprises an area of about 9.4 x 10^6 km, of which circa 53% is continental shelf, making it unique in comparison to other basins (Bates & Mathis 2009). The deep Arctic Ocean is subdivided by three nearly parallel ridges. The Lomonosov Ridge separates the ocean into two basins: the Eurasian Basin and the Canadian Basin. The Nansen-Gakkel Ridge splits the Eurasian Basin into the Amundsen Basin and the Nansen Basin. The Canadian Basin is divided into the Makarov Basin and the Canada Basin by the Alpha-Mendeleyev Ridge (Figure 1). The waters of the Arctic Ocean originate thus from the Atlantic Ocean and the Pacific Ocean. Those waters are being mixed with sea ice melt water in spring and summer, brine in winter, precipitations, and river runoff (Rudels 1989). The inflow of fresh water and the corresponding fresh water balance is of pivotal importance for the formation of sea ice and bottom water and is responsible for the strong stratification of the surface waters throughout the central Arctic Ocean (Aagaard & Carmack 1989). The waters of Atlantic and Pacific origin show different characteristics. Waters of Pacific origin are fresher and colder than waters of Atlantic origin and are relatively rich in nutrients (Jones et al. 1991, Jones 2001, Pabi et al. 2008) although nitrate is depleted relative to phosphate (Jones et al. 1998, Yamamoto-Kawai et al. 2006). Currently, the influence of waters of Pacific origin is restricted to the part of the central Arctic Ocean west of the 180° longitude (Damm et al. 2010).

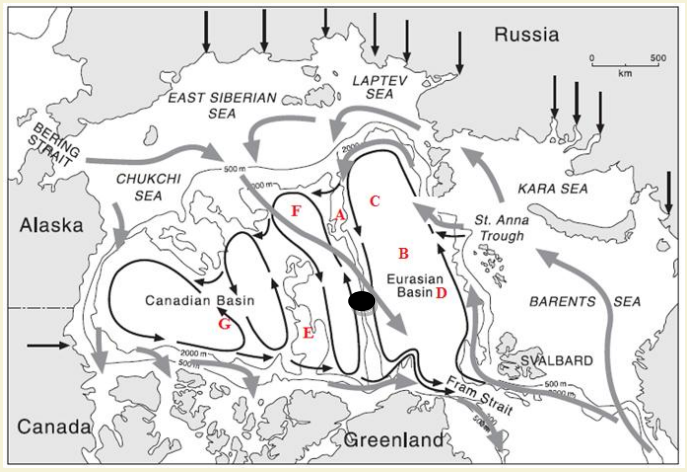

Figure 1: Arctic Ocean and adjacent seas (white areas) enclosed by land (grey areas). Letters depict the location of the Lomonosov Ridge (A), the Nansen-Gakkel Ridge (B), the Amundsen Basin (C), the Nansen Basin (D), the Alpha-Mendeleyev Ridge (E), the Makarov Basin (F) and the Canada Basin (G). The black dot represent the North Pole. Grey arrows represent the surface circulation and the black arrows represent the Atlantic Layer and the Upper Polar Deep water to depths of 1700 m. Straight black arrows represent the mouths of major rivers. Modified from: (Jones, 2001).

In spring and summer, when snow and ice in the central Arctic Ocean melt to a certain extent, phytoplankton biomass increases due to an increase of available light. However, phytoplankton blooms do not occur since light remains limited. Also, nutrient concentrations in the surface waters become depleted during the course of the phytoplankton growing season because the strong stratification prevents vertical mixing of essential nutrients from the deeper water to the euphotic zone. As such, nutrients do not become replenished (Sakshaug 2004, Tremblay & Gagnon 2009). Due to the strong stratification, the central Arctic Ocean is thought of as being an oligotrophic ocean of low phytoplankton abundance, low biomass, and regenerative production instead of new production (Wheeler et al. 1996). Traditionally, the central Arctic Ocean was regarded as being dominated by microplankton > 20 µm (e.g. a review of von Quillfeldt (1997)).

However, more recent papers show that cells < 3 µm can dominate, that the waters contain an active microbial food web, that cells < 5 µm are responsible for most of the carbon fixation, and that phytoplankton species have a circumpolar distribution (Booth & Horner 1997, Gosselin et al. 1997, Lee & Whitledge 2005). On the other hand, phytoplankton has been related to different water masses for 150 years (Lovejoy et al. 2002). Since the waters of the central Arctic Ocean are being influenced by water from several sources (see Box 1), it might be expected that the general picture of the phytoplankton composition of the central Arctic Ocean as written down in this paragraph is more complex.

For decades, the Arctic Ocean was characterised by the presence of a multiyear sea ice cover that hindered navigation by icebreakers and therefore studies of the unicellular plankton of the central Arctic Ocean are scarce. Much of the current knowledge is produced before 1905 and stems from coastal areas, voyages of exploration and drifting ice camps (Booth & Horner 1997). Nowadays, the decreasing multiyear sea ice cover due to climate induced changes results in a new accessibility of the central Arctic Ocean for research expeditions by icebreakers, and new opportunities to study this region are arising. However, most research is still conducted in the Arctic shelf regions (e.g. (Horner & Schrader 1982, Sakshaug 1997, von Quillfeldt 1997, Lovejoy et al. 2002, Lovejoy et al. 2006, Ardyna et al. 2011, Poulin et al. 2011)) or in the marginal sea ice zone and at the ice edge (e.g. (Perrette et al. 2010).

The most detailed investigation of unicellular plankton of the central Arctic Ocean was carried out during the Arctic Ocean Section 1994 (Booth & Horner 1997, Gosselin et al. 1997, Rich et al. 1997, Wheeler et al. 1997). More recent papers focus on particular regions of the central Arctic Ocean, for example the Western Arctic Ocean (e.g. (Min Joo et al. 2011)), Canadian Arctic (e.g (Ardyna et al. 2011)), or the Eurasian Basin and the Makarov Basin (e.g. (Olli et al. 2007). The research conducted by Damm et al. (2011) is an exception. They crossed the entire central Arctic Ocean in summer 2007. This and other recent investigations show indeed correlations of unicellular plankton with water masses of the central Arctic Ocean (Damm et al. 2010) and the Canadian High Arctic (Ardyna et al. 2011).

Box 2: The Arctic marine ecosystem. Phytoplankton and sea ice algae are the basis for the Arctic marine pelagic food web. Large diatoms and dinoflagellates are food for zooplankton like *Calanus glacialis* and *Calanus hyperboreus* (Auel & Hagen 2002, Darnis et al. 2008). Other important grazers are the ice related amphipods that feed mainly on sea ice algae while some species predate on zooplankton. Arctic Cod is however the main consumer of Arctic zooplankton and is responsible for 75% of the energy transfer to higher trophic levels (Welch 1992). Arctic Cod is known to live under pack ice at least for parts of their life cycle (Gradinger & Bluhm 2004) and is an important food source for seals and polar bears (Sakshaug & Slagstad 1991)(Figure 2).

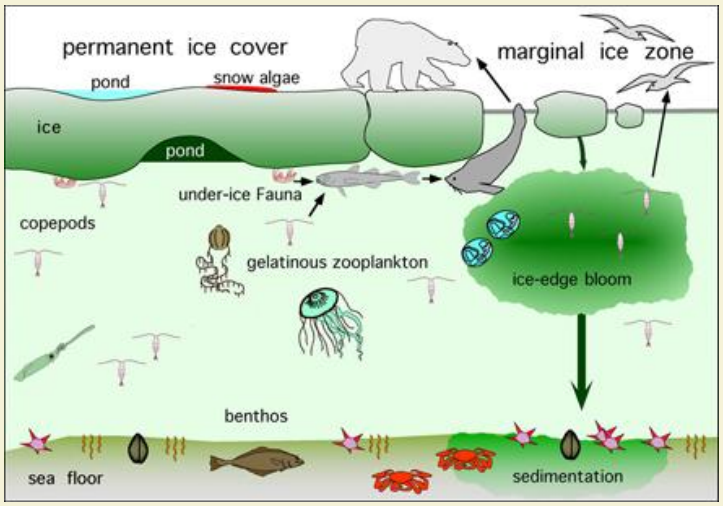

Figure 2: Schematic overview of the Arctic marine ecosystem (Bluhm et al. 2011).

To continue the research conducted since the mid-nineties and to verify the general picture of the central Arctic Ocean marine ecosystem, a *Polarstern* cruise (ARK-XXVI/3) crossed the central Arctic Ocean via the North Pole during summer 2011. This resulted not only in the unique opportunity to describe the unicellular plankton community but also to relate the abundance, biomass, taxonomic diversity and size distribution of unicellular plankton to different water masses and other environmental variables in great detail. This thesis will focus on phytoplankton, and picoplankton and nanoplankton.

Therefore, I try to address the following research questions:

I. How can the phytoplankton community of the central Arctic Ocean be described and quantified in terms of abundance, biomass, taxonomic diversity and size distribution?
II. What is the influence of the different water masses on the phytoplankton abundance, biomass and taxonomic diversity of the whole size spectrum?
III. Which environmental and chemical variables constrain phytoplankton abundance, biomass and taxonomic diversity of the whole size spectrum?

Traditionally, the phytoplankton community abundance was measured by means of inverted light microscopy (Llewellyn et al. 2005), which will also be used to address the research questions. Complementary, High Pressure Liquid Chromatography (HPLC) and flow cytometry will be used. It is important to address the research questions, since it might lead to a better understanding of the role of the phytoplankton community in the pelagic ecosystem of the central Arctic Ocean and the importance of the different water masses and other environmental and chemical constrains, especially in the light of climate change.

2. Materials and methods

2.1 Sampling procedure

Sampling took place in the central Arctic Ocean in a *Polarstern* cruise 'TransArc' (ARK-XXVI/3) in August and September 2011. Sampling was carried out on eleven stations in the ice covered central Arctic Ocean (Figure 3).

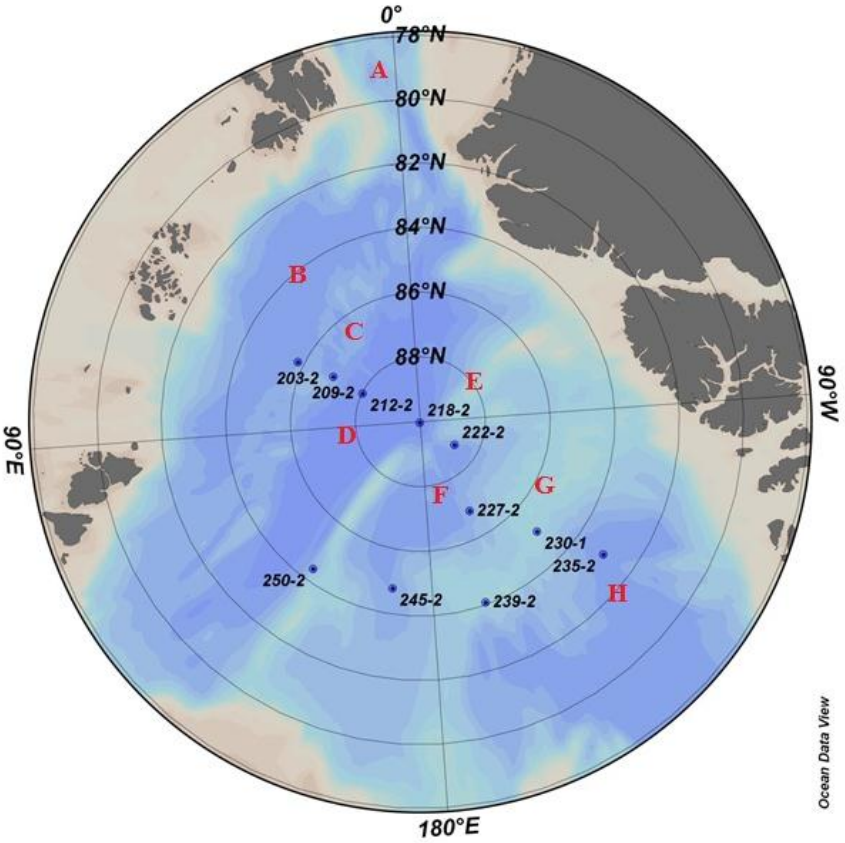

Figure 3: Biological stations performed during the TransArc cruise with *Polarstern* (ARK-XXVI/3) during August and September 2011. Sampling took place in different areas of the central Arctic Ocean. Fram Strait (A) (not sampled), Nansen Basin (B), Nansen-Gakkel Ridge (C), Amundsen Basin (D), Lomonosov Ridge (E), Makarov Basin (F), Alpha-Mendeleyev Ridge (G) and the Canada Basin (H) (Schlitzer, 2011).

Samples were taken of the water column in open waters next to the sea ice between 2 m and 200 m deep (2m, 10m, 25m, 50m, 75m, 100m, 150m and 200m) by use of a CTD rosette (Table 1). The CTD records continuously conductivity, temperature and density and is attached to a frame that contains large Niskin bottles to collect the water. The bottles can be closed electronically to sample water at a specific depth of the water column, while keeping this water separated from water collected at other depths. To determine the pigments (HPLC), 1 to 3 l of sea water from the Niskin bottles were filtered onto 25 mm Whatman GF/F filters with a pressure of less than 12 mbar. After filtration, the filters were folded and stored in 2 ml micro Apex vials at -80°C for HPLC analysis. To determine the species composition by use of a light microscope, subsamples were taken from Niskin bottles and stored in 250 ml brown bottles. The samples were preserved in a buffered formalin (1%) seawater solution until further analysis. The water samples taken for analysis be means of Flow Cytometry were also taken from Niskin bottles and counted fresh on board of the ship by using a Accuri® C6 Flow Cytometer (details see below).

On the CTD, additional sensors were mounted which recorded oxygen concentrations and the fluorescence of the phytoplankton. Hydrography data was measured by Schauer et al. (AWI). Nutrients were taken from each depth and measured directly on board by the group of Kattner et al. (AWI) according to Kattner & Becker (1991).

Table 1: Sampling locations and dates for the different methods: HPLC, light microscopy and flow cytometry. * For analysis by means of light microscopy, samples were taken from the surface (2 m) and the fluorescence maximum.

Station	203	209	212	218	222	227	230	235	239	245	250
Sampling date	14.08	17.08	19.08	22.08	26.08	29.08	31.08	02.09	05.09	08.09	11.09
HPLC	x	x	x	x	x	x	x	x	x	x	x
Light microscopy	-	x*	x*	x*	x*	x*	x*	x*	x*	x*	x*
Flow cytometry	x	x	x	x	x	x	x	x	x	x	x
Sampling depth	2 and 25m	All	All	All	All	All	All	All	All	All	All

2.2 HPLC

Pigment samples were measured by means of a Waters HPLC-system, equipped with an auto sampler (717 plus), pump (600), PDA (2996), a fluorescence detector (2475) and EMPOWER software. In order to prepare the HPLC analysis, glass pearls, 50 µm internal standard (cantaxanthin), and 1.5 ml acetone were added to the 2 ml vials containing the frozen filters. The absorption of the internal standard was measured by means of a spectrophotometer at 474 nm. The filters were homogenized for 20 sec in a Precellys® tissue homogenizer and afterwards the vials were centrifuged for 15 minutes. The supernatant was poured in another cup containing a 0.2µm filter (VWR). These vials were centrifuged for 2 minutes to allow the sample to run through the filter. Afterwards, the filters were removed and the samples were kept at -80°C prior to analyses. A subsample was transferred to the auto sampler (4°C) and mixed with 1M ammonium acetate solution (ration: 1:1) prior to injection. The analysis of the pigments was conducted by reverse-phase HPLC, by the utilization of a VARIAN Microsorb-MV3 C8 column (4.6x100 mm) and HPLC-grade solvent (Merck). The gradient was modified after Barlow et al. (1997). Each pigment of a chromatogram has been compared with the library of standards to identify the correct pigments. In the end, the peak area of the pigments, multiplied by the calibration factor, the internal standard and the amount of filtered sea water was used to calculate the concentration of the different pigments in ng L^{-1}. The taxonomic structure of the phytoplankton communities was calculated by I. Peeken (AWI) from marker pigment ratios using the CHEMTAX® program (Mackey et al. 1996). Microscopic results of the species distribution were used to constrain the pigment ratio as suggested by Higgings et al. (2011). The resulting phytoplankton group composition was expressed in chlorophyll *a* concentrations and comprised prasinophyceae / chlorophyceae, euglenoceae, dinophyteae, cryptophyteae, pelagophyteae, haptophyteae, and diatoms.

To determine the biomass (in µg chl-*a* L^{-1}) of picoplankton, nanoplankton and microplankton, the algal divisions 'Prasinophyceae' and Chlorophyceae' were considered to be picoplankton and the algal divisions 'Diatoms' and 'Dinophyteae' were considered to be microplankton. All other algal divisions were considered to be nanoplankton (Dr. Peeken, personal communication). Unfortunately most water samples taken below 50 m were close to the detection limit of the Diodearray detector.

Therefore, accurate estimates of the phytoplankton groups could only be done between samples from 2 to 50 m, except for some stations in the Pacific waters, where a deep fluorescence maximum was observed. In order to compare the biomass obtained by means of HPLC and the biomass obtained by means of light microscopy, biomass of the phytoplankton groups of the flagellates and the diatoms (in µg chl-*a* L^{-1}) was multiplied by 40 to obtain biomass data in µg C L^{-1}. Biomass of dinoflagellates (in µg chl-*a* L^{-1}) was multiplied by 60 in order to obtain biomass data in µg C L^{-1} (Dr. Peeken, personal communication).

2.3 Inverted light microscopy

From each station, the samples from the surface (2 m) and the depth of the fluorescence maximum (depth differed between stations) were analysed by inverted light microscopy by means of the Utermöhl technique. Due to previous studies from this region it was expected that the samples contained only a few amount of cells, and therefore the samples were poured into a 50 ml cylinder and stored for 48 hours to allow the cells to settle in a 3 ml chamber. The concentrated samples were investigated by different magnifications (160x, 250x and 400x) of an inverted light microscope to count at least 400 cells as recommended by Edler et al. (1979).

Annex I contains the counting protocol used to count the cells, and the procedure can be summarised as follows: The individuals counted were divided into categories based on shape and size. The shapes included: spheres, prolate spheroid, rectangular boxes and droplets. Magnification 40 (400x) was used to count picoplankton cells < 2 µm on one stripe and small nanoplankton (mainly flagellates and small pennate diatoms) on two stripes. Magnification 25 (250x) was used to count medium nanoplankton on two stripes (flagellates, small dinoflagellates and small diatoms) and magnification 16 (160x) was used to count the big nanoplankton and microplankton (dinoflagellates, diatoms and ciliates) present in half the chamber. Of every individual, the following information was noted down: size category, shape, class (dinoflagellates, flagellates, diatoms, ciliates, upos), when possible the genus and when possible an indication of the type of organism (autotrophic or heterotrophic). Annex III contains a table with the real counts per sample. However, the counting protocol used did not allow to count all required 400 cells in the samples due to the low cell numbers in some of the samples. Table 2 gives an overview of the cell numbers that were counted per sample.

Table 2: The amount of cells counted per sample excluding the picoplankton counts. Surface samples indicate the samples taken at a depth of 2 m and the deep samples indicate the samples taken at the depth of the fluorescence maximum. At the stations indicated with red numbers it was impossible to count the required 400 cells.

Station	**209**	**212**	**218**	**222**	**227**	**230**	**235**	**239**	**245**	**250**
Sample (surface)	45	53	76	96	118	130	151	163	179	195
Depth	2m	2m	2m	2m	2m	2m	2m	2m	2m	2m
Remaining cells	552	639	683	669	588	223	212	337	268	262
Sample (deep)	47	55	78	98	120	132	154	165	181	197
Depth	14m	25m	20m	25m	25m	35m	52m	28m	18m	24m
Remaining cells	452	205	470	605	541	300	290	234	221	201

Based on the size categories and the shape, the cell volume and plasma volume were calculated in order to calculate the biomass in the form of protozoan carbon based on Edler (1979) and Hillebrandt et al (1999). The following formula's has been used to calculate the cell volume (v):

Sphere: $v = \frac{\pi}{6} * d^3$ [1]

The sphere has been used for all picoplankton and sphere shaped flagellates, dinoflagellates and ciliates (d: diameter).

Prolate spheroid: $v = \frac{\pi}{6} * d^2 * h$ [2]

The prolate spheroid has been used for all prolate spheroid shaped flagellates and dinoflagellates (d: diameter and h: height).

Cone: $v = \frac{\pi}{12} * d^2 * z$ [3]

The cone has been used for all droplet shaped organisms like ciliates and heterotrophic dinoflagellates (d: length and z: height).

Rectangular box: $v = a * b * c$ [4]

The rectangular box has been used for all small unidentified small pennate diatoms in the size category 2-5 x 2-5 (a: length and b: width and c: b).

Elliptic based prism: $v = \frac{\pi}{4} * a * b * c$ [5]

The elliptic based prism has been used to calculate the cell volume of pennate diatoms (a: width and b: length and c: $\frac{b}{2}$).

Cylinder: $v = \frac{\pi}{4} * d^2 * h$ [6]

The cylinder has been used to calculate the cell volume for centric diatoms (d: diameter and h: height).

In order to determine the plasma volume, the vacule volume needs to be calculated for the diatoms, except for the small unidentified pennate diatoms in the size category 2-5 x 2-5. They are too small to subtract a vacule volume from the cell volume. Two formulas have been used to calculate vacule volume:

Pennate diatoms: $\frac{\pi * (a-2) * (b-2) * (c-2)}{4}$ [7]

Centric diatoms: $\frac{\pi * (d-2)^2 * (h-2)}{4}$ [8]

The vacule volume * 0.9 was subtracted from the cell volume to determine the plasma volume. For the flagellates, the dinoflagellates and the ciliates cell volume = plasma volume.

To calculate the protozoan carbon per cell (in ng C), the plasma volume was multiplied by 0.11 for all organisms except for armoured dinoflagellates for which the plasma volume was multiplied by 0.13 (Edler, 1979; Hillebrand et al. 1999).

The real counts of the individuals were multiplied with the 'streibenfactor' to calculate the amount of this cells in the chamber and were eventually multiplied by 20 to calculate the abundance (amount of cells) per L. The 'streibenfactor' for picoplankton was 85, the 'streibenfactor' for all other individuals counted at magnification 40 was 42,5, 27 was the 'streibenfactor' for all individuals counted at magnification 25, and the cells counted at magnification 16 where multiplied by 2. Cells were identified to the lowest possible taxonomic level by a book from Throndsen et al. (2007).

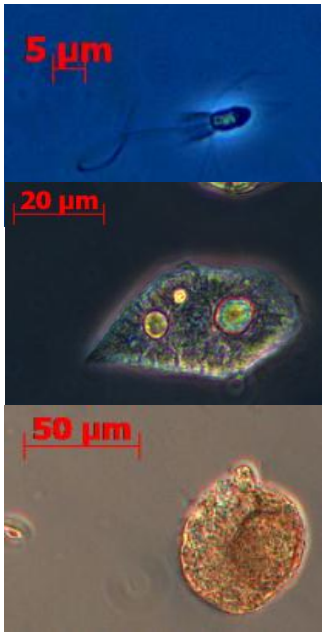

Figure 4: Choanoflagellate (A), heterotrophic dinoflagellate (B), and autotrophic dinoflagellate (C) (Photos: H. Tonkes)

Microplankton cells were cells with a diameter > 20 µm, nanoplankton were cells with a diameter between 2.5 and 20 µm and picoplankton cells were cells with a diameter < 2.5 µm.

It was difficult to distinguish between autotrophic and heterotrophic species of flagellates and dinoflagellates and due to the existence of mixotrophs, a flagellate or dinoflagellate that can be classified into both categories. Therefore it was decided to consider 50% of the unidentified flagellates and 50% of the unidentified dinoflagellates as being autotrophic unless individuals were clearly autotrophic or heterotrophic (Figure 4). The flagellates and dinoflagellates that were identified to genus level are classified in one of the two categories based on the genus. The Choanoflagellates and *Dinobryon* spp. were considered to be heterotrophic and the flagellates *Euglena* spp., *Dictyocha* spp. and *Meringosphaera tenerrima* were considered to be autotrophic. The dinoflagellates *Amphidinium* spp., *Gyrodinium* spp., *Protoperidinium* spp. and *Micracanthodinium claytonii* were considered to be heterotrophic.

The organisms that could not become identified were categorised in the category 'upos' (Figure 5). These organisms were counted in order to calculate abundance and biomass, but this category will be however always separately depicted.

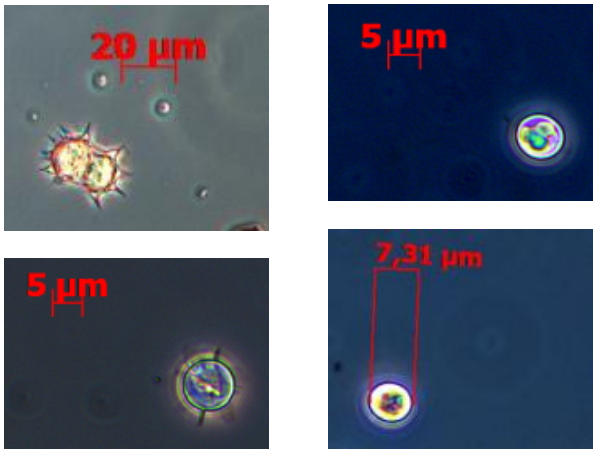

Figure 5: Examples of individuals counted as upos. (Photos: H. Tonkes).

2.4 Flow Cytometry

The data used in this thesis were measured directly on board of the Polarstern from fresh water samples of the water column using an Accuri C6 flow cytometer. The instrument was used to measure abundance, size (FSC signal was calibrated with the Invitrogen size calibration kit F-13838), as well as red (670LP) and orange (585/40) autofluorescence after excitation with a blue (488 nm) and a red (620 nm) laser. Each sample was measured for 3 min at fast flow rate (66 µl min^{-1}). Phytoplankton cells were separated from detritus using scatter plots of FL3 vs. FL2 (Figure 6 A), followed by group identification based on their specific signature in FL3 vs. FL2 (Figure 6 B) according to Marie et al. (2005). Polychromatic latex beads (1 µm, Polysciences) were added to every sample to monitor the performance of the optical system and to control the internal volume calibration of the instrument. As mentioned before, processing the flow cytometer samples took place on the ship and therefore only the analysis of this data will be part of this project. Analysing the data started with the graphs depicted in Figure 6 A and B. Figure 6 A shows the separation of the detritus and the phytoplankton and also the beads are visible. Especially Figure 6 B has been used to determine the abundance and biomass of picoplankton and the two nanoplankton groups. The green box includes all picoplankton of a particular sample. The orange box contained all nanoplankton of the first category (the small nanoplankton) and the red box contained the larger nanoplankton of the second category. For this thesis, the flow cytometer has been used to separate picoplankton (algae with a size < 3,5 µm and nanoplankton (algae with a size between 3.5 and 20 µm, summary of group small and large nanoplankton, Figure 6 B). Since the counts of cells were very low below 50 m (except for some stations in the Pacific waters, which showed a deep fluorescence maximum), only the samples of 2 to about 50 m were taken into consideration for this thesis. The size of the individual groups were used to calculate the carbon per cell and thus multiplied with the cell per ml to estimate the phytoplankton carbon of the cells.

A B

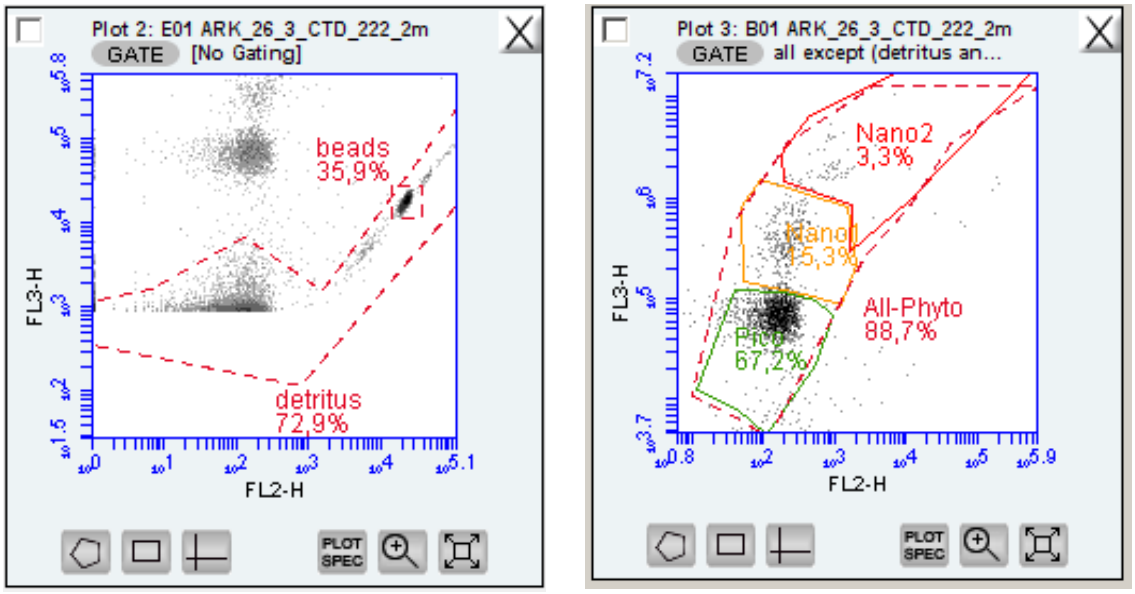

Figure 6: Plot of the red fluorescence (Fl3-H) against the orange fluorescence (Fl3-H) to indicate the detritus and the beads (A) and the picoplankton (green box), small nanoplankton (red box) and the large nanoplankton (yellow box). Both the detritus and beats are not shown in this graph (B).

2.5 Water masses

Based on profiles of nutrients, salinity, temperature and the depth of the surface mixed layer of the Arctic Ocean in summer 2011, different water masses have been distinguished by Damm et al. (unpublished data) (Figure 7).

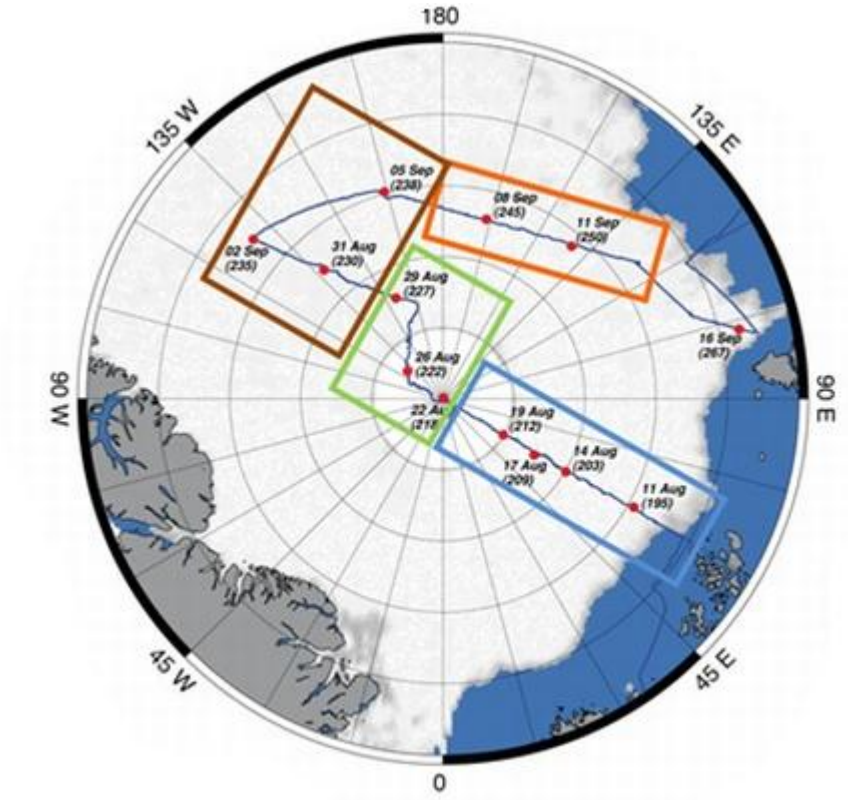

Figure 7: Grouping of stations based different source waters indicated by different coloured boxes. Blue: Adw, Green: MwI, Brown: Pdw, Orange: MwII. White area indicates the average sea ice concentration of 15 September 2011 (groupings based on unpublished work of Dr. Damm et al. (AWI) and Kattner et al. (AWI). Map made by Dr. Nicolaus (AWI)).

Those water masses were: Atlantic water (Adw), Mixed waters I (MwI), Pacific water (Pdw) and Mixed water II (MwII). Stations 203, 209, 212 and 218 were mainly characterised by waters of Atlantic origin (Adw). Waters at stations 222 and 227 contained a mixture of both Atlantic and Pacific waters (MwI). Stations 230, 235 and 239 were mainly characterised by waters of Pacific origin (Pdw) and stations 245 and 250 were again influenced by both Atlantic and Pacific waters (MwII) (Damm et al., unpublished data). These water masses will be applied in this thesis.

2.6 Statistics

After processing the samples, Kruskal-Wallis tests were conducted to investigate significant differences between abundance and biomass of phytoplankton and the different size categories ($\alpha < 0.050$). The Mann-Whitney-U-test was conducted as a post-hoc when a significant difference was found, to determine which of the four groups was significantly different ($\alpha < 0.050$). These non-parameter tests are used because the data was not normally distributed.

MDS plots were constructed to investigate similarities between stations and depths for the data of the HPLC and the light microscope. In case of the HPLC data (x'=ln(x+1) transformed), the pigment information was used to construct the plot. The four water masses were indicated with different colours to give insight in the similarity between water masses. The Bray-Curtis dissimilarity was used to quantify dissimilarities in ecological data between stations, depths and water masses. The MDS plot constructed for the data of the presence / absence data of the light microscopy was constructed with the Jaccard dissimilarity, which is used to quantify dissimilarities in presence / absence ecological data. Again, the four water masses were indicated with four different colours.

To investigate the correlation of phytoplankton biomass and abundance with the environmental and chemical parameters, Generalized Linear Models (GLMs) are conducted based on the Poisson distribution. A GLM is an example of a regression model to investigate the relationship of a response variable (in this case phytoplankton abundance or biomass) with one or more predictor variables (in this case for example average sea ice cover or salinity). GLMs assuming a Poisson distribution are suitable for applying on ecological datasets as it enables working with counted data (Dr. Aarts, personal communication). GLMs are conducted for the data sets of the HPLC, light microscopy and flow cytometry. Generally, linear relationships had been investigated, except for the relationship of phytoplankton biomass obtained by light microscopy and the average sea ice cover. This data set showed a maximum biomass value at an ice cover of 90% and therefore ice cover had been square root transformed and as such implemented as a covariate. The GLM was conducted based on a Poisson distribution with a ln-linear function. To relate the real numbers of the HPLC data and the flow cytometry data to densities, an offset was defined as the ln (x'=ln x) of the amount of the sample processed. The scale parameter was fixed on deviance to account for samples that showed a larger variance than the mean. The significant threshold was set on $\alpha < 0.050$. Significant linear relations were indicated with a regression line (y=e^beta0+beta1*X).

3 Results

3.1 Environmental and chemical variables

Sea ice cover of summer 2011 varied between 80 and 100% of the winter sea ice cover (Figure 8 A). Hydrography parameters of these ice covered waters were recorded to approximately 200 m depth. However, since phytoplankton abundance and biomass occurred to be minimal in waters deeper than 50 m (paragraph 3.2), hydrography parameters are presented for the first 50 m of the water column only. In principle, these surface waters were characterized by potential temperatures (sea water temperatures that are not influenced by differences in pressure) around -1.5 or -2 °C (Figure 8 B). The Adw were relatively cold and the Pdw relatively warm. Salinity (psu) varied substantially between stations (Figure 8 B): the Adw were relatively saline and the Pdw and the MwII relatively fresh.

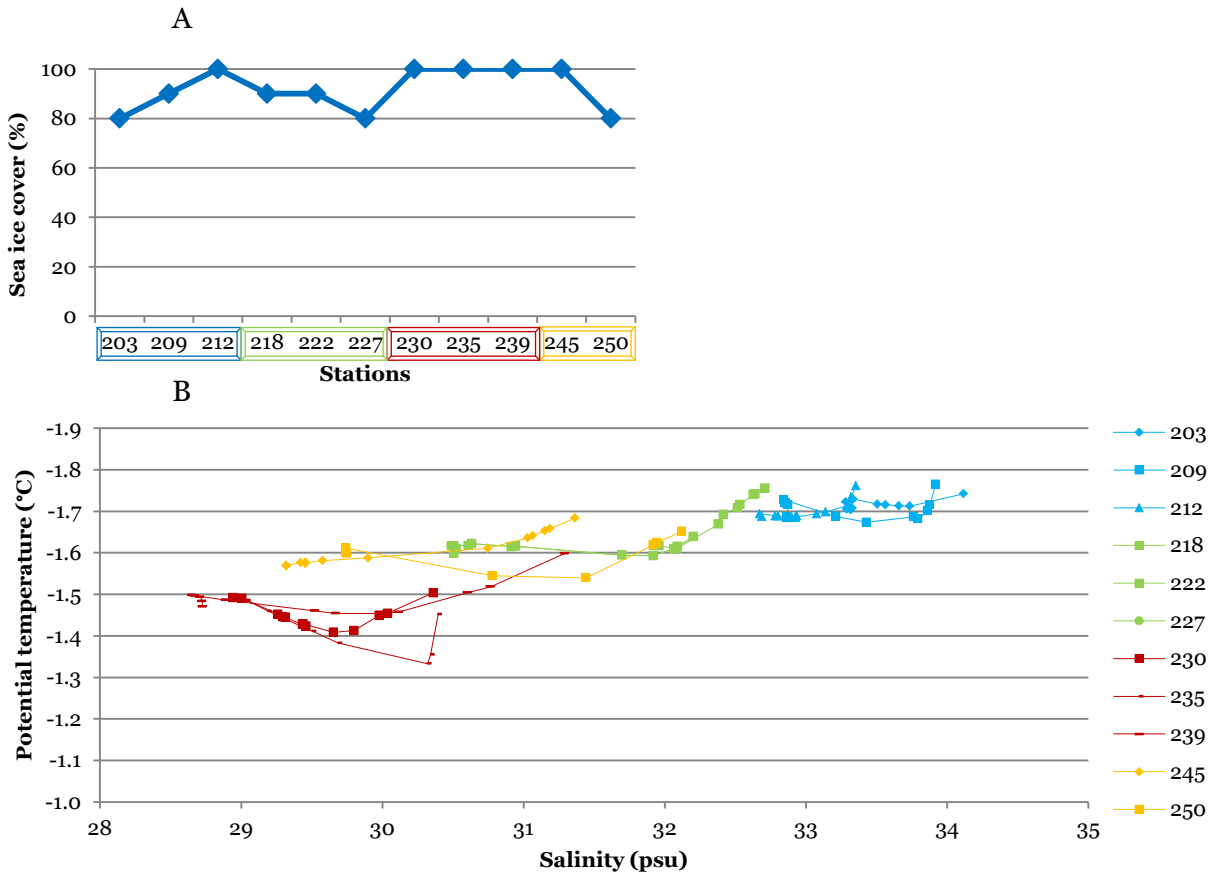

Figure 8: Average sea ice cover (in %) (A) and potential temperature (in °C) plotted against salinity (in psu) (B) The coloured boxes around the station numbers and data indicate the water masses: Blue box: Adw, Green Box: MwI, Brown Box: Pdw, Orange box: MwII.

Similar to the hydrography parameters, the nutrient concentrations are presented for the upper 50 m of the water column solely (Figure 9). In general, nutrient concentrations increased with depth, except for nitrogen (NO_2) which varied substantially between stations and depths. Nitrate (NO_3) is more or less depleted in the upper 40 m of the water column, except in the MwI and the Adw. Silicate (Si) is also depleted in the upper 40 m of the water column, except at the MwI. Phosphorus (PO_4) concentrations seemed not to be depleted in the MwI and the Pdw and ammonium (NH_4) concentrations were generally low in the entire upper 50 m of the water column.

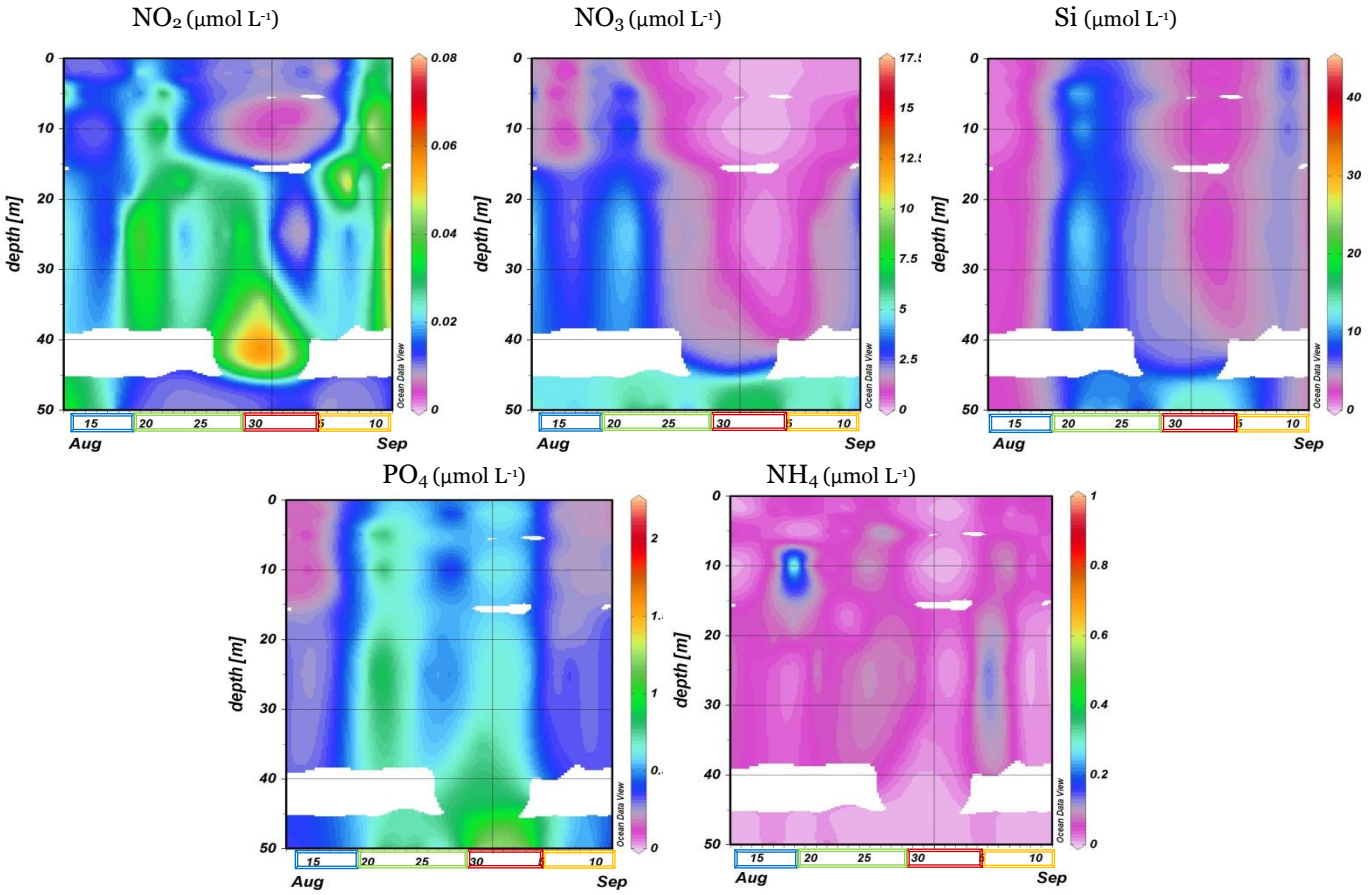

Figure 9: Depth profiles of different nutrients concentrations of NO_2, NO_3, Si, PO_4 and NH_4 (in µmol L^{-1}) against time. White areas indicate no data. Boxes around the data represent the water masses: Blue boxes: Adw, Green boxes: MwI, Brown boxes: Pdw, Orange boxes: MwII.

The Adw and the MwII showed relatively high nitrate concentrations and low phosphate concentrations. The MwI showed relatively high concentrations of both nutrients and the Pdw showed generally high concentrations of phosphate and low nitrate concentrations (Figure 10).

Conducting Kruskal-Wallis tests indicated that the salinity ($p < 0.001$) and the nutrient concentrations for nitrate, silicate and phosphorus (NO_4: p 0.050, Si: $p < 0.010$, and PO4: $p < 0.001$) differed between water masses. These results indicated that the station groupings based on these water masses is reliable and therefore these station groupings will be used in the rest of this thesis.

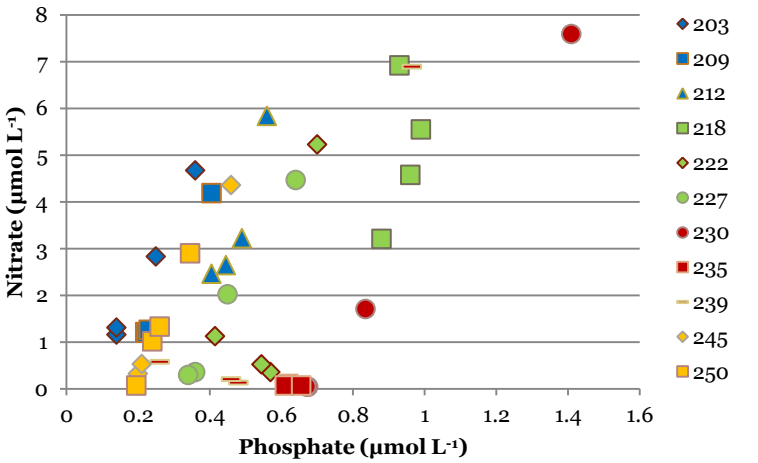

Figure 10: Phosphate-nitrate relationship for all stations up to a depth of 50 m. Colours indicate the water masses. Blue: Adw, Green: MwI, Brown: Pdw, Orange: MwII.

3.2 HPLC

3.2.1 Identified pigments and taxa

The most important pigments found in the samples were chlorophyll-*a*, fucoxanthin and chlorophyll-*b*. The distribution of these pigments in the water column showed that phytoplankton biomass was concentrated in the upper 50 to 60 m (Figure 11). Station 203 in Adw showed unusually high pigment concentrations compared to the other stations, especially for chlorophyll-*a* and fucoxanthin. Of the remaining stations, the stations of the MwI showed the highest pigment concentrations in the surface waters. The depth of the chlorophyll-*a* maximum varied among stations and could be found at the surface, around 10 m deep as was the case for station 218 and 227 in the MwI, or in deeper waters at 35 or 52 m as was the case for station 230 and 235 in Pdw. Those stations showed also a deep chlorophyll-*b* maximum. As explained in Chapter 2, the following taxonomic divisions could be identified based on differences in the concentrations of all identified algal pigments: Prasinophyceae / Chlorophyceae, Euglenoceae, Dinophyteae, Cryptophyteae, Pelagophyteae, Haptophyteae, and Diatoms.

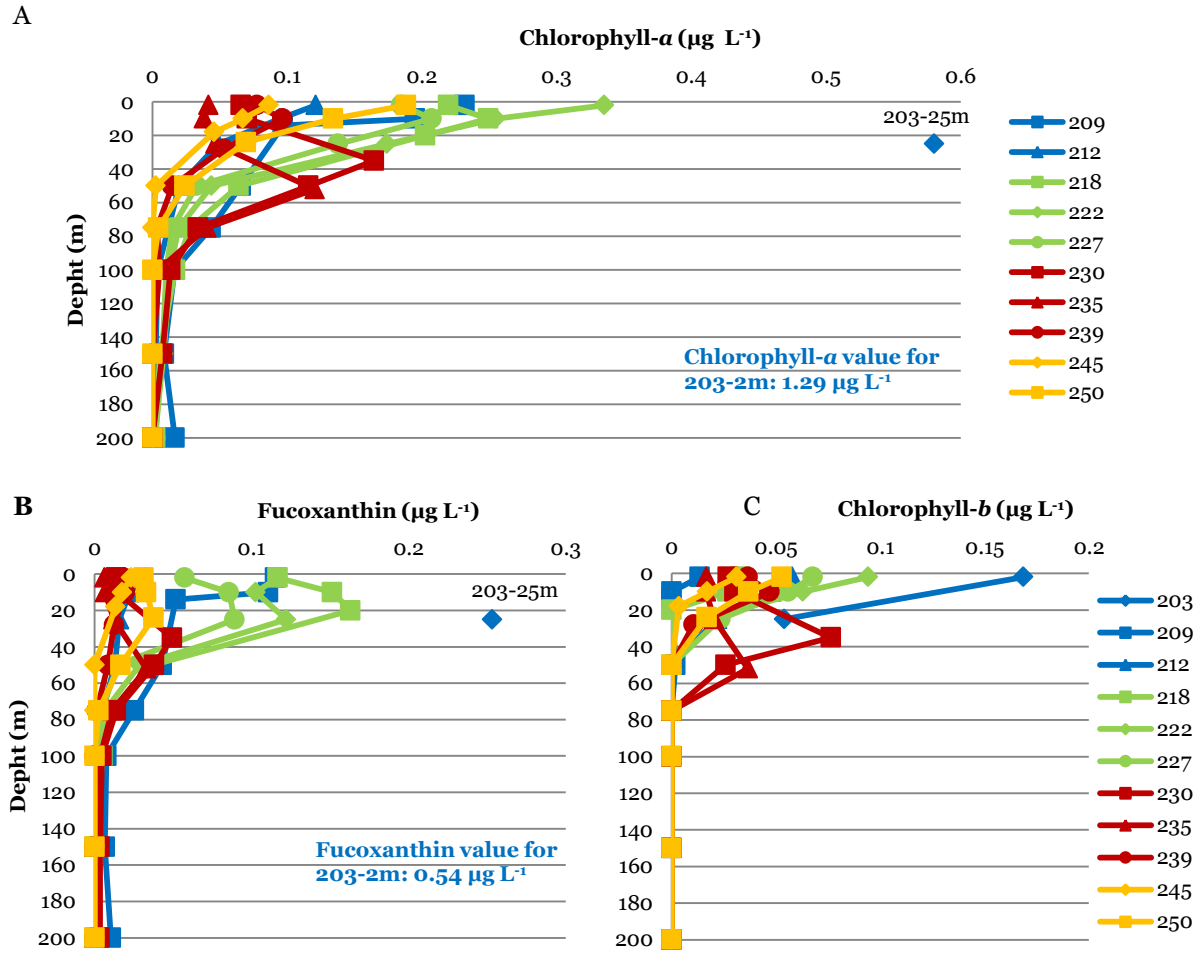

Figure 11: Chlorophyll-*a* concentration (in µg L^{-1}) against depth (in m) (A) Fucoxanthin concentration (in µg L^{-1}) against depth (in m) (B) and Chlorophyll-*b* concentration (in µg L^{-1}) against depth (in m) (C). Colours indicate the different water masses: Blue: Adw, Green: MwI, Brown: Pdw, Orange: MwII.

3.2.2 Biomass

The amount of chlorophyll-*a* of the pigment based algal classed varied substantially between the stations and depths. Annex II contains a table showing the amount of chlorophyll-*a* (in µg L^{-1}) for the taxonomic divisions as found at the different stations and depths (Figure 12).

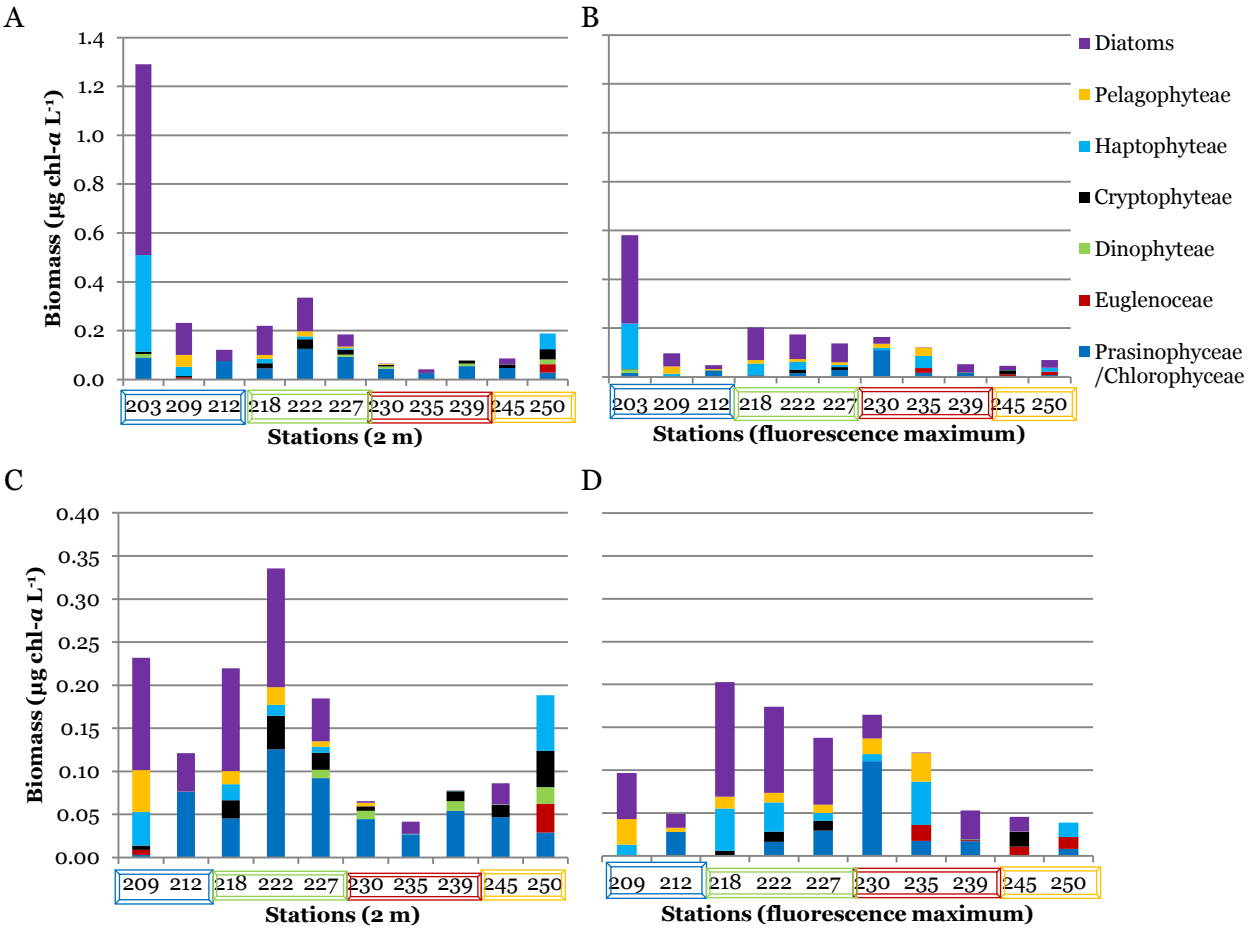

Figure 12: Biomass (µg chl-*a* L^{-1}) for the algal divisions at 2 m deep (A) and the depth of the fluorescence maximum for the different stations (station 203 included) (B). Biomass (µg chl-*a* L^{-1}) for the algal divisions at 2 m deep (C) and the depth of the fluorescence maximum for the different stations (station 203 excluded) (D). Blue boxes: Adw, Green boxes: MwI, Brown boxes: Pdw, Orange boxes: MwII.

Total biomass (µg chl-*a* L^{-1}) found at the stations varied between 0.04 and 1.3 µg chl-*a* L^{-1} and was generally lower at the depth of the fluorescence maximum than in the surface waters, except for station 230 and 235 in the Pdw. Station 203 showed an unusually high biomass at both depths as already was indicated by the elevated pigment concentrations found at this station. In general, both the stations at the Adw and the MwI showed the highest phytoplankton biomass at the surface, which is however not so straightforward at the depth of the fluorescence maximum (Figure 12). The Adw and MwI stations were characterized by diatoms, while all other stations were characterized by flagellates. Biomass of cryptophyteae, dinophyteae and euglenoceae was in principle low at all stations and all depths. prasinophyceae/chlorophyceae contributed substantially to phytoplankton biomass at the surface waters, while haptophyteae considerably important in deeper waters. At stations 230 and 235 in the Pdw, the biomass of Pelagophyteae, Haptophyteae and Euglenoceae increased with depths to 35 or 50 m (Figure 12 and Annex II).

3.2.3 Size distribution

The contribution of picoplankton, nanoplankton and microplankton to phytoplankton biomass varied between stations and depths. Picoplankton contributed in general more to biomass at the surface, especially at the stations influence by Pdw, while nanoplankton or microplankton contributed more to biomass in deeper waters. Stations influenced by Adw were dominated by microplankton at all depths, except for station 209 at the Nansen-Gakkel Ridge. The elevated phytoplankton biomass at station 203 consisted mainly of nanoplankton and microplankton and hardly of picoplankton biomass (Figure 13).

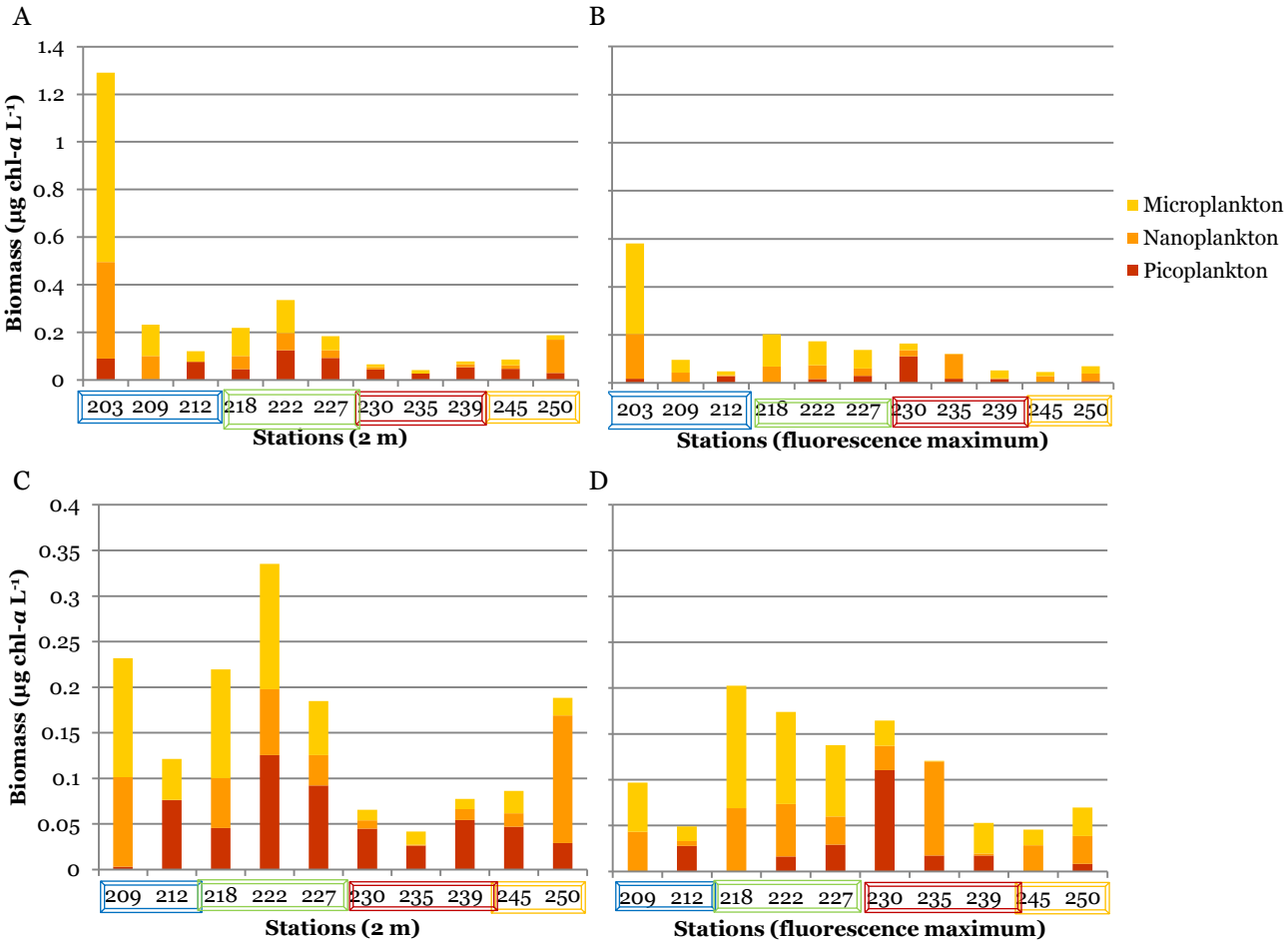

Figure 13: Contribution to biomass (µg chl-*a* L^{-1}) of picoplankton, nanoplankton and microplankton at a depth of 2 m (A) and the depth of the fluorescence maximum (station 203 included) (B) Contribution to biomass (µg chl-*a* L^{-1}) of picoplankton, nanoplankton and microplankton at a depth of 2 m (C) and the depth of the fluorescence maximum (station 203 excluded) (D). Coloured boxes around the station number indicate the different water masses: Blue boxes: Adw, Green boxes: MwI, Brown boxes: Pdw, Orange boxes: MwII.

3.2.4 Biomass related to water masses

To investigate the amount of similarity between pigment concentrations (in µg L^{-1}) in relation to the water masses of all stations up to 50 m deep, the biomass was plotted in a 3D MDS plot (Figure 14). Although it was difficult to distinguish a pattern either between water masses or between depths, the stations characterized by MwI showed most similarity, however, not significantly. The stations of the Adw showed least similarities.

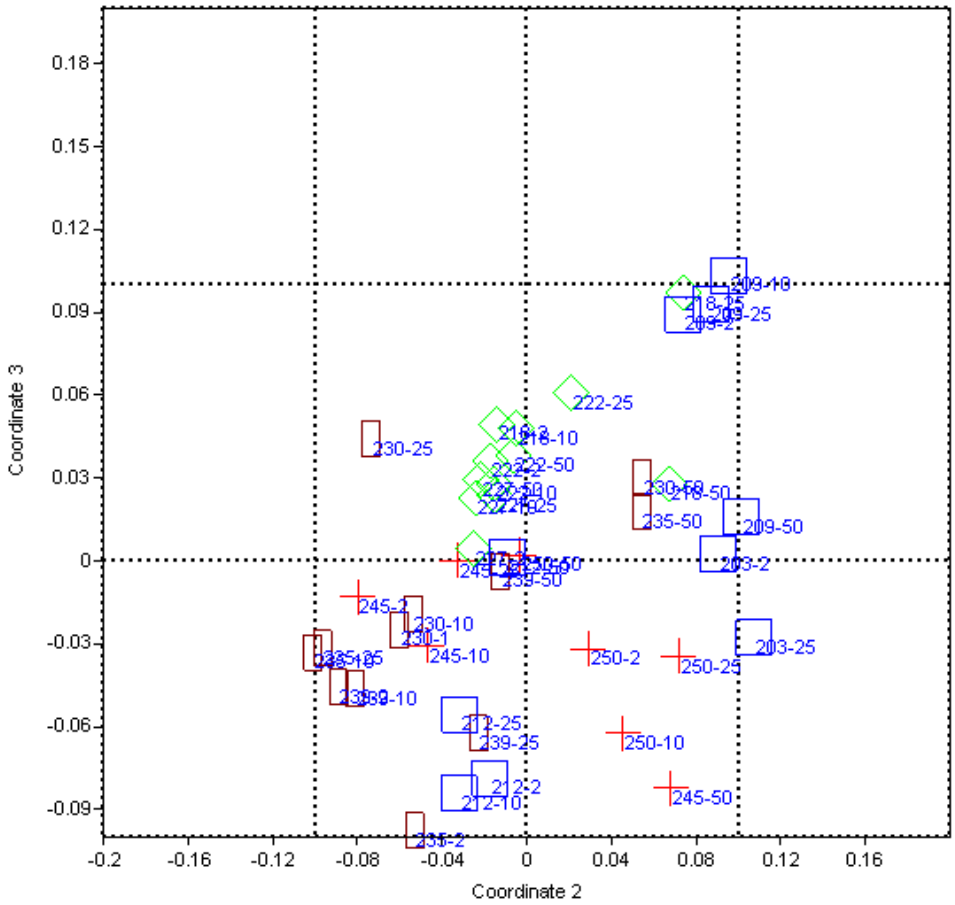

Figure 14: 3D MDS plot of biomass of pigment concentrations in relations to the water masses for all stations up to a depth of 50 m (stress: 8%). Blue boxes: Adw, Green triangles: MwI, Brown rectangles: Pdw, Red crosses: MwII.

To test whether the biomass of the various taxonomic divisions and size classes showed significant differences between water masses, Kruskal-Wallis and Mann-Whitney tests were conducted. Total phytoplankton biomass (µg chl-*a* L^{-1}) differed significantly between the station grouping based on the water masses ($p < 0.010$) (Table 3). The stations characterized by Adw and MwI showed a significantly higher biomass than the biomass found at the stations influenced by Pdw. Furthermore, the biomass in the MwI was significantly higher than in the MwII (Figure 15).

Of all taxonomic divisions, the euglenoceae, cryptophyteae, pelagophyteae and the diatoms showed significant differences between stations groupings based on the water masses. The euglenoceae showed at the stations characterized by MwII a significantly higher biomass than the biomass found at the MwI influenced stations. Cryptophyteae biomass differed significantly between almost all station groupings as well as the diatom biomass. Pelagophyteae biomass was significantly lower at the stations characterized by MwII in comparison with all other water masses. Microplankton biomass differed significantly between all water masses, while no significant differences were found for both picoplankton and nanoplankton biomass.

Table 3: Results Kruskal-Wallis test for the differences in biomass (µg chl-*a* L^{-1}) of different taxonomic divisions for the different water masses to a depth up to about 50 m ($\alpha < 0.050$). One star (*) indicates a significance < 0.050, two stars (**) indicate a significance of < 0.010 and three stars (***) indicate a significance of < 0.001. ns indicate no significance

	χ^2	df	p
Total biomass	12.642	3	**
Prasinophyceae / Chlorophyceae	2.439	3	ns
Euglenoceae	8.626	3	*
Dinophyteae	1.746	3	ns
Cryptophyteae	21.567	3	***
Haptophyteae	4.265	3	ns
Pelagophyteae	8.799	3	*
Diatoms	23.032	3	***
Picoplankton	2.439	3	ns
Nanoplankton	5.707	3	ns
Microplankton	25.139	3	***

The outcome of the statistical tests was highly influenced by the high phytoplankton biomass of station 203 in the Nansen Basin, which showed an outlier value in the biomass found at a depth of 25 m (o35) and an extreme biomass value (*36) found at the surface (Figure 15).

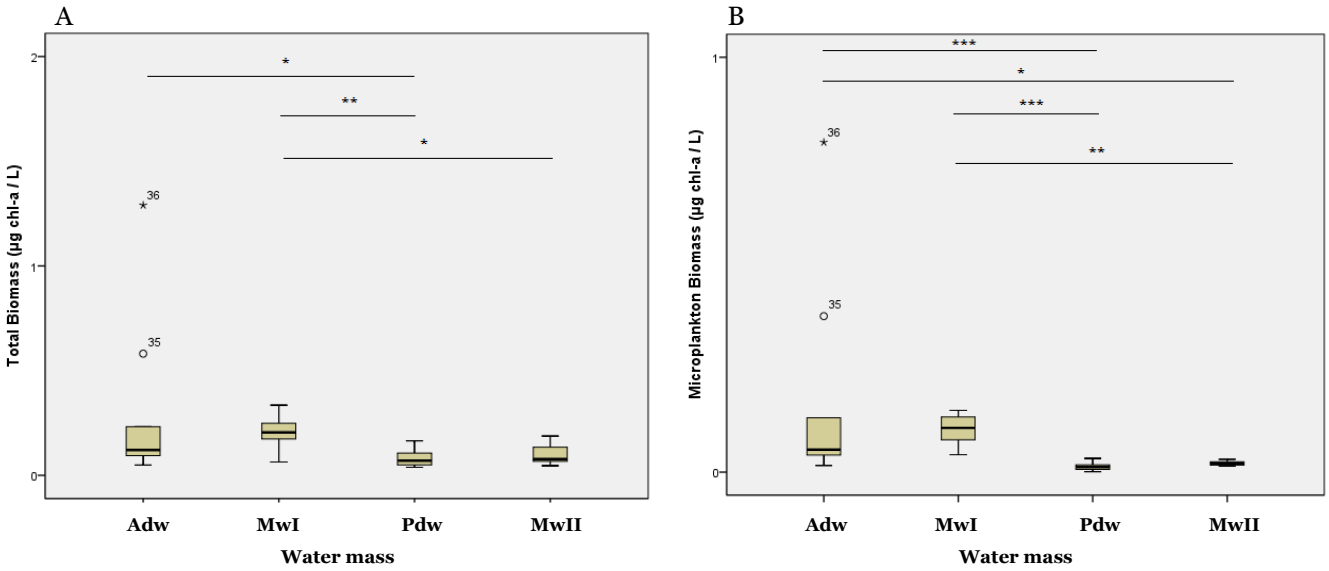

Figure 15: Boxplots showing significant differences between total phytoplankton biomass (µg chl-*a* L^{-1}) (A) and microplankton biomass (µg chl-*a* L^{-1}) (B) for the different water masses: Adw, MwI, Pdw and MwII. o indicates an outlier value and * indicates an extreme value, both found in phytoplankton biomass of station 203. One star (*) indicates a significance < 0.050, two stars (**) indicate a significance < 0.010, and three starts (***) indicate a significance of < 0.001.

3.2.5 Relation to environmental and chemical variables

Phytoplankton biomass of the central Arctic Ocean as identified by means of HPLC was significantly influenced by salinity ($p < 0.010$), temperature ($p < 0.010$), average sea ice cover ($p < 0.001$) and nutrient concentrations ($p < 0.001$) (Table 4a). This implied that waters with a higher salinity also contained a higher phytoplankton biomass as was the case for colder waters. The relationship between phytoplankton biomass and average sea ice cover was negative: the higher the average sea ice cover, the lower the phytoplankton biomass (Figure 16). The relationship with nutrient concentrations was more complicated in the sense that the individual nutrient concentrations did not show any significant relationship with total phytoplankton biomass. When all nutrients were added to the model together, the relationship became however significant ($p < 0.001$).

Microplankton biomass was also significantly influenced by salinity ($p < 0.001$), temperature ($p < 0.001$) and average sea ice cover ($p < 0.001$). Furthermore, the microplankton biomass was significantly influenced by phosphorus concentrations: the higher the phosphorus concentration, the lower the biomass of microplankton (Table 4b).

Nanoplankton was significantly influenced by salinity ($p < 0.010$), temperature ($p < 0.050$) and average sea ice cover ($p < 0.001$). Even when all nutrients were added in the model together, nanoplankton biomass did not show a significant relationship with nutrient concentrations. The only variable influencing the picoplankton biomass was the concentration of nitrate. This relationship was negative: the higher the nitrate concentration, the lower the picoplankton biomass (Table 4b).

Table 4: Results GLM for the relationship of total phytoplankton biomass (µg chl-*a* L^{-1}) (A) and biomass of picoplankton, nanoplankton and microplankton (µg chl-*a* L^{-1}) (B) with environmental and chemical variables of the water column ($\alpha < 0.050$). One star (*) indicates a significance < 0.050, two stars (**) indicate a significance of < 0.010 and three stars (***) indicate a significance of < 0.001, ns indicates no significance.

A	χ^2	df	p
Salinity	9.407	1	**
Temperature	6.638	1	**
Sea ice cover	27.787	1	***
NO_3	0.005	1	ns
NO_2	0.244	1	ns
Si	1.499	1	ns
PO_4	3.016	1	ns
NH_4	0.165	1	ns

B	Microplankton			Nanoplankton			Picoplankton		
	χ^2	df	p	χ^2	Df	p	χ^2	df	p
Salinity	19.122	1	***	7.012	1	**	2.416	1	ns
Temperature	12.866	1	***	4.020	1	*	1.191	1	ns
Sea ice cover	23.462	1	***	23.563	1	***	0.000	1	ns
NO_3	0.190	1	ns	0.4125	1	ns	6.116	1	**
NO_2	0.190	1	ns	0.087	1	ns	0.264	1	ns
Si	1.656	1	ns	0.434	1	ns	0.705	1	ns
PO_4	4.254	1	*	1.837	1	ns	0.000	1	ns
NH_4	0.091	1	ns	2.490	1	ns	0.275	1	ns

A

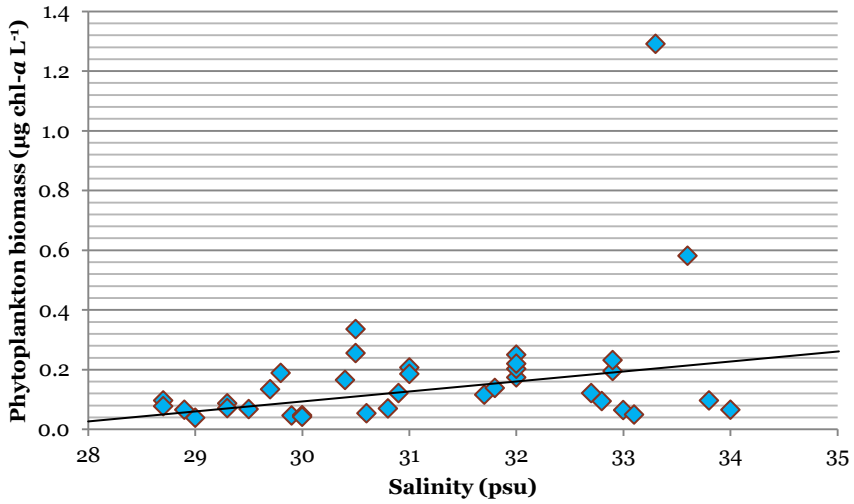

B

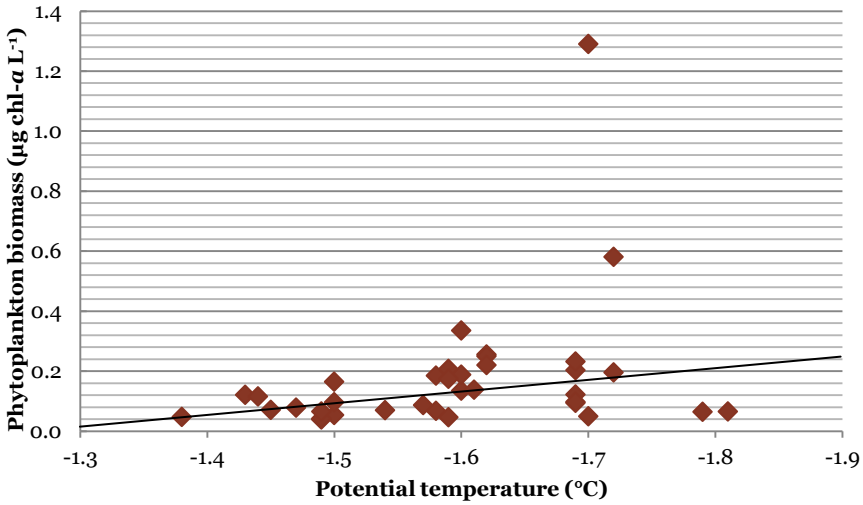

C

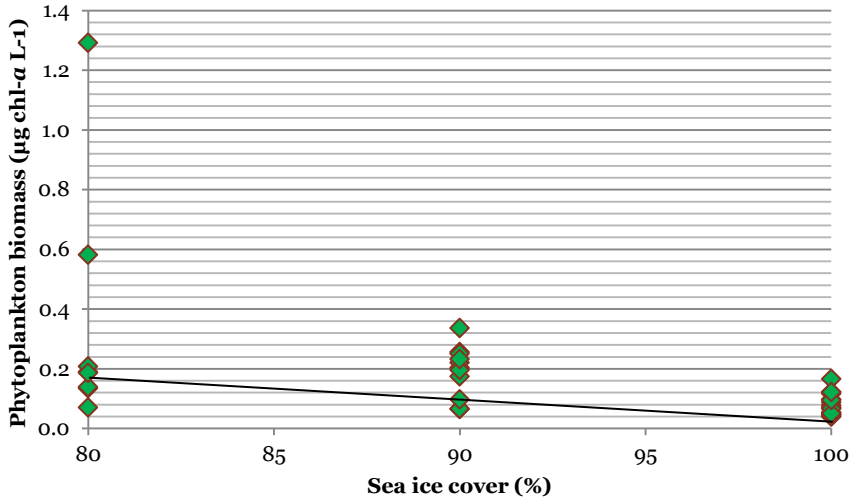

Figure 16: Significant relationship including the regression line of total phytoplankton biomass (µg chl-*a* L^{-1}) with salinity (psu) (A), temperature (°C) (B) and sea ice cover (%) (C).

3.3 Light Microscopy

3.3.1 Identified taxa

In total 11,694 cells were counted and 786 cells were taxonomically accounted, which was ca. 7% of the total number of cells. Annex III gives an overview of the real counts per sample. These samples contained flagellates, dinoflagellates, diatoms, ciliates and upos (see Chapter 2) of which flagellates dominated by far in cell numbers, both in surface as in deeper waters (Figure 17). Diatoms were mainly counted at the stations influenced by MwI, but also in the deeper waters of the stations characterized by Pdw and MwII. At station 209 at the Nansen-Gakkel Ridge, the highest amount of dinoflagellates was counted and the ciliates were mainly counted at station 250 at the Lomonosov Ridge north of Russia.

The flagellates comprised the autotrophs *Euglena* spp., *Dictyocha* spp., *Meringosphaera tenerrima*, the mixotroph *Dinobryon* spp., and the heterotrophic Choanoflagellates. Although it is difficult to find real evidence, it seemed that fresh water flagellates like *Haematococussus* spp. and *Pandorina* spp. were present in the samples. Dinoflagellates comprised the heterotrophs *Amphidinium* spp., *Gyrodinium* spp., *Protoperidinium* spp., *Micracanthodinium claytonii*. Most of the counted dinoflagellates were athecate, which was 93.7% of the dinoflagellates. Diatoms comprised: *Navicula* spp., *Thalassiosira* spp., *Cylindrotheca* spp./*Nitzschia longissima*, *Chaetoceros* spp., *Eucampia groenlandica*, *Rhizosolenia* spp., *Melosira arctica*, *Attheya* spp., *Nitzschia* spp./*Pseudonitzschia* spp., *Pleurosigma* spp., *Guinardia* spp. Identified ciliates comprised *Stromtium* spp. and *Myrionecta rubra*.

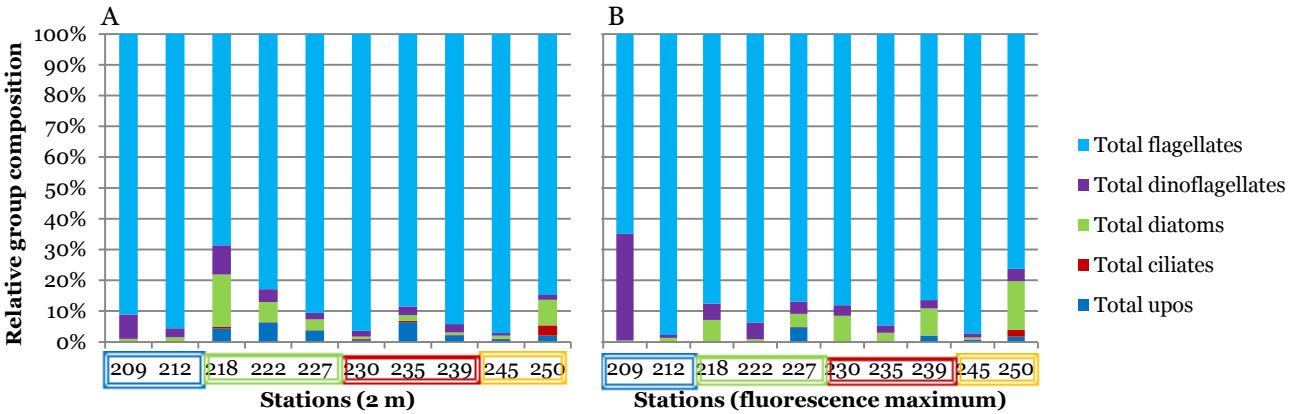

Figure 17: Relative group composition comprising of flagellates, dinoflagellates, diatoms, ciliates and upos at the surface (A) and the depth of the fluorescence maximum (B). The coloured boxes around the station numbers indicate the water masses: Blue boxes: Adw, Green boxes: MwI, Brown boxes: Pdw, Orange boxes: MwII.

The condition of the cells varied among samples. On average the percentage of empty cells, which comprised mainly pennate diatoms, was 5% but varied substantially among stations. The percentage of empty cells was for example < 1% at station 209 at the Nansen-Gakkel Ridge and 17% in the deeper waters of station 245 in the Makarov Basin north of Russia. Cysts of diatoms and flagellates were observed at almost all stations but in low numbers. Diatom chains of pennate diatoms were also counted in most of the samples. Those chains contained mainly two or three cells. Chains of *Chaetoceros* spp. were generally longer and could comprise six to seven cells, except at the surface of stations 212 and 218 influenced by MwI. At those stations, chains up to 11 and 33 cell were counted.

3.3.2 Abundance and biomass

Total abundance varied between 82,675 and 1,519,080 cells per litre and was higher at the surface then in deeper waters (Figure 18). Annex IV shows the abundance of the various taxa per station. The stations characterized by Adw and MwI showed the highest abundance at the surface when compared to the stations influenced by Pdw and MwII. This pattern is less strong in the deeper waters, especially because the Pdw influenced stations 230 and 235 showed an increase in abundance with increasing depth. The previous paragraph already explained that the flagellates were most important in terms of abundance at all stations and depths.

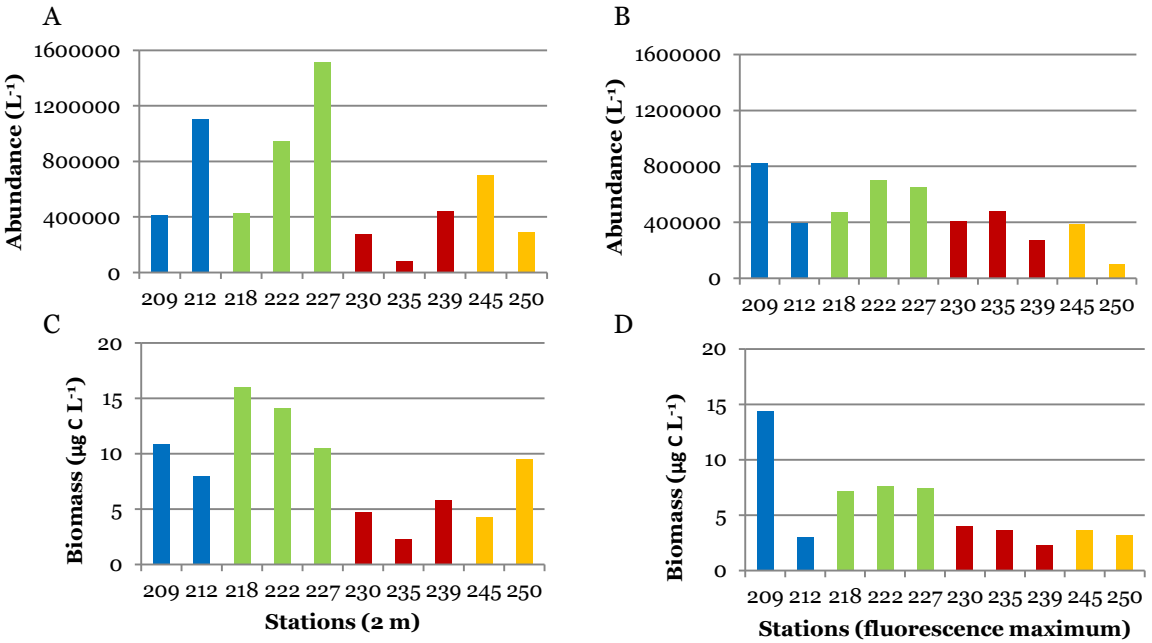

Figure 18: Abundance (amount of cell per litre) at 2 m depth (A) and the depth of the fluorescence maximum (B) and biomass (µg C per litre) at 2 m depth (C) and the depth of the fluorescence maximum (D) of phytoplankton and other unicellular protists per station and water mass: Blue bars: Adw, Green bars: MwI, Brown bars: Pdw, Orange bars: MwII.

A high abundance was not automatically correlated with a high biomass. Total biomass ranged between 2.3 and 16 µg C L^{-1} and was generally higher at the surface than in deeper waters, except for the stations 209 at the Nansen-Gakkel Ridge and station 235 in the Canada Basin. Annex IV shows the biomass of the various taxa per station. The stations influence by MwI showed the highest biomass at the surface. The high biomass of the deeper waters of station 209 prevents this pattern to continue to the deeper waters. At the stations influenced by Adw, the dinoflagellates contributed mostly to biomass. Biomass of flagellates, diatoms and ciliates was negligible at those stations. At all other stations, biomass of both dinoflagellates and flagellates was about equally important at the surface, while biomass of flagellates became more important in deeper waters. Ciliates contributed substantially to biomass, especially at the surface and especially at the stations influenced by Pdw and MwII. At those stations, ciliates were as important as flagellates and dinoflagellates. Diatom biomass was negligible at all stations and depths (Figure 19).

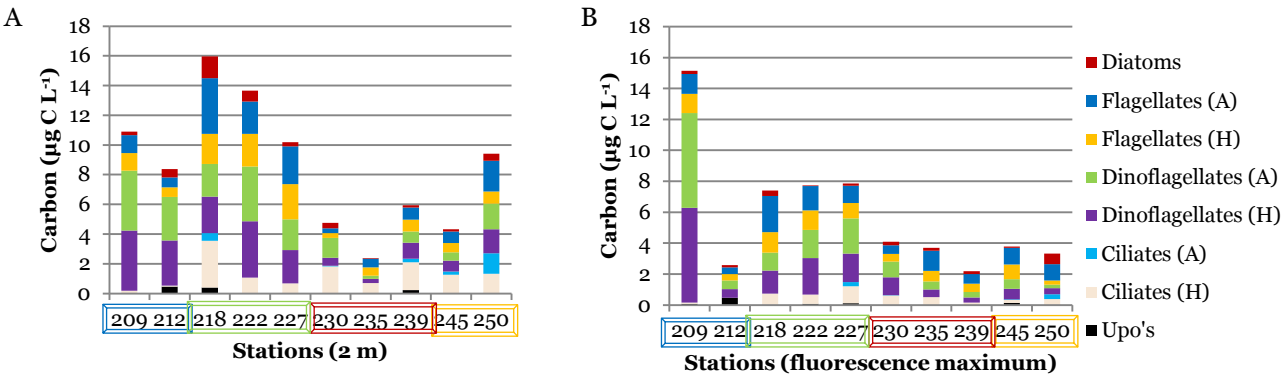

Figure 19: Contribution to protozoan carbon (µg C L^{-1}) for diatoms, flagellates, dinoflagellates, ciliates and upos for both autotrophic organisms (indicated with A) and heterotrophic organisms (indicated with H) at 2 m deep (A) and at the depth of the fluorescence maximum (B). The coloured boxes around the station numbers represent the water masses: Blue boxes: Adw, Green boxes: MwI, Brown boxes: Pdw, Orange boxes: MwII.

Only in a few cases autotrophic flagellates are more important than heterotrophic flagellates, for example at station 218 at the North Pole and station 250 at the Lomonosov Ridge north of Russia. However, in most cases the decision to consider 50% of all unidentified flagellates and dinoflagellates as being autotrophic explains the equal contribution. The ciliates on the other hand showed a clearly importance of heterotrophic ciliates in comparison to the autotrophic ciliates (Figure 19).

Investigating the taxonomic diversity within flagellates and dinoflagellates showed that most organisms were unidentified, especially in the surface waters. *Dictyocha* spp. however, contributed between 25% and 45% to flagellate biomass at stations 218 at the North Pole and station 250 at the Lomonosov Ridge north of Russia. The deeper waters showed a higher diversity. *Dictyocha* spp. contributed at more than two stations and also *Euglena* spp. contributed to flagellate biomass. The contribution of identified dinoflagellates to biomass is negligible at all stations, although *Micracanthodinium claytonii* contributed mainly at station 230 at the Alpha-Mendeleyev Ridge and *Amphidinium* spp. contributed mainly in the deeper waters of station 250 at the Lomonosov Ridge north of Russia (Annex IV). Separation of the flagellates between autotrophs and heterotrophs showed the same pattern as in Figure 17: flagellates are most important in terms of abundance.

3.3.3 Size distribution

In general, protist abundance (L^{-1}) was dominated by picoplankton or nanoplankton and the contribution of microplankton was negligible on all stations and depths. Exceptions were the surface waters of stations 218 at the North Pole and deep waters at station 250 at the Lomonosov Ridge north of Russia. Both stations were characterized by a very low picoplankton biomass (Figure 20). Protist biomass (µg C L^{-1}) was characterized by very low biomass of picoplankton. In general, microplankton contributed mostly to biomass at the surface waters of all stations, except at the stations influenced by MwI on which nanoplankton contributed the most to biomass. The contribution of nanoplankton to biomass became more important in the deeper waters (Figure 20).

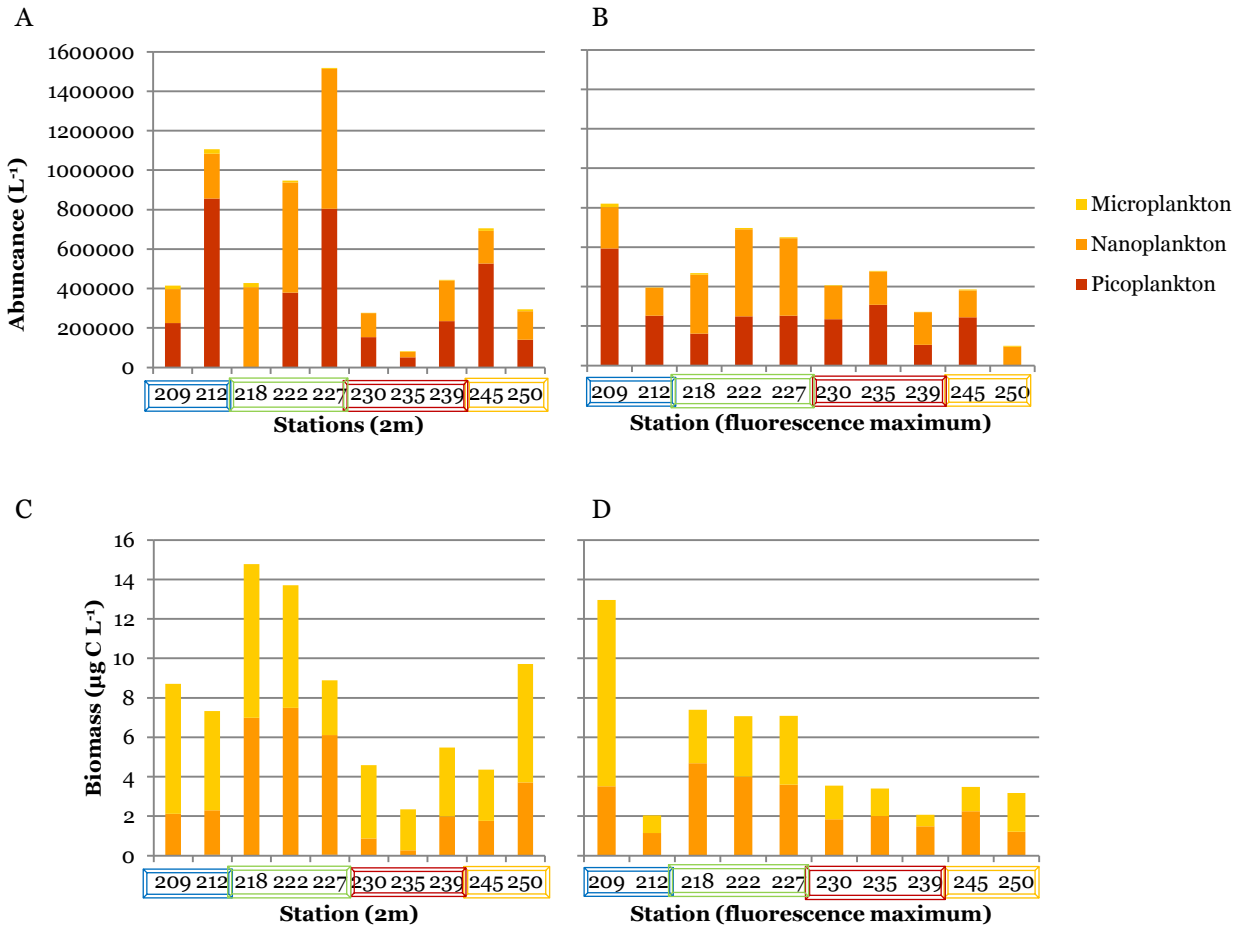

Figure 20: Abundance (L^{-1}) of picoplankton, nanoplankton and microplankton at 2 m deep (A) and at the depth of the fluorescence maximum (B) and biomass (µg C L^{-1}) of picoplankton, nanoplankton and microplankton at 2 m deep (C) and the depth of the fluorescence maximum (D). The coloured boxes around the station numbers indicate water masses: Blue boxes: Adw, Green boxes: MwI, Brown boxes: Pdw, Orange boxes: MwII.

3.3.4 Relation to water masses

To investigate the amount of similarity between identified presence and absence of identified taxa in relation to the water masses of all stations at the surface and the deeper waters, the biomass was plotted in a 3D MDS plot (Figure 21). Again, it is difficult to distinguish a pattern for the data, especially for the stations influenced by MwI, Pdw and MwII. It seemed however, that the taxa present at the Adw varied from taxa present in all other water masses, but not significantly.

To test whether the abundance and biomass of unicellular protists showed significant differences between water masses, Kruskal-Wallis and Mann-Whitney tests were conducted. Total unicellular protists abundance did not significantly differ between water masses ($p > 0.050$), which was not the case for the different algal divisions. The abundance of diatoms and flagellates did not show significant differences, but dinoflagellates on the other hand, occurred in higher abundances in the Adw and the MwI than in the Pdw and the MwII. Ciliates occurred significantly less in the Adw in comparison with all other water masses and most of the upos were counted in the MwI in relation to the other water masses (Table 5A and Figure 22 A and B).

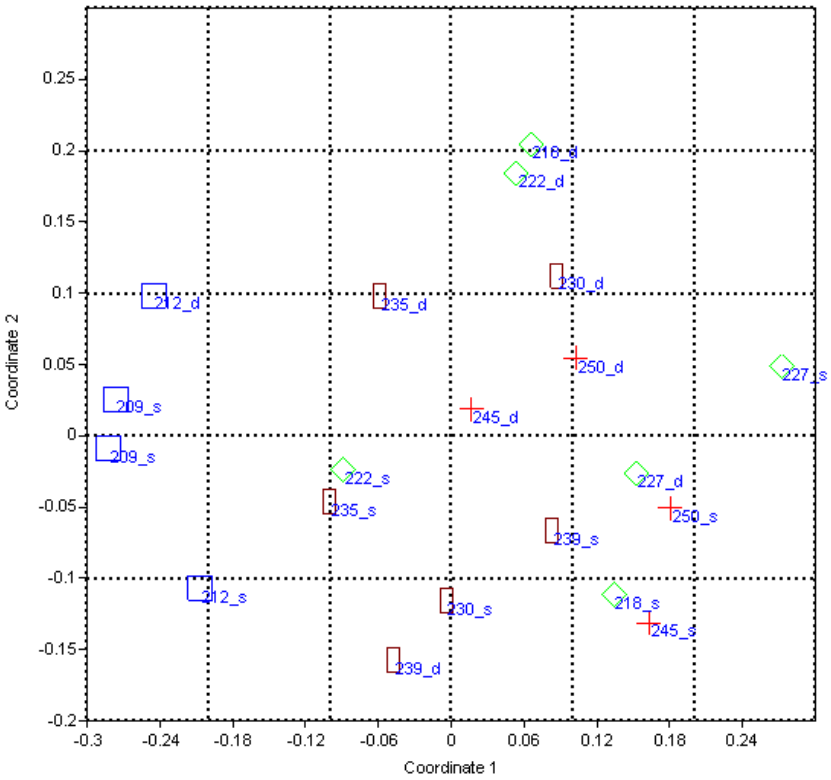

Figure 21: 3D MDS plot of similarity of the taxonomic composition of the stations at a depth between 2 m (indicated with –s) and the depth of the fluorescence maximum (indicated with –d), as indicated by different colours. Blue boxes: Adw, Green triangles: MwI, Brown rectangulars: Pdw, Red crosses: MwII (Stress 25%).

Total unicellular plankton biomass showed significant differences between water masses ($p < 0.050$), which meant that the biomass found at the MwI was significantly higher than the biomass found at the Pdw. Furthermore, the biomass of flagellates ($p < 0.010$), dinoflagellates ($p < 0.050$) and ciliates ($p < 0.050$) indicated significant differences between water masses. The biomass of flagellates found at the MwI was significantly higher than the biomass identified at all other stations, and the biomass found at the Adw was significantly higher than the biomass found in the Pdw. Biomass of dinoflagellates was high at both the Adw and the MwI, but only the MwI counted a significantly higher biomass than the Pdw and the MwII. Ciliates biomass at last, was significantly lowest in the Adw (Table 5B and Figure 22 C, D, E and F).

Table 5: Results Kruskal-Wallis test for the differences in total abundance (L^{-1}) and total biomass (µg C L^{-1}), abundance and biomass of the algal divisions: diatoms, flagellates, dinoflagellates, ciliates and upos and for the different size categories for the different water masses ($\alpha < 0.050$). One star (*) indicates a significance < 0.050, two stars (**) indicate a significance < 0.010, ns indicates no significance.

A

Abundance	χ^2	df	p
Total	7.660	3	ns
Diatoms	0.070	3	ns
Flagellates	4.755	3	ns
Dinoflagellates	13.762	3	**
Ciliates	9.956	3	*
Upos	8.934	3	*
Picoplankton	3.989	3	ns
Nanoplankton	13.964	3	*
Microplankton	8.724	3	*

B

Biomass	χ^2	df	p
Total	7.983	3	*
Diatoms	1.945	3	ns
Flagellates	11.717	3	**
Dinoflagellates	10.662	3	*
Ciliates	8.917	3	*
Upos	4.391	3	ns
Picoplankton	4.165	3	ns
Nanoplankton	12.952	3	**
Microplankton	4.576	3	ns

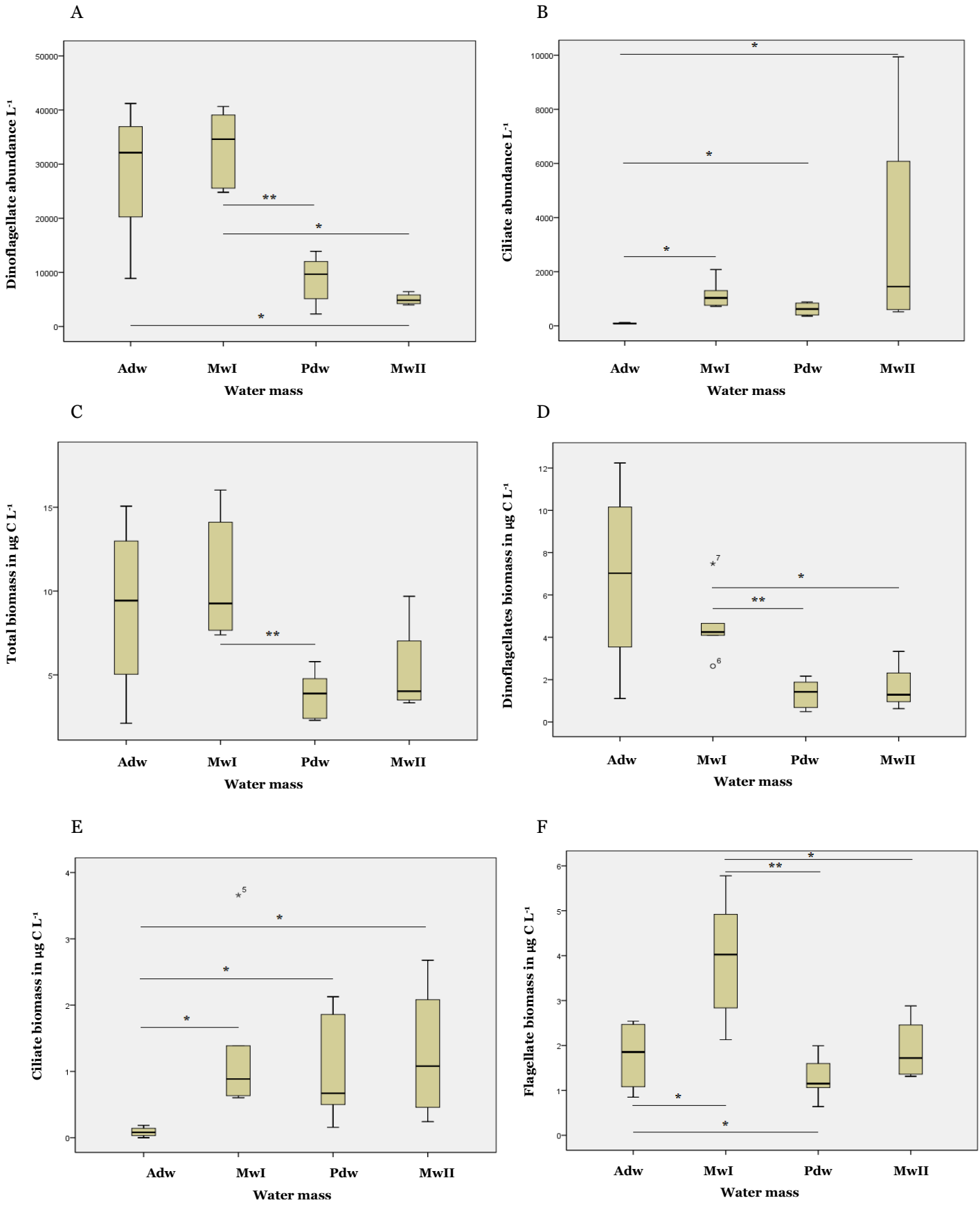

Figure 22: Boxplots showing differences of algal divisions between water masses for dinoflagellate abundance (A), Ciliate abundance (B), total unicellular plankton biomass (C), dinoflagellate biomass (D), ciliate biomass (E) and flagellate biomass (F). One star (*) indicates significant differences < 0.050. Two stars (**) indicate a significant difference of < 0.010.

The size distribution of unicellular plankton also showed significant differences between water masses. Abundance of both nanoplankton and microplankton differed significantly between water masses ($p < 0.050$ and $p < 0.010$ respectively). Nanoplankton biomass was significantly higher in the MwI compared to the other water masses. The same held true for microplankton abundance, which was also significantly higher in the Adw. The investigation of the biomass indicated only significant differences between water masses for the nanoplankton ($p < 0.010$), being significantly higher in MwI in relation to the other water masses (Table 5).

3.3.5 Relation to environmental parameters

No significant linear relationships were found between abundance of unicellular plankton and the environmental and chemical variables salinity, water temperature, average sea ice cover, and nutrients concentrations, even when all variables were included in the model (Table 6).

Table 6: Results GLM for the relationship of total phytoplankton abundance (L^{-1}) and total biomass (µg chl-*a* L^{-1}) (A) and relations of biomass of picoplankton, nanoplankton and microplankton (µg chl-*a* L^{-1}) with environmental and chemical variables (B) ($\alpha < 0.050$). One star (*) indicates a significance < 0.050, two stars (**) indicate a significance of < 0.010 and three stars (***) indicate a significance of < 0.001, ns indicates no significance. Black numbers indicate linear relationships and red numbers indicate a quadratic relationship.

A	Abundance			Biomass		
	χ^2	df	P	χ^2	df	p
Salinity	2.158	1	ns	3.545	1	ns
Temperature	2.669	1	ns	7.151	1	**
sea ice cover	1.160	1	ns	7.361	1	**
NO_3	0.018	1	ns	0.015	1	ns
NO_2	2.526	1	ns	0.626	1	ns
Si	0.059	1	ns	0.007	1	ns
PO_4	0.374	1	ns	1.184	1	ns
NH_4	0.115	1	ns	0.628	1	ns

B	Microplankton			Nanoplankton			Picoplankton		
	χ^2	df	p	χ^2	Df	p	χ^2	df	p
Salinity	2.149	1	ns	1.679	1	ns	0.475	1	ns
Temperature	7.020	1	**	2.539	1	ns	0.713	1	ns
Sea ice cover	5.002	1	*	6.241	1	*	0.998	1	ns
NO_3	0.129	1	ns	0.547	1	ns	0.002	1	ns
NO_2	1.114	1	ns	0.054	1	ns	0.210	1	ns
Si	0.018	1	ns	6.826	1	**	0.398	1	ns
PO_4	0.337	1	ns	0.685	1	ns	0.025	1	ns
NH_4	0.205	1	ns	2.190	1	ns	0.911	1	ns

The biomass of unicellular plankton was constrained by water temperature ($p < 0.010$) and sea ice cover ($p < 0.010$), however, only the relationship with temperature is linear. The relationship between total unicellular organisms and the average sea ice cover was quadratic, which meant that biomass increased up to an ice cover of 90% and from that point decreased again. In this case, an ice cover of 90% would lead to the highest biomass. Total biomass did not show a significant relationship to nutrient concentrations, even when all nutrients were included in the model (Table 6A). Unicellular microplankton was constrained by water temperature ($p < 0.010$) and average sea ice cover ($p < 0.050$). Again, the relationship with sea ice cover is quadratic instead of linear. Unicellular nanoplankton was constrained by sea ice cover ($p < 0.050$) in a quadratic relationship and unicellular picoplankton showed no significant relationship to one of the variable (Table 6B) (Figure 23).

A

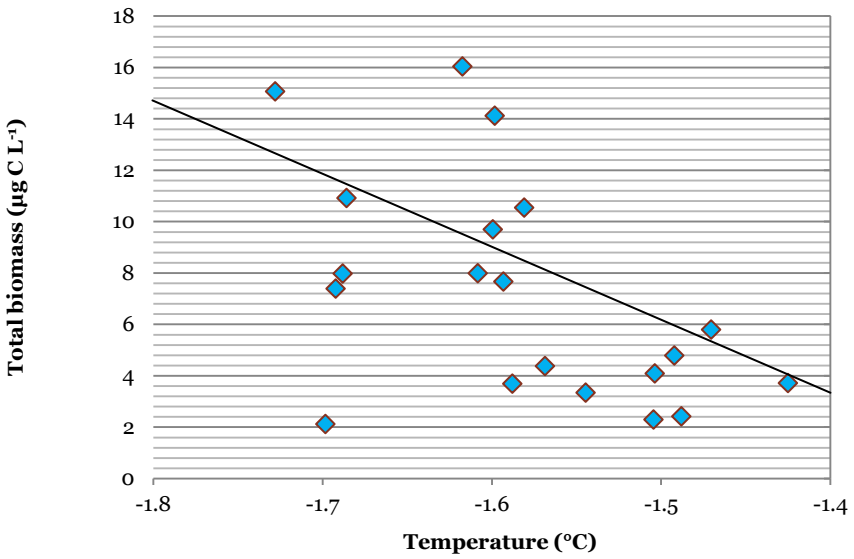

B

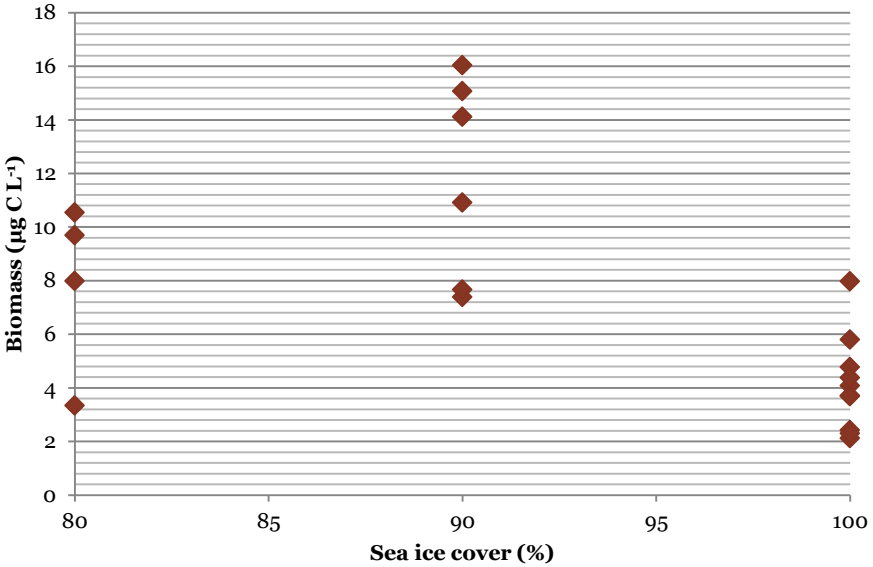

Figure 23: Significant relationship including the regression line of total biomass of unicellular plankton (µg C L^{-1}) with temperature (°C) (A) and sea ice cover (%) (B). No regression line is depicted for sea ice cover, but this quadratic relationship is significant.

3.4 Flow Cytometry

3.4.1 Abundance and biomass

Total abundance (L^{-1}) varied between 615,522 and 17,058,342 cells L^{-1} and varied substantially between stations and depth. The surface waters showed a higher abundance on every station than the deeper waters of the fluorescence maximum (Figure 24 A and B). Annex X contains a table showing the abundance for all stations and depths. At both depths, station 203 at the Nansen Basin showed an unusually high biomass, which was also indicated by the HPLC. Although situated in the Adw like station 203, station 209 at the Nansen-Gakkel Ridge contained an unusually low abundance, especially at the surface. Total biomass (µg C L^{-1}) varied between 0.81 and 41.17 µg C L^{-1} and was generally lower in deeper waters, except for station 209. While differences in abundance between the different water masses is not so obvious, the MwI contained the highest biomass in the surface waters (except station 203).

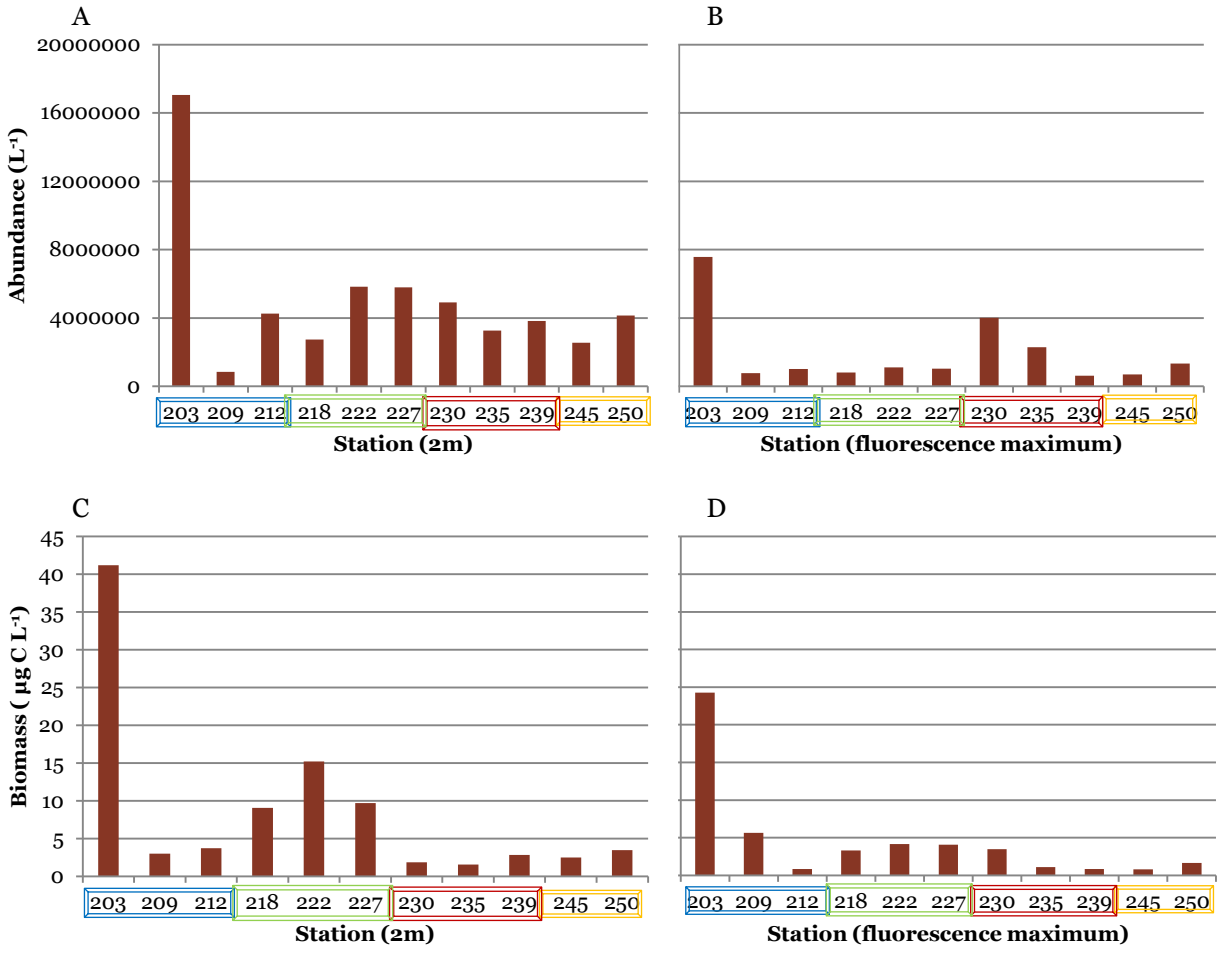

Figure 24: Phytoplankton abundance (cells L^{-1}) at the different stations at a depth of 2 m (A) and the depth of the fluorescence maximum (A) and phytoplankton biomass (µg C L^{-1}) at the different stations at the depth of 2 m (C) and the depth of the fluorescence maximum (D). The coloured boxes around the stations indicate the different water masses: Blue boxes: Adw, Green boxes: MwI, Brown boxes: Pdw, Orange boxes: MwII.

3.4.2 Size distribution

Total phytoplankton abundance was generally dominated by picoplankton, at all stations and all depths. Station 203 in the Nansen Basin and the stations of the MwI showed the highest contribution of nanoplankton, but cell concentrations were minor compared to the total abundance (Figure 25 A and B). Total phytoplankton biomass on the other hand was mainly dominated by nanoplankton (Figure 25 C and D), except station 212 in the Amundsen Basin at the surface and the deeper waters. The contribution of picoplankton to biomass increased however with depth at the stations of the Pdw and the MwII (Figure 25 E and F).

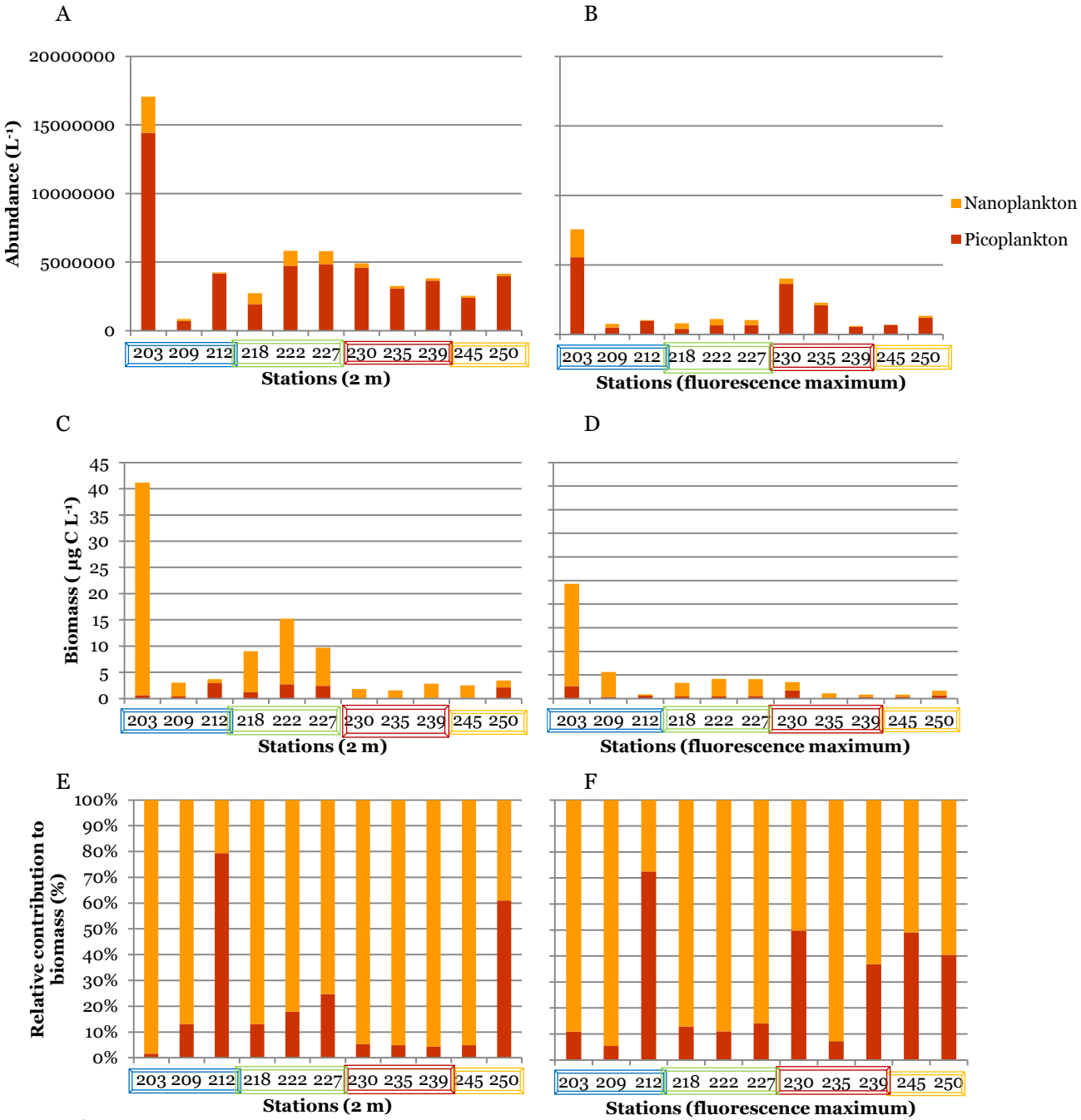

Figure 25: Contribution of picoplankton and nanoplankton to abundance (cells L-1) for the depth of 2 m (A) and the fluorescence maximum (B) and to biomass (µg C L^{-1}) for the depth of 2 m (C) and the fluorescence maximum (D). And relative contribution (%) of picoplankton and nanoplankton to biomass for the surface (E) and the deep waters (F). Coloured boxes around the stations indicate water masses: Blue boxes: Adw, Green boxes: MwI, Brown boxes: Pdw, Orange boxes: MwII.

3.4.3 Relation to water masses

Total phytoplankton abundance determined by flow cytometer did not show a significant relationship with the four water masses, although nanoplankton was significantly higher in the MwI compared to the Pdw and the MwII ($p < 0.010$) (Table 7 and Figure 26). Total phytoplankton biomass however, did show significant differences between water masses ($p < 0.050$). Biomass of the Adw and the MwI were higher than the biomass found at the other stations, but this correlation was influenced by the high biomass at station 203. Nanoplankton biomass followed the same pattern ($p < 0.050$). Picoplankton however, showed significant lower biomass at the Pdw compared to the Adw and the MwI ($p < 0.050$). Also these correlations were influenced by the high biomass of station 203.

Table 7: Results Kruskal-Wallis test for the differences in total abundance (cells L^{-1}) and total biomass (µg C L^{-1}) and abundance and biomass of picoplankton and nanoplankton for the different water masses ($\alpha < 0.050$). One star (*) indicates a significance < 0.050 and two stars (**) indicate a significance < 0.010, ns indicates no significance.

Abundance	χ^2	df	p	Biomass	χ^2	df	p
Total	0.970	3	ns	**Total**	10.950	3	*
Picoplankton	0.933	3	ns	**Picoplankton**	9.192	3	*
Nanoplankton	12.792	3	**	**Nanoplankton**	11.015	3	*

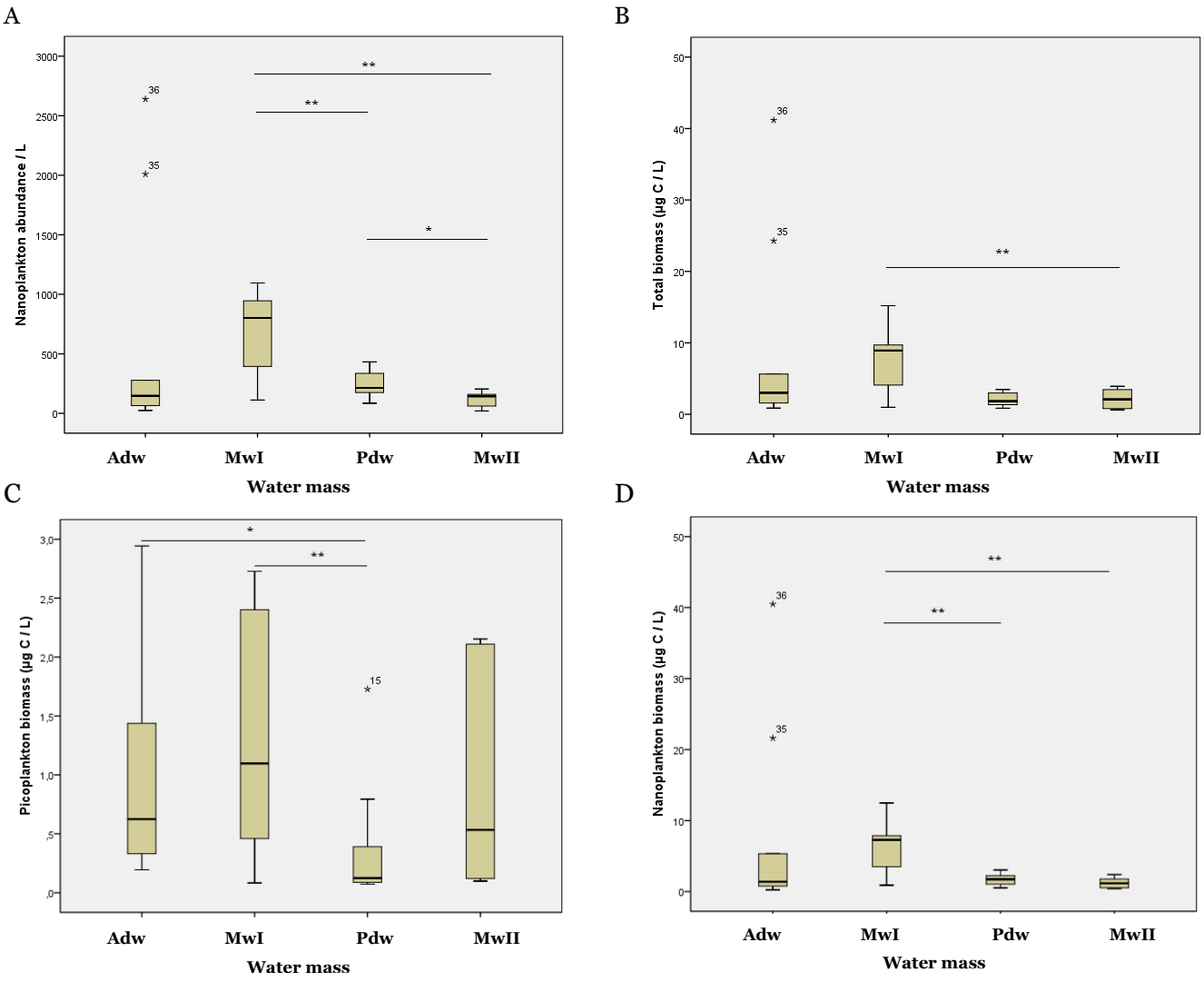

Figure 26: Boxplots showing differences between water masses for nanoplankton abundance (in L^{-1}) (A), total phytoplankton biomass (in µg C L^{-1}) (B), picoplankton biomass (in µg C L^{-1}) (C), nanoplankton biomass (in µg C L^{-1}) (D). One star (*) indicates significant differences < 0.050. Two stars (**) indicate a significant difference of < 0.010.

3.4.4 Relation to environmental and chemical variables

Total phytoplankton abundance was constrained by concentrations of both NO_3 and Si: the higher the concentration in the water column, the lower the phytoplankton abundance ($p < 0.050$ for both of them). Phytoplankton biomass however, was only constrained by the average sea ice cover ($p < 0.001$): the more sea ice was present, the lower was the phytoplankton biomass (Figure 27). Also the biomass of picoplankton ($p < 0.010$) and nanoplankton ($p < 0.001$) were in this way correlated to the sea ice cover. When all nutrients were added together to the model, it correlated to total phytoplankton biomass ($p < 0.001$) and the biomass of nanoplankton ($p < 00.001$) (Table 8 A and B). Picoplankton abundance was constrained by concentrations of NO_3 and Si ($p < 0.050$ for both). Nanoplankton abundance was correlated with sea ice cover ($p < 0.001$): the less sea ice, the higher the nanoplankton abundance. When all nutrients were added to the model, it correlated with nanoplankton abundance ($p < 0.001$) (Table 8 C).

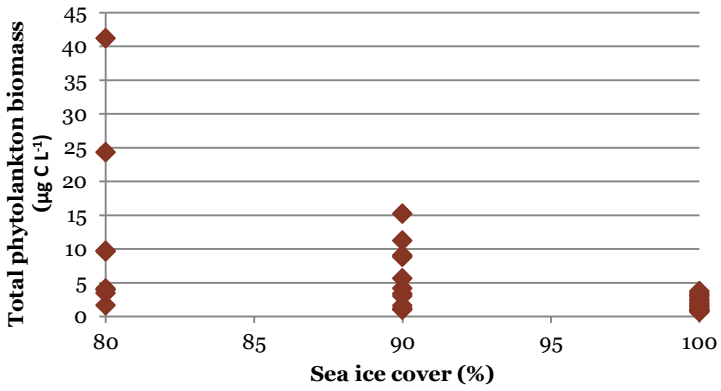

Figure 27: Phytoplankton biomass (µg C L^{-1}) plotted against sea ice cover (%). The linear relationship is significant.

Table 8: Results GLM for the relationship of total phytoplankton abundance (L^{-1}) and biomass (µg chl-*a* L^{-1}) (A), the relations of biomass of picoplankton and nanoplankton (µg chl-*a* L^{-1}) (B) and the relations of abundance of picoplankton and nanoplankton (L^{-1}) (C) with environmental and chemical variables ($\alpha < 0.050$). One star (*) indicates a significance < 0.050, two stars (**) indicate a significance of < 0.010 and three stars (***) indicate a significance of < 0.001, ns indicates no significance.

A	Abundance			Biomass		
	χ^2	Df	P	χ^2	df	p
Salinity	0.818	1	ns	2.719	1	ns
Temperature	0.225	1	ns	2.154	1	ns
sea ice cover	3.440	1	ns	19.065	1	***
NO_3	4.442	1	*	0.157	1	ns
NO_2	1.859	1	ns	0.435	1	ns
Si	4.993	1	*	1.170	1	ns
PO_4	1.529	1	ns	2.006	1	ns
NH_4	0.117	1	ns	0.344	1	ns
B	**Picoplankton**			**Nanoplankton**		
	χ^2	Df	P	χ^2	df	p
Salinity	0.020	1	ns	3.210	1	ns
Temperature	0.585	1	ns	2.189	1	ns
sea ice cover	7.868	1	**	17.805	1	***
NO_3	0.222	1	ns	0.128	1	ns
NO_2	1.026	1	ns	0.819	1	ns
Si	0.124	1	ns	1.619	1	ns
PO_4	0.441	1	ns	2.094	1	ns
NH_4	0.023	1	ns	0.610	1	ns
C	**Picoplankton**			**Nanoplankton**		
	χ^2	Df	P	χ^2	df	p
Salinity	1.623	1	ns	1.426	1	ns
Temperature	0.486	1	ns	0.651	1	ns
sea ice cover	2.048	1	ns	16.357	1	***
NO_3	6.111	1	*	0.016	1	ns
NO_2	2.111	1	ns	0.346	1	ns
Si	6.372	1	*	0.253	1	ns
PO_4	1.776	1	ns	0.207	1	ns
NH_4	0.043	1	ns	0.855	1	ns

3.5 Combining results

3.5.1 Carbon to chlorophyll-*a* ratio

Phytoplankton biomass as identified with the aid of the microscope combined with the chlorophyll-*a* concentrations obtained by HPLC enabled to calculate the carbon to chlorophyll-*a* ratio (C:Chl-*a* ratio) for all stations (except station 203). The C:Chl-*a* ratio varied between 11 in the deeper waters of station 230 in the Pdw and 79 in deeper waters of station 209 in the Adw. The average C:Chl-*a* ratio was 29 (Table 9).

Table 9: Phytoplankton carbon (PPC) in µg C L^{-1} obtained with the microscope, chlorophyll-*a* concentration (Chl-*a*) in µg C L^{-1} obtained by HPLC and the carbon : chlorophyll-*a* ratio (C:Chl-*a* ratio) for all stations and depths.

Station	Depth	PPC (µg C L^{-1})	Chl-*a* (µg C L^{-1})	C:Chl ratio
209	2	5.475	0.232	24
209	14	7.609	0.097	79
212	2	4.163	0.121	34
212	25	2.041	0.049	42
218	2	7.929	0.22	36
218	20	3.867	0.203	19
222	2	6.610	0.335	20
222	25	3.432	0.174	20
227	2	4.983	0.185	27
227	25	3.8	0.138	28
230	2	2.071	0.066	31
230	35	1.829	0.165	11
235	2	0.832	0.042	20
235	52	2.004	0.121	17
239	2	1.989	0.078	26
239	29	1.154	0.053	22
245	2	1.692	0.086	20
245	18	1.825	0.046	40
250	2	5.658	0.188	30
250	24	2.291	0.07	33

3.5.2 HPLC and light microscopy

In order to compare the biomass obtained by HPLC (µg chl-*a* L^{-1}) and light microscopy (µg C L^{-1}), the biomass of autotrophic flagellates, autotrophic dinoflagellates and diatoms found by the two methods was summarized in a table (Table 10). HPLC biomass (in µg chl-*a* L^{-1}) was converted to µg C L^{-1} by multiplying the biomass of flagellates by 40 and biomass of dinoflagellates by 60 (see Chapter 2), of which flagellates comprised the algal divisions prasinophyceae / chlorophyceae, euglenoceae, cryptophyteae, haptophyteae and pelagophyteae. After converting, the biomass obtained by HPLC and obtained by light microscopy were plotted in the same graph (Figure 28). The biomass found by the aid of HPLC was generally higher than the biomass found by means of light microscopy. For example, the biomass of flagellates found by means of HPLC was twice as much as flagellates biomass found by means of light microscopy at half of the stations. The biomass of dinoflagellates found by both methods showed the highest deviation between both methods. In a substantial amount of stations no dinoflagellates were found by the HPLC, while those were indeed identified by means of light microscopy. Despite this difference, two patterns are comparable: (1) an increasing biomass when navigating from the stations characterized by Adw to the stations influenced by MwI and a decreasing biomass when navigating from these stations to the stations characterized by Pdw and MwII and (2) the contribution of diatoms to biomass seemed more important in the Adw and the MwI than in the other water masses and this biomass seemed to decrease when navigating from the Adw, via the MwI to the Pdw (Figures 28 and 29).

Table 10: Biomass (µg C L^{-1}) of flagellates (F.), dinoflagellates (Dino.) and diatoms (Dia.) identified by HPLC and light microscopy for the stations at 2 m deep (– s) and at the depth of the fluorescence maximum (– d).

Station	HPLC F.	Micro F.	HPLC Dino.	Micro Dino.	HPLC Dia.	Micro Dia.	Total HPLC
209_s	4.05	1.20	0.00	4.03	5.22	0.24	9.27
209_d	1.72	0.32	0.00	1.34	2.15	0.19	3.87
212_s	3.06	1.30	0.00	6.12	1.79	0.57	4.85
212_d	1.31	0.56	0.00	1.02	0.64	1.04	1.95
218_s	4.02	0.66	0.00	2.93	4.77	1.47	8.79
218_d	2.76	0.57	0.00	0.20	5.34	0.35	8.1
222_s	7.91	0.45	0.00	0.56	5.51	0.73	13.42
222_d	2.94	1.30	0.00	0,51	4.02	0.03	6.96
227_s	5.02	3.74	0.57	2.19	1.99	0.27	7.58
227_d	2.39	0.82	0.00	0.77	3.11	0.15	5.5
230_s	2.16	2.35	0.56	1.16	0.09	0.37	2.81
230_d	5.48	0.62	0.00	0.35	1.11	0.21	6.59
235_s	1.10	2.19	0.00	3.69	0.57	0.06	1.67
235_d	4.80	0.78	0.00	0.54	0.02	0.19	4.82
239-s	2.65	1.57	0.66	1.82	0.01	0.16	3.32
239_d	0.78	1.09	0.01	0.62	1.34	0.19	2.13
245_s	2.47	2.55	0.00	2.07	0.98	0.15	3.45
245_d	1.14	2.07	0.00	1.72	0.69	0.07	1.83
250_s	6.76	1.13	1.16	2.26	0.00	0.49	7.92
250_d	1.55	1.05	0.00	0.25	1.23	0.51	2.78

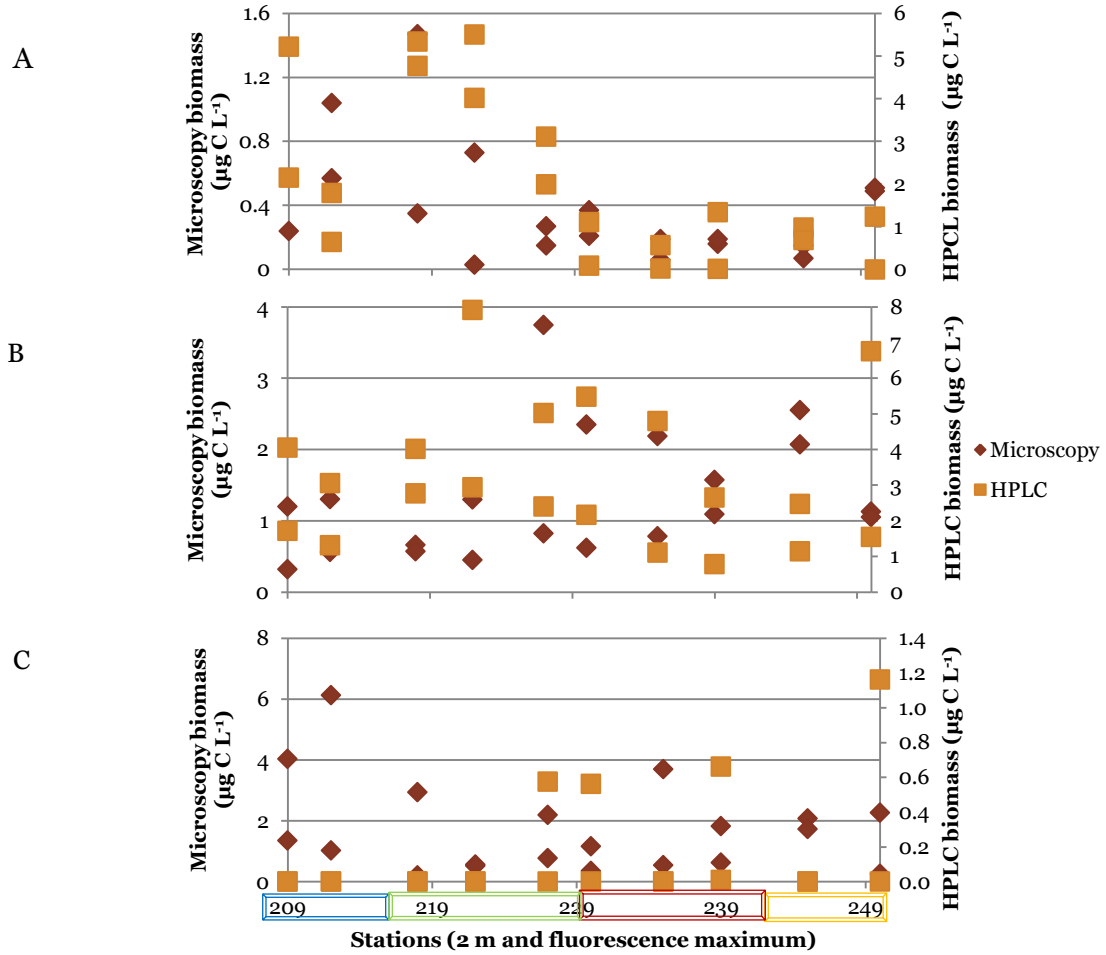

Figure 28: Microscopy biomass (µg C L^{-1}) and HPLC biomass (µg C L^{-1}) plotted for all stations for diatoms (A), autotrophic Flagellates (B) and autotrophic dinoflagellates (C) for different water masses: Blue boxes: Adw, Green boxes: MwI, Brown boxes: Pdw, Orange boxes: MwII.

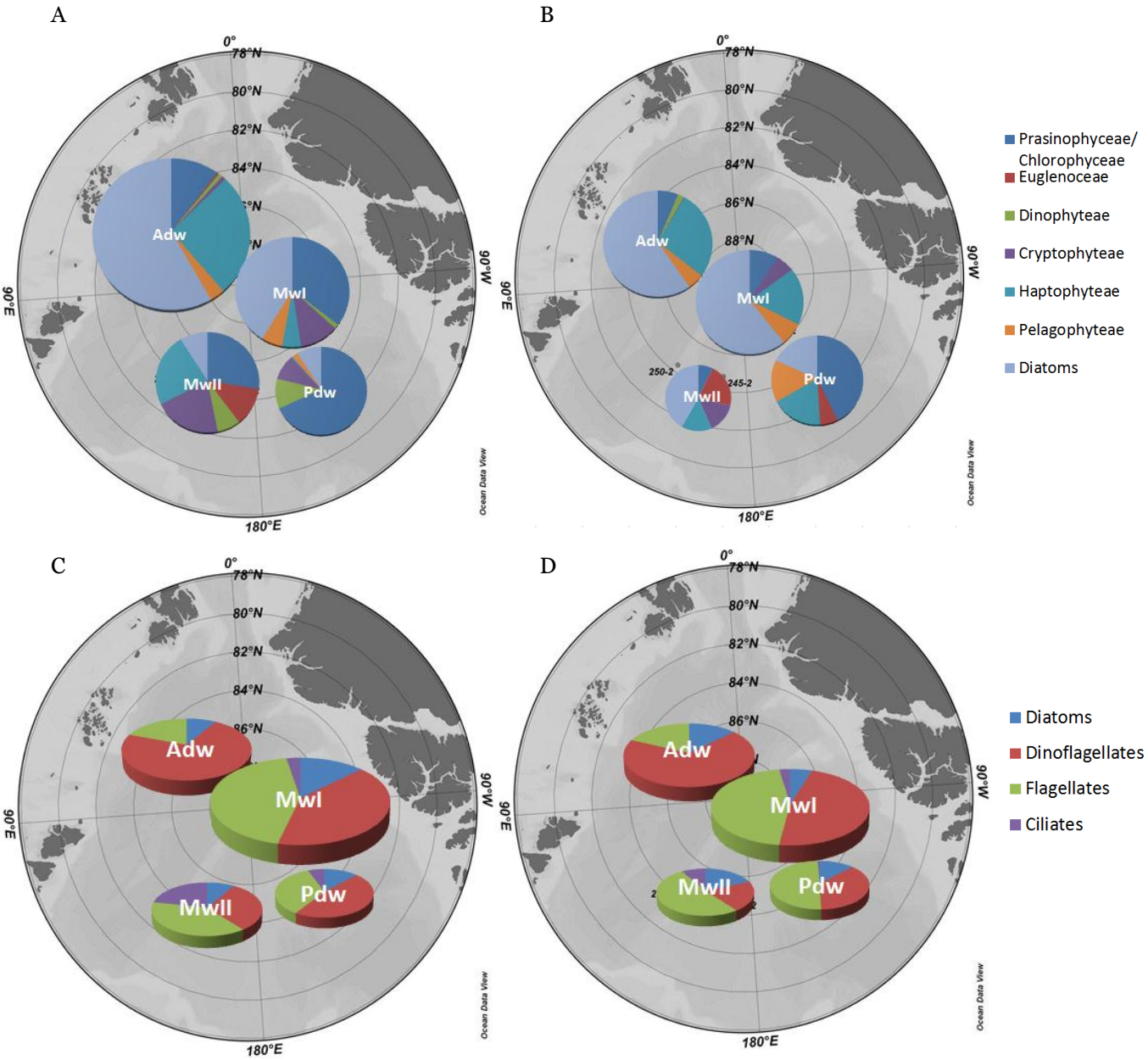

Figure 29: Relative importance of the algal divisions to biomass (in µg chl-*a* L^{-1}) found at the different water masses by means of HPLC for the surface (A) and the depth of the fluorescence maximum (B). And the relative importance of the algal divisions to biomass (in µg C L^{-1}) as found by means of light microscopy for the surface (C) and the depth of the fluorescence maximum (D). The size of the pies represent the schematically representation of the amount of biomass found at a certain water mass. All figures indicate the autotrophic biomass. Please note that station 203 is NOT included the microscopy biomass.

3.5.3 Light microscopy and flow cytometry

To compare the biomass obtained by light microscopy and by flow cytometry, the biomass of nanoplankton obtained by the two methods is plotted in one graph (Figure 30). The relationship between flow cytometry obtained biomass and the biomass obtained by light microscopy seemed to be linear. A simple linear regression showed that this relationship was significant ($p < 0.001$) with a R^2 of 68%.

The regression equation for this relationship is the following:

$$Nanoplankton\ biomass\ flow\ cytometry = -0.642 + 2.3 * nanoplankton\ biomass\ microscopy \quad [9]$$

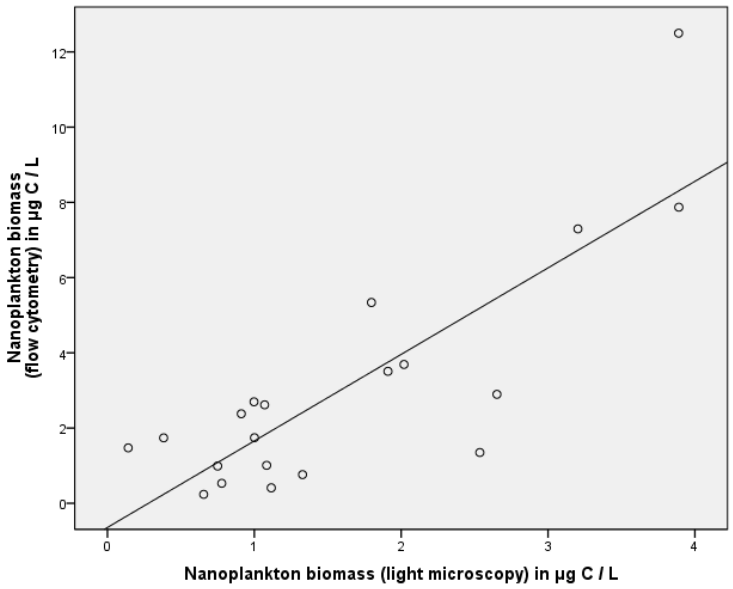

Figure 30: Nanoplankton biomass obtained by Flow Cytometry (in µg C L^{-1}) plotted against the nanoplankton biomass obtained by Light Microscopy (µg C L^{-1}).

The significant relationship between the nanoplankton data of flow cytometry and light microscopy, enables combining both datasets to obtain a more realistic impression of the phytoplankton biomass (Figure 31 A and B). For this combination, the biomass of picoplankton and nanoplankton are obtained from the flow cytometry dataset and biomass of microplankton of the microscopy dataset. As such, total phytoplankton biomass ranged between 1 – 18 µg C L^{-1}.

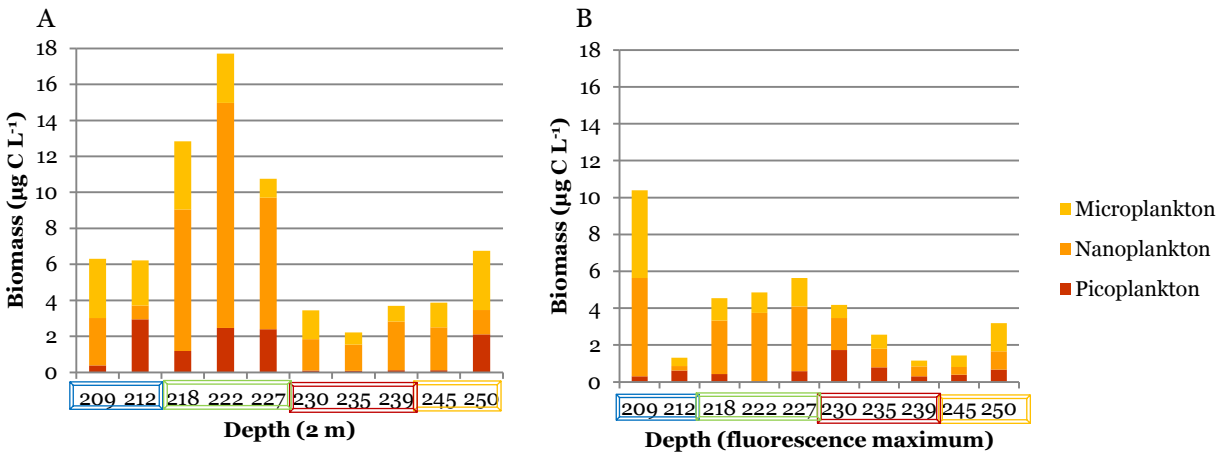

Figure 31: Biomass of picoplankton (flow cytometry), nanoplankton and microplankton (both light microscopy) for the surface waters (A) and the depth of the fluorescence maximum (B) for the different water masses: Blue boxes: Adw, Green boxes: MwI, Brown boxes: Pdw, Orange boxes: MwII.

Biomass of nanoplankton could be separated into small nanoplankton (about < 5 μm) and big nanoplankton (between about 5 – 20 μm). The biomass of the small nanoplankton comprised for 55% of small nanoplankton and for 45% of big nanoplankton.

Total phytoplankton biomass was higher at the surface than in the deeper water. Generally, picoplankton biomass was only of minor importance in contributing to total phytoplankton biomass except on the station 212 (at the surface) and station 230 (in the deeper water). Picoplankton biomass was negligible at the Pdw stations and station 245 (at the surface) and station 222 (deeper waters). In general, nanoplankton contributed most to phytoplankton biomass especially in the MwI and the Pdw.

4. Discussion

4.1 Methodological considerations

In this thesis, the phytoplankton community of the central Arctic Ocean by summer 2011 has been investigated by means of three methods: High Pressure Liquid Chromatography (HPLC), inverted light microscopy and flow cytometry. Although the three methods indicated the same pattern and the data of the different methods can be combined to a certain extent, a substantially between-method variability occurred. Therefore, it was needed to consider strengths and weaknesses of all methods to indicate which data is best applicable to address the research questions of this thesis and to discuss the results.

4.1.1 Flow cytometry and light microscopy

Total phytoplankton abundance obtained by flow cytometry was considerably higher than the total phytoplankton abundance obtained with the aid of the light microscope (Figure 20 and 25). The difference was the biggest in the picoplankton fraction, since it was impossible to recognize picoplankton sized cells at all by means of the microscope. The flow cytometry gave a more reliable estimation of the picoplankton fraction of the phytoplankton community. Because picoplankton abundance was much higher than nanoplankton abundance at all stations, the between-method difference was considerable. On the other hand, due to the set-up of the flow cytometer, it was impossible to measure microplankton cells > 20 µm. The nanoplankton biomass obtained by flow cytometry differed also considerably from the nanoplankton biomass obtained with the microscope. The biomass obtained by flow cytometry[1] was 0.2 – 12 µg C L^{-1} and comprised only autotrophic organisms. Biomass obtained by light microscopy however was 2 – 7.4 µg C L^{-1} and comprised of both autotrophic and heterotrophic organisms. The decision to consider 50% of the unidentified nanoplankton as being heterotrophic, increased the difference and resulted in the fact that the nanoplankton biomass obtained by the flow cytometer could be about two times more than the nanoplankton biomass obtained with the aid of light microscopy (Figure 30). Also without this decision, the flow cytometry nanoplankton biomass could be substantially higher than the biomass of the microscope (Figure 20 and 25), most likely caused by the state of the samples. The flow cytometer processed life organisms and measured their real biological properties. By doing so it gave a realistic estimate of both abundance and biomass (Marie et al. 2005). The samples processed with the microscope were formalin preserved. This preservation might induce shrinking of cells, might increase the clustering of cells, and might increase the loss of cells after some time when the samples are stored in liquid. This leads to underestimations of abundance and biomass (as reviewed by Lovejoy et al. (2002)). Microplankton biomass however, was overestimated at the Pdw and the MwII since it was impossible to count the 400 cells per microscopy sample as recommended by Edler (1979).

The nanoplankton biomass obtained by flow cytometry might be biased by the fact that cell volume was calculated based on the geometric shapes sphere (small nanoplankton) and cone (big nanoplankton). It is unlikely that this bias resulted in an overestimation of nanoplankton biomass by flow cytometry. The amount of under- or overestimation by choosing the inappropriate shapes is determined by the species dominating in the samples (Hillebrand et al. 1999).

[1] For the purpose of the comparison, the biomass estimate does not included the biomass of station 203 since no microscopy data for this stations was available.

Regarding the microscopy samples, the geometric shape prolate spheroid seemed more appropriate for the bigger nanoplankton, but the decision to take the formula for the cone would result in an underestimation. This possible underestimation can to a certain extend be compensated when cone or prolate spheroid shaped organisms passed the beam in their length instead of their width. Applying the sphere formula on their length would then result in an overestimation.

4.1.2 Light microscopy and HPLC

Unless the negative implication of formalin on the organisms, working with the microscope is of pivotal importance to determine the taxonomic diversity in the samples because the flow cytometry did not indicate any taxonomic diversity. Although the data of the HPLC in combination with the output of CHEMTAX also gave an insight in the taxonomic diversity, reliable observations of the taxonomic diversity can only be obtained with the help of the microscope (Irigoien et al. 2004). In order to define the algal divisions present with the help of CHEMTAX, input ratios for the different pigments were needed. The pigment peridinin is for example associated with dinoflagellates and the pigment fucoxanthin with diatoms (Irigoien et al. 2004). Problems arise in cases when dinoflagellates contain fucoxanthin instead of peridinin (Dr Peeken, personal communication). As such, a dinoflagellate bloom can become identified as a diatom bloom (Irigoien et al. 2004, Llewellyn et al. 2005).

Also in this thesis, the HPLC and CHEMTAX data indicated diatom biomass instead of dinoflagellate biomass as indicated by light microscopy in Adw and MwI (Figure 29). It is very well possible that the amount of diatoms have been overestimated by the HPLC and CHEMTAX by assigning too much fucoxanthin to diatoms. A complicating factor, is the decision to consider 50% of the unidentified dinoflagellates as being autotrophic. It is also possible that heterotrophic dinoflagellates dominated in the Adw and MwI and that therefore autotrophic dinoflagellates are overestimated, leading to a dominance of dinoflagellates instead of diatoms. Despite those contradictions, HPLC and CHEMTAX data indicated the dominance of flagellates and dinoflagellates (65%) and to a less extend diatoms (35%). The same pattern was found by microscopy: 85% and 11% respectively.

Although difficulties might arise in determining the algal divisions present in the samples, HPLC (in combination with CHEMTAX) is an accepted method in quantifying phytoplankton communities (e.g. (Havskum et al. 2004)) and has been used earlier for describing Arctic phytoplankton communities (e.g. Min Joo et al. (2011)). Furthermore, the method is fast, the HPLC data provides reliable estimates of concentrations of chlorophyll-*a* and degradation products of chlorophyll-*a*. This since the samples were shock frozen with liquid nitrogen and therefore did not show the disadvantages formalin had on the microscopy samples.

4.1.3 HPLC and flow cytometry

The biomass data of the HPLC and CHEMTAX is expressed in chlorophyll-*a* instead of phytoplankton carbon. It is complicated to transform the chlorophyll-*a* data to carbon based biomass data. In this thesis, the transformation is conducted to multiplying chlorophyll-*a* biomass of all phytoplankton except dinoflagellates by 40 and by multiplying the chlorophyll-*a* biomass of dinoflagellates by 60. This transformation was applied to determine the C:Chl-*a* ratios for the samples.

Although the ratios seemed reliable (the average C:Chl-*a* ratio was 29, while Booth & Horner (1997) found an average of 26 and Sherr et al. (2003) found a ratio of 31 in the Canadian Basin), the biomass data obtained by flow cytometry (for picoplankton and nanoplankton) and light microscopy (for microplankton) will be used. Also, because picoplankton biomass is underestimated by the HPLC since the pigment concentrations of these small cells are so small that the detection limit is reached (Llewellyn et al. 2005).

4.1.4 Decisions

Considering the strengths and weaknesses of all methods, the fact that all methods gave the same patterns and that the methods are able to compensate each other when a method is weak (see paragraph 3.5), the following decisions have been made to address the research questions and to discuss the results:

- Total phytoplankton abundance and biomass will be obtained by combining the data of the flow cytometry and the light microscopy;
- The biomass of picoplankton and nanoplankton will be obtained from the flow cytometer and the microplankton biomass will be obtained of the light microscopy data;
- Chlorophyll-*a* data will be obtained from the HPLC.
- The taxonomic diversity of the flagellates will be obtained by the HPLC data;
- The contribution of diatoms and dinoflagellates to total biomass of all water masses will be obtained from both HPLC and light microscopy, taking into account that both the HPLC biomass of diatoms and the microscopy biomass of dinoflagellates are overestimations. More information concerning the environmental variables is needed to formulate a solution.

4.2 Phytoplankton abundance and biomass of the whole size spectrum

The central Arctic Ocean is considered as being an oligotrophic and low productivity and biomass ocean (Wheeler et al. 1996, Fahl & Nöthig 2007). It was therefore not surprising to find a phytoplankton biomass of 1 – 18 µg C L^{-1} by the summer of 2011. A biomass close to values of 5 – 10 mg C m^{-3} characteristic for oligotrophic regions of the Atlantic Ocean (Maranon et al. 2000). The observed biomass of 1 – 18 µg C L^{-1} was also close to the values of 2 – 10 µg C L^{-1} of the central Arctic Ocean by summer of 1994 (Booth & Horner 1997), when two stations with extreme diatom biomass were ignored. An average picophytoplankton biomass of 2.6 µg C L^{-1} was also not incorporated in this value. The sampling period conducted by Booth & Horner (1997), the average sea ice cover, and nutrient concentrations where comparable with those in this thesis. In determining the phytoplankton biomass, Booth & Horner (1997) compensated for the negative effects of preservation. Taking all these elements into consideration, one might conclude that the phytoplankton biomass by the summer of 2011 was higher than by the summer of 1994. One might even hypothesize that the biomass of the central Arctic Ocean is increasing, although annual variability exists. The before mentioned biomass values as found in this thesis did not include the surface biomass > 40 µg C L^{-1} of station 203 in the Nansen Basin. This value was unusually high in comparison with the biomass found at all other stations and corresponded to average phytoplankton biomass values of 20 – 60 µg C L^{-1} of temperate Atlantic Ocean waters (Maranon et al. 2000). The values found corresponded however also to findings of Booth & Horner (1997). They found a phytoplankton biomass of 30 µg C L^{-1} in the Nansen Basin, mainly comprising of diatoms.

Also the low phytoplankton biomass of station 212 on the Nansen-Gakkel Ridge was in accordance to the findings of Booth & Horner (1997).

The phytoplankton growing season is very short in the Arctic Ocean and decreases with increasing latitude. The presence of sea ice has an important influence of the light availability under the ice and is able to hamper primary production. As such, light availability in combination with the thickness and extent of the sea ice cover are important limiting factors for the central Arctic Ocean phytoplankton community (Horner & Schrader 1982, Cota et al. 1996).

The results of this thesis emphasised the importance of the sea ice cover in constraining the phytoplankton community of the central Arctic Ocean in summer 2011. In this study, the highest phytoplankton biomass values were associated with the lowest ice cover, and vice versa. This inverse relationship became apparent from regression analysis in two out of three methods, in spite of the narrow range of sea ice cover (80 – 100 %). This relationship has been reviewed by Sakshaug (2004) and Tremblay et al. (2009). They argued that light determines when phytoplankton starts to growth and how much energy can be obtained for primary production. Once there is enough light for net growth, the ability of cells to harvest this light efficiently determines whether phytoplankton biomass increases or not (Sakshaug 2004, Tremblay & Gagnon 2009). This ability is influenced by the physiological state of the cells and possibly by temperature (Tremblay et al. 2006). In the case of this thesis, a decrease is sea ice cover resulted in an increase of phytoplankton biomass. This pattern is also known from the ice edge regions (e.g. (Perrette et al. 2010)). Since photoacclimation is not likely to occur in combination with the cold waters of the central Arctic Ocean (Sakshaug & Slagstad 1991) clear linear relationships have been indicated between sea ice cover and primary production, at least in coastal regions (e.g. (Rysgaard et al. 1999, Tremblay & Gagnon 2009)). This linear relationship diminishes when nutrients become depleted. Tremblay & Gagnon (2009) showed that variability in production is caused by nutrient supply rather than light availability.

Sea ice is not only important in determining the circumstances in the water column, but also seeds the water column with pennate diatoms and flagellates during ice melting processes to a certain extend (Gradinger et al. 1999). The diatoms found in this thesis were a mixture of planktonic taxa, for example *Chaetoceros* spp. and sea ice taxa, for example *Nitzschia* spp. / *Pseudonitzschia* spp. The sea ice taxa contributed mostly to diatom biomass and almost all empty diatom cells were sea ice-associated pennate diatoms, which indicates a seeding of sea ice taxa from sea ice to the water column. The full and alive diatoms contributed only minimal to phytoplankton biomass in the central Arctic Ocean.

Nutrients in combination with vertical stratification are thus important in constraining the phytoplankton community of the central Arctic Ocean. Vertical stratification is tightly coupled to the sea ice cover: sea ice melt freshens the waters in spring and summer and freezing increases salinity in winter (Carmack 2007). The amount of vertical stratification determines the amount of nutrients that are exported from below the euphotic zone to the surface waters. A strong stratification prevents replenishment of nutrients from below the euphotic zone (Springer & McRoy 1993, Tremblay & Gagnon 2009). Stratified waters can be characterized by regenerative production since no input of nutrients from below the euphotic zone occurs. In these systems biomass exists mainly of phytoplankton cells < 5 µm, mainly flagellates, and these systems are characterized by low phytoplankton biomass and production.

Less stratified waters, characterized by new production and thus the input of nutrients from below the euphotic zone, show a higher production and biomass and are characterized by bigger phytoplankton, mainly diatoms (Damm et al. 2010, Ardyna et al. 2011). Due to its oligotrophic and stratified character, the central Arctic Ocean is considered as being an flagellate based ecosystem (Booth & Horner 1997, Ardyna et al. 2011) as also the oligotrophic regions of the Atlantic Ocean are flagellate based ecosystems (Maranon et al. 2000). Also Sherr et al. (2003) found that phytoflagellates were the most important component of phytoplankton biomass. Diatoms contributed substantially in spring (Sherr et al. 2003). This thesis indicated that the contribution of both flagellates and dinoflagellates together was substantially more important than the contribution of diatoms, although geographical differences occurred and uncertainty exists (see paragraph 4.3). Furthermore, nanoplankton < 5 µm contributed more to phytoplankton biomass than nanoplankton between 5 – 20 µm.

Booth & Horner (1997) indicated that also autotrophic picoplankton < 2 µm could contribute substantially to phytoplankton biomass in the central Arctic Ocean in summer 1994, on average 2.6 µg C L^{-1} or 36%. In summer 2011, autotrophic picoplankton dominated at all stations in terms of abundance, but the average contribution to biomass was only on average 1 µg C L^{-1} or 28%. Autotrophic nanoplankton (and in some cases autotrophic microplankton) contributed mostly to phytoplankton biomass at almost all stations. As such, the before mentioned increase in phytoplankton biomass seemed to be caused by an increase in biomass of nanoplankton and microplankton. This thesis indicated a flagellate based ecosystem, characterized by the dominance of flagellates in terms of abundance and the dominance of flagellates and dinoflagellates together in terms of biomass. In accordance to Sakshaug (2004), the flagellates found at the central Arctic Ocean consisted of prasinophyceae / chlorophyceae, euglenoceae, cryptophyteae, haptophyteae, pelagophyteae (all indicated by HPLC) and chrysophytes (found in the microscopy samples). No cyanobacteria were found during this research.

4.3 Geographical patterns of phytoplankton distribution

The results of this thesis showed that the phytoplankton community differed substantially between water masses. This difference correlated with dissimilarities in biomass: from moderately to high biomass in the Adw and the MwI and lower biomass in the Pdw and the MwII. The high biomass at the Adw and MwI can be explained by a relatively low ice cover of 80% in combination with relatively high concentration of NO_2 and NO_3 in comparison with the Pdw and the MwII. The MwI was furthermore characterized by relatively high concentrations of PO_4 and Si. The Adw and to a certain extend the MwI were characterized with relatively cold waters compared to the MwII and especially the Pdw. Station 203 in the Adw might be influenced the most compared all other stations of the Adw by the inflow of Atlantic water from the Fram Strait (Rudels 2011), which might explain the high biomass found at this station. This Atlantic water did not only contain high nitrate concentrations which seem to increase Arctic phytoplankton biomass (Margalef 1978), but these waters might also contain phytoplankton organisms originating from the Fram Strait that as such increased the biomass. The low biomass of station 212 might indicate that the influence of the Fram Strait in case of the organisms was already negligible. The high phytoplankton biomass at the MwI might be caused by the high nutrient concentrations of nitrate, phosphate and silicate, in combination with a low ice cover.

As such, it might be concluded that the nitrate concentrations indicate a Atlantic water influence, but that the high phosphate concentrations show a clear Pacific water influence. This was also found by Jones (2001) which argued that the surface waters in the area of the North Pole originate mainly from the Pacific Ocean and the Chukchi Sea. As such, it is very well possible that the influence of the Pacific waters is not only restricted to the Canada Basin, but that these waters are restricted to the part of the central Arctic Ocean west of the 180° longitude (Damm et al. 2010).

This would indicate that the MwII can be considered as Adw. The low biomass at those stations might be caused by the fact that the available nutrient concentrations are consumed to a certain extent on its journey to these stations via the basin and the shelf areas in that regions (Grahl et al. 1991, Tremblay & Gagnon 2009, Cai et al. 2010). Although warmer water should have a positive influence on the metabolic rate of phytoplankton (Behrenfeld 2011), an opposite relationship between phytoplankton biomass and water temperature was found: the lower the temperature of the surface waters, the higher the phytoplankton biomass. This relationship was caused by a significant correlation of microplankton biomass with water temperature. In autotrophic nanoplankton and picoplankton, this relationship was not found. The cold waters of the Adw and the MwI might thus have influenced the phytoplankton biomass at these stations positively. However, the Pdw and the MwII to a certain extend seemed to be more stratified than the Adw and the MwI, due to a layer of warm water on top of the water column. Both waters are more nutrient depleted, which became visible in the deep maxima of both fluorescence and chlorophyll-*a* that could be observed in both water masses. Especially the phytoplankton community of station 230 and 235 in the Pdw had to survive in the deeper waters of the water column in order to obtain enough nutrients. The strong stratification at the Pdw and MwII caused a lower phytoplankton abundance and biomass and therefore phytoplankton biomass correlated with the relatively low temperatures of the Adw and MwI. As such, one might hypothesize that temperature in this case is a proxy for other patterns, like stratification in combination with nutrient availability, and not the reason for the high biomass of the Adw and MwI.

Until now, one other study has been conducted after the phytoplankton biomass of the central Arctic Ocean in relation to different water masses. This study is conducted by Damm et al. (2010) in September 2007. Two water masses were distinguished: Atlantic derived waters (comparable with Adw, MwI and MwII) and Pacific derived waters (comparable with Pdw). Although chlorophyll-*a* concentrations are no good indicator for phytoplankton biomass (Sakshaug 2004), chlorophyll-*a* concentrations were substantially higher in Atlantic derived water than in Pacific derived water. Damm et al. (2010) found concentrations of 0.19 – 0.48 µg L^{-1} and 0.06 – 0.22 µg L^{-1} respectively in the upper 10 m of the water column. The values found for the Pacific derived water were in accordance with the values found in this thesis for the Pdw, which was 0.04 – 0.09 µg L^{-1}, although chlorophyll-*a* concentrations in the deep Pdw could increase to 0.16 µg L^{-1}. Damm et al. (2010) concluded that the Pacific derived water is an area of regenerated production with low biomass and production, dominated by nanoplankton sized flagellates. The chlorophyll-*a* concentrations found in this thesis for the Adw/MwI/MwII, which are comparable with the Atlantic derived waters, are substantially higher than found by Damm et al. (2010). The chlorophyll-*a* concentrations were 0.06 – 1.29 µg L^{-1} and mainly influenced by the high chlorophyll-*a* concentration at station 203 in the Nansen Basin. Damm et al. (2010) concluded that the Atlantic derived water was an area of new production dominated by diatoms.

The results of this thesis indicated that the contribution of diatoms is more important in the Adw and the MwI and less important in the Pdw and the MwII. But diatoms did not dominate in terms of production, although the exact contribution is uncertain. In the MwI for example, Si concentrations increased with depth so it might be that diatoms indeed contributed substantially to total phytoplankton biomass as indicated by HPLC. In the Adw of summer 2011 it is more likely that flagellates and dinoflagellates were more important than diatoms as indicated by the light microscope since Si concentrations in the water column were low. Considering the microscopy samples, it is still reasonable to consider 50% of the unidentified dinoflagellates as being autotrophic. Also, Olli et al. (2007) found that about 50% of the unicellular plankton found in the Eurasian Basin was autotrophic. The high biomass of dinoflagellates as indicated by figure 29 in the Adw was possible too high, but diatoms seemed not to dominate. The difference might be caused by the fact that Damm et al. (2010) only counted easy identifiable cells, such as diatoms.

Other research focused on different regions of the central Arctic Ocean. Olli et al. (2007) investigated for example the biomass of unicellular plankton in the Eurasian Basin, which was comparable to the Adw. In accordance to the results of my thesis and the results of Booth & Horner (1997), small flagellates and dinoflagellates dominated in the Eurasian Basin in summer 2001. The contribution of diatoms was less important. As such, the phytoplankton community of summer 1997, summer 2001 and summer 2011 was significantly different from the blooms of diatoms or *Phaeocystis* sp. as known for the Barents Sea (Olli et al. 2002, Ratkova & Wassmann 2002), other Arctic shelves (Sakshaug 2004), polynyas (Lovejoy et al. 2002), coastal waters of Western Greenland (Nielsen & Hansen 1999) and coastal waters of Western Svalbard (Lasternas & Agustá 2010). No picoplankton sized cyanobacteria were found by the summer of 2001 (Olli et al. 2007), as also no cyanobacteria were observed in this thesis, not only in the Adw but nowhere in the central Arctic Ocean. This is in accordance to findings of for example Sherr et al. (2003). The importance of *Phaeocystis* sp. has not been investigated in this thesis, since it was not possible to distinguish this taxa properly.

Min Joo et al. (2011) investigated the phytoplankton composition of the Western Arctic Ocean of summer 2007, which was more or less comparable with the Pdw of this thesis. The Western Arctic Ocean phytoplankton composition of summer 2007 was characterized by the importance of both picoplankton and nanoplankton in terms of abundance, consisting of dinoflagellates and flagellates (Min Joo et al. 2011). This corresponds to the findings in this thesis. The microplankton found by Min Joo et al. (2011) however, comprised mainly of diatoms and therefore differed with the results of this thesis. This might be caused by the fact that Min Joo et al. (2011) sampled the Canada Basin, but closer to the Bering Strait than the location of the sample locations of this thesis. The average ice cover could be substantially smaller, influencing the phytoplankton composition.

4.4 Outlook: central Arctic Ocean phytoplankton under change?

Phytoplankton biomass is the basis of central Arctic Ocean marine ecosystem and is responsible for an autotrophic production of 50 x 106 t C y^{-1} (Sakshaug 2004) . Sea ice algae are responsible for a substantially amount of this primary production (Gosselin et al. 1997). The sea ice, but also the ice water interface are important habitats for central Arctic Ocean algae (Horner et al. 1992, Melnikov 1997, Melnikov et al. 2002, Gradinger 2009). Investigation of the biomass of ice algae at some of the stations of this thesis revealed that algal biomass in multiyear sea ice was substantially higher than the phytoplankton biomass found in the water column (Hänselmann, unpublished data). Other habitats are melt ponds (e.g. (Lee et al. 2012)) and the water column (e.g. Booth & Horner (1997)). Ice algae are important food sources for amphipods, while phytoplankton is an important food source for zooplankton. Both amphipods and zooplankton are an important food source for the Arctic Cod *Boreaogadhus saida,* which in their turn serve as a food source for seals and polar bears. The Arctic Cod is responsible for transferring 75% of the energy in the food web to higher trophic levels (Sakshaug & Slagstad 1991, Welch 1992, Gradinger & Bluhm 2004). Due to the restricted growing season, the food web is highly developed and phytoplankton is effectively grazed down by zooplankton and heterotrophic protists (Grahl et al. 1991, Sherr et al. 2003).

The multiyear sea ice cover is an important feature of the central Arctic Ocean and the previous paragraphs already stated the importance of this sea ice cover in constraining the phytoplankton community. Currently, the multiyear sea ice cover on the central Arctic Ocean is decreasing, both in thickness and extend (Stroeve et al. 2007, Comiso et al. 2008, Kwok et al. 2009). The consequences for the phytoplankton community is subject of high speculation: the melting processes will for example probably lead to an increasing input of fresh water, especially in the Canada Basin (Rabe et al. 2010, Rudels 2011) and will as such enhance the stratification of the water column and reducing phytoplankton growth (McPhee et al. 2009, Yamamoto-Kawai et al. 2009). On the other hand, a decreasing ice cover will increase the available light in the water column, and is therefore expected to enhance phytoplankton growth (Olli et al. 2007). The ice edge and the marginal sea ice zone are expected to shift north wards resulting in phytoplankton blooms in areas where blooms were not visible before and phytoplankton is expected to start growing earlier in the season (Wassmann 2011). A decreasing ice cover might also increase the wind induced mixing of the water column, which might party undo the stratification of the water column. This process might lead to the release of some of the nutrient concentrations stored in the deeper layers of the central Arctic Ocean (Zhang et al. 2004).

Another important consequence of climate change is the expectation that the temperature of waters of the central Arctic Ocean will increase (Polyakov et al. 2005, McLaughlin et al. 2009). It is speculated that this warming might increase metabolic activities within phytoplankton resulting in an increase in phytoplankton biomass (Behrenfeld 2011). The results of this thesis however, seemed to show that the water temperature was not the reason for a high biomass, but a proxy of other patterns like stratification and nutrient availability. This is an important finding since climate induce changes are expected to increase the water temperature of the central Arctic Ocean. The results of this thesis indicated that this will probably not influence the community directly, but indirectly by influencing stratification and water circulation.

Another consequence of a warming Arctic Ocean might be the migration of temperature species further to the North, changing the food source for grazers, a food source which certainly will change since the habitat of sea ice algae is disappearing. Although phytoplankton did not became identified until species level, Northwards migrating coccolithophores (Hegseth & Sundfjord 2008) seemed not to occur in the samples.

The different regions will probably respond differently to the changes. The Pdw and MwII are already relatively warm and a reduced ice cover might probably not induce phytoplankton growth because nutrients are limiting (unless an increase in storm events will decrease the stratification). The Adw and MwI are now relatively cold. A decreasing ice cover leads probably to an increasing biomass early in the season because nutrients seem not to limit immediately. But, warmer waters will increase the stratification in these regions which might decrease nutrient concentrations and as such may hamper the increase in biomass. As such, an increase in the during of the growing season due to a decrease in sea ice cover, does not automatically have to result in an increase in phytoplankton biomass, because of the strong stratification and the low replenishment of nutrients. Also an earlier start of the growing season is unlikely to increase the average annual phytoplankton biomass due to the low nutrient concentrations, unless zooplankton is not able to adapt to the change in timing of phytoplankton growth. Since grazing pressure is currently very high and effective, a mismatch with the phytoplankton growing season might be of great influence.

Due to the expected stronger stratification, the size spectrum of phytoplankton is probably also going to change. Li et al. (2009) found a decreasing abundance of nanoplankton and an increasing abundance of picoplankton due to an increase in stratification and a decrease of nitrate concentrations in the Arctic Ocean. As such, it was expected to find a contribution of picoplankton to biomass in summer 2011 which was higher than the contribution of picoplankton as find by Booth & Horner (1997) in summer 1994, but this was not the case. Instead of picoplankton, nanoplankton or microplankton contributed mostly to phytoplankton biomass as found in this thesis. Furthermore, biomass of picoplankton was not necessarily the most important size class in determining the total biomass of the Pdw, the most fresh and nutrient depleted region of the central Arctic Ocean in summer 2011. The results of the flow cytometer indicated moreover that the picoplankton biomass at the Pdw was significantly lower than in the Adw and MwI. This contradicted with the results of Li et al. (2009). What would cause this difference?

All in all, a lot of uncertainty exists concerning the 'real' phytoplankton composition of the central Arctic Ocean, let alone that is known what consequences climate change would possible have. This is all speculation. At this stage, the most important part would be to conduct more research to the central Arctic Ocean phytoplankton community and the importance of diatoms, picoplankton and nanoplankton, in order to increase the understanding of the marine ecosystem in general.

5. Conclusions & Recommendations

5.1 Conclusions

The central Arctic Ocean showed a phytoplankton biomass characteristic for an oligotrophic ocean. It was a flagellate and picoplankton based ecosystem in terms of abundance and a nanoplankton and flagellate/dinoflagellate based system in terms of biomass. The phytoplankton community was concentrated in the upper 50 – 60 m of the water column. This community comprised a total phytoplankton biomass between 1 and 18 µg C L^{-1}. The Adw and MwI showed a significantly higher biomass than the Pdw and the MwII. The biomass at station 203 in the Adw was unusually high: > 40 µg C L^{-1} and was not included in the before mentioned range. The phytoplankton community was especially limited by light. Sea ice, as a proxy for light availability showed to be of significant importance. The higher the sea ice cover was, the lower was the phytoplankton biomass. The phytoplankton community was also influenced by the nutrient concentrations. The MwII showed not only the highest biomass, also the highest nutrient concentrations of nitrate, phosphate and silicate, and the lowest sea ice cover. Temperature also seemed to influence the phytoplankton community and especially microplankton: the lower the temperature, the higher was the biomass. It was however hypothesized that the temperature was only a proxy for other patterns and not so much the reason for the high biomass of the Adw and MwI. But despite the low nutrients, and the warm, fresh and stratified waters of the Pdw, this water mass contained a significantly lower picoplankton biomass compared the Adw and the MwI. A lot of speculation exists about the consequences of a decreasing ice cover and an increase in warm water for the phytoplankton composition. Based on the results of this thesis it might be hypothesized that especially the phytoplankton community at the Adw and MwI will change the most.

5.2 Recommendations

Since only few studies have been conducted to the phytoplankton community of the central Arctic Ocean, more research is needed. Not only out of scientific interest in order to reach a better understanding of the marine ecosystem, but also because this region is changing. Ideally, cruises that cross the central Arctic Ocean will be repeated every year in other to start time series and create a dataset that can be used to compare future research outcomes with. Ideally, the cruises cover the whole growing season to investigate the phytoplankton community at the start of the growing season, in the course of the growing season and at the end of the growing season. At the same time, it would be interesting to add the zooplankton composition as a biological variable to the environmental and chemical variables already used to create a more complete overview of the ecosystem. Also the microbial food web should not become forgotten. Concerning the methods, I would recommend to verify which dinoflagellates could contain fucoxanthin by growing dinoflagellates in cultures when possible. It is important to know what the degree of overestimation for diatoms can be when HPLC is used. Furthermore, it would be recommended to also make use of epifluorescence microscopy, although a lot of experience is needed to apply this method. This method enables to identify phytoplankton to the species level, but can also be used to get a more precise idea of the amount of autotrophic and heterotrophic organisms is the sample. Lastly, the correlation between nanoplankton biomass of both flow cytometry and light microscopy needs to be verified every year.

References

Aagaard K, Carmack E (1989) The role of sea ice and other fresh water in the Arctic circulations. Journal of Geophysical Research 94(C10): pp. 14 485-14 498

Ardyna M, Gosselin M, Michel C, Poulin M, Tremblay JÉ (2011) Environmental forcing of phytoplankton community structure and function in the Canadian High arctic: Contrasting oligotrophic and eutrophic regions. Marine Ecology Progress Series 442: pp. 37-57

Auel H, Hagen W (2002) Mesozooplankton community structure, abundance and biomass in the central Arctic Ocean. Marine Biology 140: pp. 1013-1021

Barlow RG, Cummings DG, Gibb SW (1997) Improved resolution of mono-and divinyl chlorophylls *a* and *b* and zeaxanthin and lutein in phytoplankton extracts using reverse phase C-8 HPLC. Marine Ecology Progress Series 161: pp. 303-307

Bates NR, Mathis JT (2009) The Arctic Ocean marine carbon cycle: Evaluation of air-sea CO2 exchanges, ocean acidification impacts and potential feedbacks. Biogeosciences 6: pp. 2433-2459

Behrenfeld MJ (2011) Uncertain future for ocean algae. Nature Climate Change: pp. 33-34

Bluhm, BA, Gradinger, R, Hopcroft, RR (2011) Editorial – Arctic Ocean Diversity: Synthesis. Marine Biodiversity 41: pp. 1-4

Booth BC, Horner RA (1997) Microalgae on the Arctic ocean section, 1994: Species abundance and biomass. Deep-Sea Research Part II: Topical Studies in Oceanography 44: pp. 1607-1622

Cai P, Rutgers Van Der Loeff M, Stimac I, Nöthig EM, Lepore K, Moran SB (2010) Low export flux of particulate organic carbon in the central Arctic Ocean as revealed by 234Th: 238U disequilibrium. Journal of Geophysical Research C: Oceans 115

Carmack EC (2007) The alpha/beta ocean distinction: A perspective on freshwater fluxes, convection, nutrients and productivity in high-latitude seas. Deep-Sea Research Part II: Topical Studies in Oceanography 54: pp. 2578-2598

Comiso JC, Parkinson CL, Gersten R, Stock L (2008) Accelerated decline in the Arctic sea ice cover. Geophysical Research Letters 35

Cota GF, Pomeroy LR, Harrison WG, Jones EP, Peters F, Sheldon Jr WM, Weingartner TR (1996) Nutrients, primary production and microbial heterotrophy in the southeastern Chukchi Sea: Arctic summer nutrient depletion and heterotrophy. Marine Ecology Progress Series 135: pp. 247-258

Damm E, Helmke E, Thoms S, Schauer U, Nöthig E, Bakker K, Kiene RP (2010) Methane production in aerobic oligotrophic surface water in the central Arctic Ocean. Biogeosciences 7: pp. 1099-1108

Darnis G, Barber DG, Fortier L (2008) Sea ice and the onshore-offshore gradient in pre-winter zooplankton assemblages in southeastern Beaufort Sea. Journal of Marine Systems 74: pp. 994-1011

Darnis G, Robert D, Pomerleau C, Link H, Archambault P, Nelson RJ, Geoffroy M, Tremblay JÉ, Lovejoy C, Ferguson SH, Hunt BPV, Fortier L (2012) Current state and trends in Canadian Arctic marine ecosystems: II. Heterotrophic food web, pelagic-benthic coupling, and biodiversity. Climatic Change: pp. 1-27

Edler L (1979) Recommendations on methods for marine biological studies in the Baltic Sea. The Baltic Marine Biologists 5

Fahl K, Nöthig EM (2007) Lithogenic and biogenic particle fluxes on the Lomonosov Ridge (central Arctic Ocean) and their relevance for sediment accumulation: Vertical vs. lateral transport. Deep-Sea Research Part I: Oceanographic Research Papers 54: pp. 1256-1272

Gosselin M, Levasseur M, Wheeler PA, Horner RA, Booth BC (1997) New measurements of phytoplankton and ice algal production in the Arctic Ocean. Deep-Sea Research Part II: Topical Studies in Oceanography 44: pp. 1623-1644

Gradinger R, Friedrich C, Spindler M (1999) Abundance, biomass and composition of the sea ice biota of the Greenland Sea pack ice. Deep-Sea Research Part II: Topical Studies in Oceanography 46: pp. 1457-1472

Gradinger RR, Bluhm BA (2004) In-situ observations on the distribution and behaviour of amphipods and Arctic cod (Boreogadus saida) under the sea ice of the High Arctic Canada Basin. Polar Biology 27: pp. 595-603

Grahl C, Boetius A, Nöthig E (1991) Pelagic-benthic coupling in the Laptev Sea affected by Sea ice. In: Kassens H, Bauch HA, Dmitrenko IA, Eicken H, Hubberten H-W, Melles M, Thiede J, Timokhov LA (eds) Land-ocean systems in the Siberian Arctic: Dynamics and History. Lecture notes in Earch Science, Springer, Berlin

Hays GC, Richardson AJ, Robinson C (2005) Climate change and marine plankton. Trends in Ecology and Evolution 20: pp. 337-344

Havskum H, Schülter L, Scharek R, Berdalet E, Jacquet S (2004) Routine quantification of phytoplankton groups - Microscopy or pigment analyses? Marine Ecology Progress Series 273: pp. 31-42

Hegseth EN, Sundfjord A (2008) Intrusion and blooming of Atlantic phytoplankton species in the high Arctic. Journal of Marine Systems 74: pp. 108-119

Higgins HW, Wright SW, Schlüter L (2011) Chapter 6: Quantatative interpretation of chemotaxonic pigment data. In: Roy S, Llewellyn CA, Egeland ES, Johnsen G (eds) Phytoplankton pigments Characterization, Chemotaxonomy and Applications in Oceanography. Cambridge University Press: pp. 257-313

Hillebrand H, Dürselen CD, Kirschtel D, Pollingher U, Zohary T (1999) Biovolume calculation for pelagic and benthic microalgae. Journal of Phycology 35:pp. 403-424

Horner R, Schrader GC (1982) Relative contributions of ice algae, phytoplankton, and benthic microalgae to primary production in near shore regions of the Beaufort Sea. Arctic 45: pp. 485-503

Irigoien X, Meyer B, Harris R, Harbour D (2004) Using HPLC pigment analysis to investigate phytoplankton taxonomy: The importance of knowing your species. Helgoland Marine Research 58: pp. 77-82

Johannessen OM, Miles MW (2011) Critical vulnerabilities of marine and sea ice-based ecosystems in the high Arctic. Regional Environmental Change 11: pp. 239-248

Jones EP (2001) Circulation in the Arctic Ocean. Polar Research 20: pp. 139-146

Jones EP, Anderson LG, Swift JH (1998) Distribution of Atlantic and Pacific waters in the upper Arctic Ocean: implications for circulation. Geophysical Research Letters 25: pp. 765-768

Jones EP, Anderson LG, Wallace DWR (1991) Tracers of near-surface, halocline and deep waters in the Arctic ocean: Implications for circulation. Journal of Marine Systems 2: pp. 241-255

Kattner G, Becker H (1991) Nutrients and organic nitrogenous compounds in the marginal ice zone of the Fram Strait. Journal of Marine Systems 2: pp. 385-394

Kwok R, Cunningham GF, Wensnahan M, Rigor I, Zwally HJ, Yi D (2009) Thinning and volume loss of the Arctic Ocean sea ice cover: 2003-2008. Journal of Geophysical Research C: Oceans 114

Lasternas S, Agustá S (2010) Phytoplankton community structure during the record Arctic ice-melting of summer 2007. Polar Biology 33:pp. 1709-1717

Lee SH, Whitledge TE (2005) Primary and new production in the deep Canada Basin during summer 2002. Polar Biology 28: pp. 190-197

Lee SH, Stockwell DA, Joo HM, Son YB, Kang CK, Whitledge TE (2012) Phytoplankton production from melting ponds on Arctic sea ice. Journal of Geophysical Research C: Oceans 117: pp. 1-11

Li WKW, McLaughlin FA, Lovejoy C, Carmack EC (2009) Smallest algae thrive as the Arctic Ocean freshens. Science 326: pp. 539

Llewellyn CA, Fishwick JR, Blackford JC (2005) Phytoplankton community assemblage in the English Channel: A comparison using chlorophyll a derived from HPLC-CHEMTAX and carbon derived from microscopy cell counts. Journal of Plankton Research 27: pp. 103-119

Lovejoy C, Legendre L, Martineau MJ, Bâtcle J, Von Quillfeldt CH (2002) Distribution of phytoplankton and other protists in the North Water. Deep-Sea Research Part II: Topical Studies in Oceanography 49: pp. 5027-5047

Lovejoy C, Massana R, Pedrós-Alió C (2006) Diversity and distribution of marine microbial eukaryotes in the arctic ocean and adjacent seas. Applied and Environmental Microbiology 72: pp. 3085-3095

Mackey MD, Mackey DJ, Higgins HW, Wright SW (1996) CHEMTAX – a program for estimating class abundances from chemical markers: application to HPLC measurements of phytoplankton. Marine Ecology Progress Series 114: pp. 265-283

Maranon E, Holligan PM, Varela M, Mourino B, Bale AJ (2000) Basin-scale variability of phytoplankton biomass, production and growth in the Atlantic Ocean. Deep-Sea Research Part I: Oceanographic Research Papers 47: pp. 825-857

Margalef R (1978) Life-forms of phytoplankton as survival alternatives in an unstable environment. Oceanologica Acta: pp. 493-509

Marie D, Simon N, Vaulot D (2005) Chapter 17: Phytoplankton cell counting by flow cytometry. In: Algal cultruring Techniques. Elsevier Academic Press: pp. 253-268

McLaughlin FA, Carmack EC, Williams WJ, Zimmermann S, Shimada K, Itoh M (2009) Joint effects of boundary currents and thermohaline intrusions on the warming of Atlantic water in the Canada Basin, 1993-2007. Journal of Geophysical Research C: Oceans 114

McPhee MG, Proshutinsky A, Morison JH, Steele M, Alkire MB (2009) Rapid change in freshwater content of the Arctic Ocean. Geophysical Research Letters 36

Min Joo H, Lee SH, Won Jung S, Dahms HU, Hwan Lee J (2011) Latitudinal variation of phytoplankton communities in the western Arctic Ocean. Deep-Sea Research Part II: Topical Studies in Oceanography

Nielsen TG, Hansen BW (1999) Plankton community structure and carbon cycling on the western coast of Greenland during the stratified summer situation. I. Hydrography, phytoplankton and bacterioplankton. Aquatic Microbial Ecology 16: pp. 205-216

Olli K, Wassmann P, Reigstad M, Ratkova TN, Arashkevich E, Pasternak A, Matrai PA, Knulst J, Tranvik L, Klais R, Jacobsen A (2007) The fate of production in the central Arctic Ocean - top-down regulation by zooplankton expatriates? Progress in Oceanography 72: pp. 84-113

Olli K, Wexels Riser C, Wassmann P, Ratkova T, Arashkevich E, Pasternak A (2002) Seasonal variation in vertical flux of biogenic matter in the marginal ice zone and the central Barents Sea. Journal of Marine Systems 38: pp. 189-204

Pabi S, van Dijken GL, Arrigo KR (2008) Primary production in the Arctic Ocean, 1998-2006. Journal of Geophysical Research C: Oceans 113

Perrette M, Yool A, Quartly GD, Popova EE (2010) Near-ubiquity of ice-edge blooms in the Arctic. Biogeosciences Discussions 7: pp. 8123-8142

Polyakov IV, Beszczynska A, Carmack EC, Dmitrenko IA, Fahrbach E, Frolov IE, Gerdes R, Hansen E, Holfort J, Ivanov VV, Johnson MA, Karcher M, Kauker F, Morison J, Orvik KA, Schauer U, Simmons HL, Skagseth O, Sokolov VT, Steele M, Timokhov LA, Walsh D, Walsh JE (2005) One more step toward a warmer Arctic. Geophysical Research Letters 32: pp. 1-4

Poulin M, Daugbjerg N, Gradinger R, Ilyash L, Ratkova T, von Quillfeldt C (2011) The pan-Arctic biodiversity of marine pelagic and sea-ice unicellular eukaryotes: A first-attempt assessment. Marine Biodiversity 41: pp. 13-28

Rabe B, Karcher M, Schauer U, Toole JM, Krishfield RA, Pisarev S, Kauker F, Gerdes R, Kikuchi T (2010) An assessment of Arctic Ocean freshwater content changes from the 1990s to the 2006-2008 period. Deep-Sea Research Part I: Oceanographic Research Papers 58: pp. 173-185

Ratkova TN, Wassmann P (2002) Seasonal variation and spatial distribution of phyto- and protozooplankton in the central Barents Sea. Journal of Marine Systems 38: pp. 47-75

Rich J, Gosselin M, Sherr E, Sherr B, Kirchman DL (1997) High bacterial production, uptake and concentrations of dissolved organic matter in the Central Arctic Ocean. Deep-Sea Research Part II: Topical Studies in Oceanography 44:pp. 1645-1663

Rudels B (2011) Volume and freshwater transports through the Canadian Arctic Archipelago-Baffin Bay system. Journal of Geophysical Research C: Oceans 116

Rysgaard S, Nielsen TG, Hansen BW (1999) Seasonal variation in nutrients, pelagic primary production and grazing in a high-Arctic coastal marine ecosystem, Young Sound, Northeast Greenland. Marine Ecology Progress Series 179: pp. 13-25

Rudels B (1989) The formation of Polar Surface Water, the ice export and the exchange through the Fram Strait. Progress in Oceanography 22: pp. 205-248

Sakshaug E (1997) Biomass and productivity distributions and their variability in the Barents Sea. ICES Journal of Marine Science 54: pp. 341-350

Sakshaug E (2004) Chapter 3: Primary and Secondary production in the Arctic Seas. In: Stein R, Macdonald RW (eds) The Organic Carbon Cycle in the Arctic Ocean. Springer: pp. 37-82

Sakshaug E, Johnsen G, Kristiansen S, Quillfeldt C, Rey F, Slagstad D, Thingstad F (2009) Chapter 7: Phytoplankton and primary production. In: Sakshaug E, Johnsen G, Kovacs K (eds) Ecosystem Barents Sea. Tapir Academic Press: pp. 167-208

Sakshaug E, Slagstad D (1991) Light and productivity of phytoplankton in polar marine ecosystems: a physiological view. Polar Research 10: pp. 69-85

Schlitzer R (2011) Ocean Data View

Sherr EB, Sherr BF, Wheeler PA, Thompson K (2003) Temporal and spatial variation in stocks of autotrophic and heterotrophic microbes in the upper water column of the central Arctic Ocean. Deep-Sea Research Part I: Oceanographic Research Papers 50:pp. 557-571

Sieburth J, Smetacek V, Lenz J (1978) Pelagic ecosystem structure: heteroptrophic compartements of the plankton and their relationship to plankton size fractions. Limnology and Oceanography 23: pp. 1256-1263

Springer AM, McRoy CP (1993) The paradox of pelagic food webs in the northern Bering Sea-III. Patterns of primary production. Continental Shelf Research 13: pp. 575-599

Stroeve J, Holland MM, Meier W, Scambos T, Serreze M (2007) Arctic sea ice decline: Faster than forecast. Geophysical Research Letters 34

Tremblay JÉ, Gagnon J (2009) The effects of irradiance and nutrient supply on productivity of Arctic waters: a perspective on climage change. In: Nihoul CJ, Kostianoy AG (eds) Influence of Climate Change on the Changing Arctic and Sub-Arctic Condictions: pp. 73-94

Tremblay JÉ, Michel C, Hobson KA, Gosselin M, Price NM (2006) Bloom dynamics in early opening waters of the Arctic Ocean. Limnology and Oceanography 51:pp. 900-912

Throndsen J, Rytter G, Tangen K (2007) Phytoplankton of Norwegian Coastal Waters. Almater Forlag A5

von Quillfeldt CH (1997) Distribution of diatoms in the Northeast Water Polynya, Greenland. Journal of Marine Systems 10:pp. 211-240

Wassmann P (2011) Arctic marine ecosystems in an era of rapid climate change. Progress in Oceanography 90: pp. 1-17

Welch HE (1992) Energy flow through the marine ecosystem of the Lancaster Sound region, Arctic Canada. Arctic 45: pp. 343-357

Wheeler PA, Gosselin M, Sherr E, Thibault D, Kirchman DL, Benner R, Whitledge TE (1996) Active cycling of organic carbon in the central Arctic Ocean. Nature 380: pp. 697-699

Wheeler PA, Watkins JM, Hansing RL (1997) Nutrients, organic carbon and organic nitrogen in the upper water column of the Arctic Ocean: Implications for the sources of dissolved organic carbon. Deep-Sea Research Part II: Topical Studies in Oceanography 44: pp. 1571-1592

Yamamoto-Kawai M, McLaughlin FA, Carmack EC, Nishino S, Shimada K, Kurita N (2009) Surface freshening of the Canada Basin, 2003-2007: River runoff versus sea ice meltwater. Journal of Geophysical Research C: Oceans 114

Yamamoto-Kawai M, Carmack E, McLaughlin F (2006) Nitrogen balance and Arctic throughflow. Nature 443: pp. 43

Zhang X, Walsh JE, Zhang J, Bhatt US, Ikeda M (2004) Climatology and interannual variability of Arctic cyclone activity: 1948-2002. Journal of Climate 17: 2300

Annex I Counting protocol Light Microscopy

One chamber has been investigated at least five times. Firstly, the counting process was prepared by investigating the chamber in total by means of magnification 16 (160x). As such, it became clear whether the chamber contained only a few cells (resulting in about 200 real counts) or a lot cells (resulting in > 400 real counts), what the taxonomic diversity was (cells dominated by diatoms, flagellates or dinoflagellates), what the size distribution was (amount of bigger cells and diatom chains), what the proportion of autotrophic / heterotrophic cells was (only a very rough estimate) and what the condition of the cells and the general impression about the sample was (amount of empty cells, state and condition of the full cells). All this information was written down in a summary for each sample.

The next step of the counting process was to count all picoplankton cells at magnification 40 (400x). All cells < 2 µm has been counted at one stripe. Thirdly, the following protocol has been used to count all nanoplankton cells with a diameter between 2 µm and 10 µm at two stripes at magnification 40 (400x):

2-5 (1)

5-10 (2)

2-5 x 5-10 (3)

5-10 x 5-10 (4)

5-10 x 10-15 (5)

5-10 x 15-20 (6)

2-5 x 2-5 (9)

2-5 x 10-15 (10)

2-5 x 2-5 (8)

2-5 x 2-5 (11)

5-10 x 15-20 (7)

The first step was to divide the shape of the cell in one of the four categories (sphere, prolate spheroid, rectangular box and a droplet). The rectangular boxes have been used for the small and unidentified diatoms. Per count, it was noted down whether the cell belonged to the diatoms, dinoflagellates (being armoured or unarmoured), or the flagellates (in this case most of the time flagellates). And, when possible it was noted down to which family/order/genus the cells belonged (in this case for example the Choanoflagellates). The number in brackets corresponded with the number on the counting machine. In some cases other numbers on the counting machine have been chosen and all cells that did not fit into these standardized categories have been noted down individually. All real counts have been noted down in excel in the folder 'source table'.

Fourthly, the following protocol has been used to count all nanoplankton with a diameter between 10 µm and 15 µm at two stripes at magnification 25 (250x):

10-15 (1)

10-15 x 10-15 (3)

10-15 x 15-20 (4)

10-15 x 20-25 (5)

10-15 x 25-30 (6)

10-15 x 40-45 (10)

10-15 x 10-15 (9)

10-15 x 15-20 (8)

10-15 x 30-35 (11)

10-15 x 20-25 (7)

Again, the cells are divided in the different shapes and counted with a counting machine (in this case the sphere, prolate spheroid and the droplet). Since flagellates and dinoflagellates dominated the samples, all diatoms have been noted down individually. This was also the case for ciliates. Per count, it was noted down whether the cell belonged to the diatoms, dinoflagellates (being armoured or unarmoured), flagellates, ciliates or UPO's (in this case most of the time both flagellates and dinoflagellates). And, when possible it was noted down to which family/order/genus the cells belonged (in this case for example the *Dictyocha* sp.). Again, the number in brackets corresponded with the numbers on the counting machine. In some cases other numbers on the counting machine have been chosen and all cells that did not fit into these standardized categories have been noted down individually. All real counts have been noted down in excel in the folder 'source table'.

The second last step was to use the following protocol to count all nanoplankton and microplankton cells with a diameter > 15 µm at magnification 16 (160x) in half the chamber:

15-20 (10)

20-25 (1)

25-30 (2)

15-20 x 15-20 (3)

15-20 x 20-25 (4)

15-20 x 25-30 (5)

20-25 x 20-25 (6)

20-25 x 25-30 (7)

20-25 x 30-35 (8)

25-30 x 30-35 (9)

15-20 x 20-15 (11)

15-20 x 25-30 (12)

Again, the cells are divided in the different shapes and counted with a counting machine (in this case the sphere, prolate spheroid and the droplet). Since flagellates and dinoflagellates dominated the samples, all diatoms have been noted down individually. This was also the case for ciliates.

Per count, it was noted down whether the cell belonged to the diatoms, dinoflagellates (being armoured or unarmoured), flagellates, ciliates or UPO's (in this case most of the time both dinoflagellates and ciliates). And, when possible it was noted down to which family/order/genus the cells belonged (in this case for example the *Dictyocha* sp., *Protoperidinium* sp., *Gyrodinium* sp., *Amphidinium* sp., *Thalassiosira* sp. and *Chaetoceros* sp.). Again, the number in brackets corresponded with the numbers on the counting machine. In some cases, other numbers on the counting machine have been chosen and all cells that did not fit into these standardized categories have been noted down individually. All real counts have been noted down in excel in the folder 'source table'.

The last step was to count the biggest cells or chains at magnification 10 (100x) in the whole chamber, when necessary. In the end, this was only needed for sample 130 in which *Rhizosolenia* sp. has been found.

Annex II HPCL biomass

Table II a: Biomass (µg chl-*a* L^{-1}) of different algal divisions for a depth of 2 m (A) and the depth of the fluorescence maximum (B) per station for the four water masses. Blue: Adw, Green: MwI, Brown: Pdw, Orange: MwII.

A

Taxa / Stations	203	209	212	218	222	227	230	235	239	245	250
Prasinophyceae / Chlorophyceae	0.090	0.003	0.076	0.046	0.126	0.095	0.045	0.026	0.054	0.047	0.029
Euglenoceae	0	0.006	0	0	0	0	0	0	0	0	0.033
Dinophyteae	0.014	0	0	0	0	0.01	0.009	0	0.011	0	0.019
Cryptophyteae	0.010	0.005	0	0.021	0.039	0.02	0.005	0	0.012	0.014	0.042
Haptophyteae	0.396	0.039	0	0.019	0.013	0.007	0	0.001	0	0.001	0.065
Pelagophyteae	0	0.049	0	0.015	0.02	0.007	0.004	0	0	0	0
Diatoms	0.781	0.131	0.045	0.119	0.138	0.05	0.002	0.014	0	0.025	0
Total	**1.290**	**0.232**	**0.121**	**0.22**	**0.335**	**0.185**	**0.066**	**0.042**	**0.078**	**0.086**	**0.188**

B

Taxa / Stations	203	209	212	218	222	227	230	235	239	245	250
Prasinophyceae / Chlorophyceae	0.018	0	0.028	0	0.016	0.029	0.11	0.017	0.017	0	0.008
Euglenoceae	0	0	0	0	0	0	0	0.019	0.001	0.011	0.014
Dinophyteae	0.014	0	0	0	0	0	0	0	0	0	0
Cryptophyteae	0.002	0	0	0.006	0.012	0.012	0	0	0	0.017	0
Haptophyteae	0.185	0.013	0	0.049	0.034	0.009	0.008	0.09	0.001	0	0.017
Pelagophyteae	0	0.03	0.005	0.014	0.011	0.01	0.018	0.033	0	0	0
Diatoms	0.362	0.054	0.016	0.133	0.1	0.078	0.028	0	0.033	0.017	0.031
Total	**0.581**	**0.097**	**0.049**	**0.203**	**0.174**	**0.138**	**0.165**	**0.121**	**0.053**	**0.046**	**0.07**

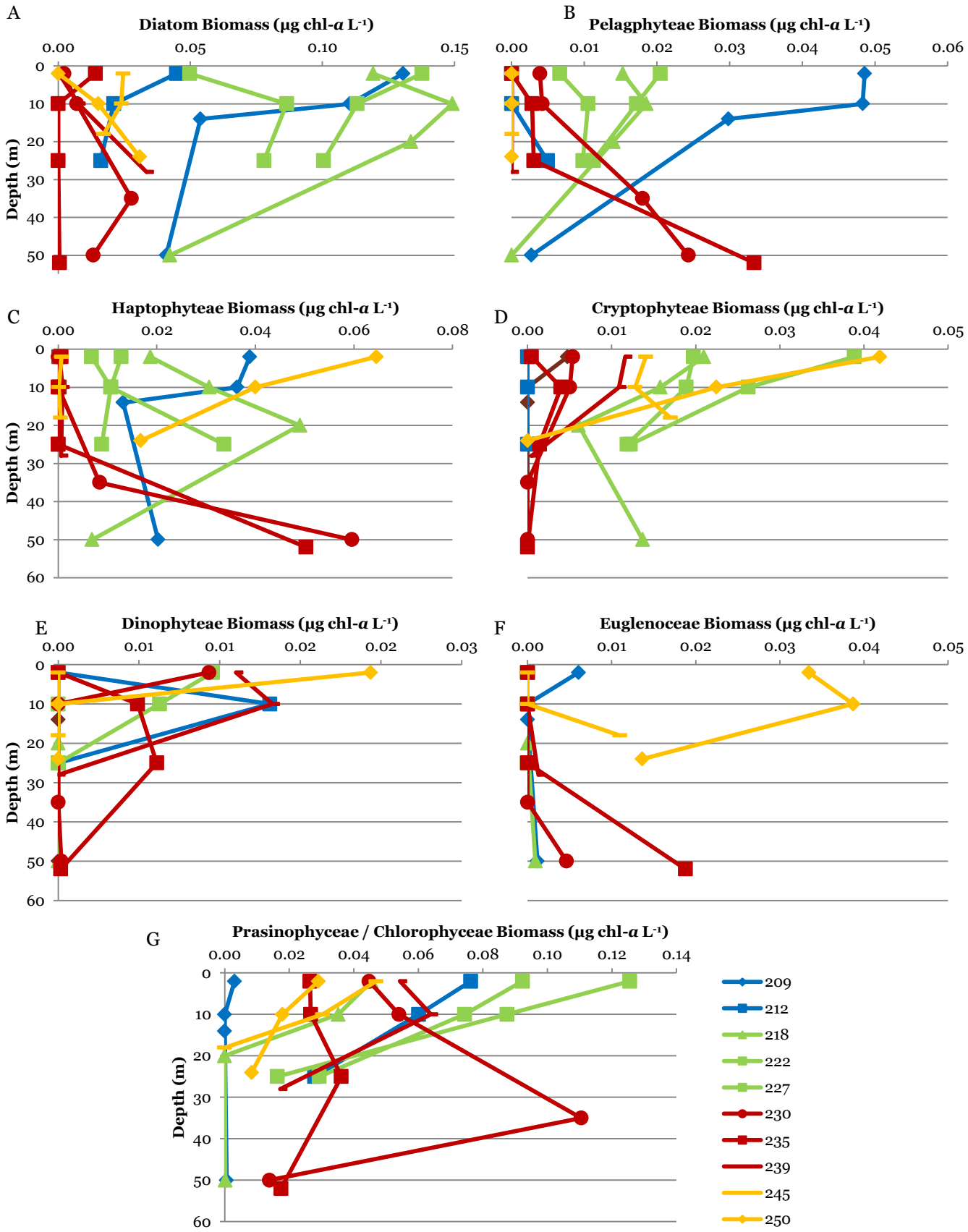

Figure II a: Biomass of Diatoms (A), Pelagophyteae (B), Haptophyteae (C), Cryptophyteae (D), Dinophyteae (E), Euglenoceae (F), and Prasinophyceae / Chlorophyceae (G) for the different stations and water masses. Blue lines: Adw, Green lines: MwI, Brown lines: Pdw, Orange lines: MwII. Since only two depths are sampled at station 203, this station is not included in this figure.

Annex III Light Microscopy: real counts

Sa.	Size µm	Shape	P	F	Di	Dia	Cil	U	Genus	M	S	C	SF
45	2-5 x 30	Prolate spheroid				1			*Cylindrotheca/nitzschia longissima*	16		0.5	2
45	2-5 x 36.3	Prolate spheroid				1			*Cylindrotheca/nitzschia longissima*	16		0.5	2
45	5 x 63	Elliptic prism				1			*Nitzschia/Pseudonitzschia*	16		0.5	2
45	15-20 x 20-25	Cone			1					16		0.5	2
45	15-20 x 25-30	Cone			1					16		0.5	2
45	17.6 x 52.1	Prolate spheroid					1			16		0.5	2
45	30.1 x 37.2	Cone					1			16		0.5	2
45	27.1 x 30.7	Prolate spheroid			1					16		0.5	2
45	10-15 x 20-25	Cone			1					25	2		27
45	20-25 x 30-35	Prolate spheroid			2					16		0.5	2
45	25 x 30	Sphere			2					16		0.5	2
45	31.8 x 41.6	Prolate spheroid			1					16		0.5	2
45	50 x 59	Cylinder				1			*Bacterosira/Guinardia*	16		0.5	2
45	20-25 x 20-25	Prolate spheroid			4					16		0.5	2
45	36.3	Sphere					1			16		0.5	2
45	15.5 x 40.4	Elliptic prism				1				16		0.5	2
45	37.0 x 42.5	Prolate spheroid			1					16		0.5	2
45	20-25 x 25-30	Prolate spheroid			6					16		0.5	2
45	20 x 25	Sphere			31					16		0.5	2
45	15-20 x 25-30	Prolate spheroid			51					16		0.5	2
45	10-15 x 20-25	Prolate spheroid			12					25	2		27
45	15-20 x 20-25	Prolate spheroid			141					16		0.5	2
45	2-5 x 5-10	Prolate spheroid		1					*Pyramimonas*	40	2		42.5
45	2-5 x 18.5	Prolate spheroid				1			*Cylindrotheca/nitzschia longissima*	25	2		27
45	2-5 x 10	Elliptic prism				1				40	2		42.5
45	2-5 x 2-5	Prolate spheroid		4						40	2		42.5
45	2-5 x 2-5	Rectangular box				3				40	2		42.5
45	5 x 10	Sphere		3						40	2		42.5
45	2-5 x 5-10	Prolate spheroid			3					40	2		42.5
45	5-10 x 15-20	Cone			1					40	2		42.5
45	10-15 x 10-15	Prolate spheroid			1					25	2		27
45	5 x 10	Sphere		105						40	2		42.5
45	5-10 x 5-10	Prolate spheroid			3					40	2		42.5
45	5-10 x 10-15	Prolate spheroid			2					40	2		42.5
45	10 x 15	Sphere			3					25	2		27
45	10-15 x 15-20	Prolate spheroid			5					25	2		27
45	15-20 x 15-20	Prolate spheroid			38					16		0.5	2
45	15 x 20	Sphere			48					16		0.5	2
45	1	Sphere	132							40	1		85
45	2 x 5	Sphere		21						40	2		42.5
45	2 x 5	Sphere		46						40	2		42.5
47	2-5 x 85.5	Elliptic prism				1			*Nitzschia/Pseudonitzschia*	16		0.5	2
47	7.5 x 39.4	Elliptic prism				1				16		0.5	2
47	2-5 x 35.5	Elliptic prism				1			*Nitzschia/Pseudonitzschia*	16		0.5	2
47	15-20 x 30-35	Prolate spheroid			1					16		0.5	2
47	22.6	Sphere					1			16		0.5	2
47	10 x 46.5	Elliptic prism				1			*Navicula*	16		0.5	2
47	25-30 x 30-35	Prolate spheroid			1					16		0.5	2
47	25-30 x 35-40	Prolate spheroid			1					16		0.5	2
47	42.2 x 49.8	Cylinder				1			*Bacterosira/Guinardia*	16		0.5	2
47	33.7 x 54.1	Cone					1			16		0.5	2
47	30-35 x 30-35	Prolate spheroid			1					16		0.5	2
47	30 x 35	Sphere			1					16		0.5	2
47	25-30 x 25-30	Prolate spheroid			2					16		0.5	2
47	20-25 x 20-25	Prolate spheroid			5					16		0.5	2
47	25 x 30	Sphere			3					16		0.5	2
47	41	Sphere			1					16		0.5	2
47	15-20 x 20-25	Prolate spheroid			1					25	2		27
47	20.3 x 24.6	Prolate spheroid			1					25	2		27
47	21.4 x 23.8	Prolate spheroid			1					25	2		27
47	20 x 25	Sphere			14					16		0.5	2
47	10-15 x 20-25	Prolate spheroid			4					25	2		27
47	25.9 x 23.9	Prolate spheroid			1					25	2		27
47	15-20 x 20-25	Prolate spheroid			38					16		0.5	2
47	15-20 x 25-30	Prolate spheroid			33					16		0.5	2
47	20-25 x 25-30	Prolate spheroid			22					16		0.5	2
47	29.9 x 27.8	Prolate spheroid			1					25	2		27
47	20-25 x 30-35	Prolate spheroid			24					16		0.5	2
47	15-20 x 25-30	Prolate spheroid			4					25	2		27

47	15-20 x 20-25	Prolate spheroid			7					25	2		27
47	2-5 x 5-10	Prolate spheroid			1					40	2		42.5
47	2-5 x 5-10	Prolate spheroid		1						40	2		42.5
47	2-5 x 7	Elliptic prism				1				40	2		42.5
47	5-10 x 5-10	Cylinder				19			*Chaetoceros*	16		0.5	2
47	2-5 x 10	Cylinder				4				40	2		42.5
47	5 x 10	Sphere		103						40	2		42.5
47	8.6 x 16.2	Prolate spheroid			1					25	2		27
47	2-5 x 2-5	Prolate spheroid		19						40	2		42.5
47	15 x 20	Sphere			5					16		0.5	2
47	5-10 x 5-10	Prolate spheroid			3					40	2		42.5
47	5-10 x 5-10	Prolate spheroid		3					*Pyramimonas*	40	2		42.5
47	5-10 x 15-20	Prolate spheroid			2					40	2		42.5
47	5-10 x 5-10	Prolate spheroid		5						40	2		42.5
47	10-15 x 10-15	Prolate spheroid			2					25	2		27
47	5-10 x 10-15	Prolate spheroid			8					40	2		42.5
47	10-15 x 15-20	Prolate spheroid			12					25	2		27
47	15-20 x 15-20	Prolate spheroid			8					25	2		27
47	2 x 5	Sphere		81						40	2		42.5
47	1	Sphere	349							40	1		85
53	20 x 20-25	Prolate spheroid						1		16		0.5	2
53	10	Sphere						1		40	2		42.5
53	24.4	Sphere					1			16		0.5	2
53	2-5 x 34.7	Elliptic prism				1				16		0.5	2
53	2-5 x 50.7	Elliptic prism				1			*Nitzschia/Pseudonitzschia*	16		0.5	2
53	2-5 x 53.8	Elliptic prism				1			*Nitzschia/Pseudonitzschia*	16		0.5	2
53	2-5 x 59.8	Elliptic prism				1			*Nitzschia/Pseudonitzschia*	16		0.5	2
53	2-5 x 67.6	Elliptic prism				1			*Nitzschia/Pseudonitzschia*	16		0.5	2
53	2-5 x 46.9	Elliptic prism				2			*Nitzschia/Pseudonitzschia*	16		0.5	2
53	2-5 x 61	Elliptic prism				4			*Nitzschia/Pseudonitzschia*	16		0.5	2
53	6 x 68.7	Elliptic prism				2				16		0.5	2
53	2-5 x 35-40	Prolate spheroid				2			*Cylindrotheca/nitzschia longissima*	25	2		27
53	20-25 x 45-50	Cone			1					16		0.5	2
53	28.9 x 30.9	Cone					1			16		0.5	2
53	20-25 x 30-35	Prolate spheroid			1					16		0.5	2
53	36.8	Cylinder				2			*Thalassiosira*	16		0.5	2
53	41.4 x 53.1	Cylinder				1			*Bacterosira/Guinardia*	16		0.5	2
53	32	Sphere			1				*Protoperidinium*	16		0.5	2
53	25 x 30	Sphere			3					16		0.5	2
53	20-25 x 25-30	Prolate spheroid			5					16		0.5	2
53	20 x 25	Sphere			8					16		0.5	2
53	15-20 x 25-30	Prolate spheroid			12					16		0.5	2
53	15-20 x 20-25	Prolate spheroid			21					16		0.5	2
53	10-15 x 20-25	Prolate spheroid			4					25	2		27
53	10-15 x 20-25	Prolate spheroid			18					40	2		42.5
53	2-5 x 2-5	Prolate spheroid			1					40	2		42.5
53	2-5 x 2-5	Cylinder				1			*Attheya*	40	2		42.5
53	2-5 x 5-10	Prolate spheroid		1					*Pyramimonas*	40	2		42.5
53	5 x 10	Sphere		5						40	2		42.5
53	2-5 x 5-10	Prolate spheroid		1						40	2		42.5
53	2-5 x 10-15	Prolate spheroid			1					40	2		42.5
53	2-5 x 5-10	Prolate spheroid			2					40	2		42.5
53	5 x 10	Sphere			2					40	2		42.5
53	2-5 x 10	Elliptic prism				2				40	2		42.5
53	5-10 x 15-20	Cone		1						40	2		42.5
53	2-5 x 2-5	Elliptic prism				3				40	2		42.5
53	9.4	Sphere		1						40	2		42.5
53	10-15 x 15-20	Cone			1					25	2		27
53	5 x 10	Sphere		28						40	2		42.5
53	10 x 15	Sphere			1					25	2		27
53	10-15 x 10-15	Prolate spheroid			1					25	2		27
53	15-20 x 15-20	Prolate spheroid			5					16		0.5	2
53	10 x 15	Sphere		1						40	2		42.5
53	5-10 x 15-20	Prolate spheroid			2					40	2		42.5
53	10-15 x 15-20	Prolate spheroid			3					25	2		27
53	10 x 5-10	Cylinder				237				16		0.5	2
53	15 x 20	Sphere			46					16		0.5	2
53	1	Sphere	504							40	1		85
53	2 x 5	Sphere		197						40	2		42.5
55	2-5 x 35-40	Prolate spheroid				4			*Cylindrotheca/nitzschia longissima*	16		0.5	2
55	5-10 x 35-40	Prolate spheroid		2					*Euglena*	16		0.5	2
55	20-25 x 20-25	Prolate spheroid			1					16		0.5	2
55	15-20 x 20-25	Prolate spheroid			2					16		0.5	2

55	20-25 x 30-35	Prolate spheroid			1					16		0.5	2
55	25-30 x 30-35	Prolate spheroid			1					16		0.5	2
55	25-30 x 55-60	Prolate spheroid			1					16		0.5	2
55	20 x 25	Sphere			4					16		0.5	2
55	30-35 x 55-60	Prolate spheroid			1					16		0.5	2
55	25 x 30	Sphere			3					16		0.5	2
55	15-20 x 25-30	Prolate spheroid			12					16		0.5	2
55	2-5 x 5-10	Prolate spheroid			1				*Pyramimonas*	40	2		42.5
55	2-5 x 2-5	Elliptic prism				3				40	2		42.5
55	2-5 x 10-15	Prolate spheroid			3					40	2		42.5
55	2-5 x 10-15	Elliptic prism				2				40	2		42.5
55	2-5 x 30-35	Elliptic prism				2			*Nitzschia/Pseudonitzschia*	25	2		27
55	5 x 10	Cylinder				1				40	2		42.5
55	5 x 10	Sphere			2					40	2		42.5
55	5-10 x 15-20	Prolate spheroid			1					40	2		42.5
55	10 x 15	Sphere		1						25	2		27
55	5 x 10	Sphere		1						40	2		42.5
55	15 x 20	Sphere			5					16		0.5	2
55	6 x 19	Cylinder				1				40	2		85
55	5-10 x 10-15	Prolate spheroid			2					40	2		42.5
55	10-15 x 10-15	Prolate spheroid		5						25	2		27
55	5 x 10	Sphere		8						40	2		42.5
55	2-5 x 2-5	Rectangular box				4				40	2		42.5
55	1	Sphere	149							40	1		85
55	2 x 5	Sphere		10						40	2		42.5
55	2 x 5	Sphere		121						40	2		42.5
76	5 x 10	Sphere						22		40	2		42.5
76	2-5 x 36	Elliptic prism				1			*Nitzschia/Pseudonitzschia*	16		0.5	2
76	2-5 x 40	Prolate spheroid				5			*Cylindrotheca/nitzschia longissima*	16		0.5	2
76	17.7 x 20.1	Cone					1			16		0.5	2
76	15-20 x 20-25	Cone			1					16		0.5	2
76	10 x 54.9	Elliptic prism				1			*Navicula*	16		0.5	2
76	18 x 24	Cone					1			16		0.5	2
76	15-20 x 20-25	Cone			1				*Protoperidinium*	16		0.5	2
76	21.9 x 18.7	Cone					1		*Stromtium*	16		0.5	2
76	18 x 30	Cone					1			16		0.5	2
76	18 x 30	Cylinder				1				16		0.5	2
76	20 x 26	Cone					1			16		0.5	2
76	15-20 x 30-35	Cone			1					16		0.5	2
76	10 x 91	Elliptic prism				1			*Nitzschia/Pseudonitzschia*	16		0.5	2
76	20.5 x 28.8	Cone					1			16		0.5	2
76	22.6 x 24.2	Cone					1			16		0.5	2
76	24.5 x 22.7	Cone					1			16		0.5	2
76	22.3 x 25.6	Cone					1			16		0.5	2
76	21.5 x 28	Cone					1			16		0.5	2
76	21.3 x 29.8	Cone					1			16		0.5	2
76	25.4 x 22	Cone					1			16		0.5	2
76	23 x 30.2	Cone					1			16		0.5	2
76	36	Cylinder				1			*Thalassiosira*	16		0.5	2
76	20-25 x 40-45	Cone			1					16		0.5	2
76	25 x 36	Cone					1		*Myrionecta*	16		0.5	2
76	29.2 x 35.1	Cylinder				1				16		0.5	2
76	24	Sphere					1			16		0.5	2
76	24	Sphere					1			16		0.5	2
76	24	Sphere					1			16		0.5	2
76	24	Sphere					1			16		0.5	2
76	24	Sphere					1			16		0.5	2
76	24	Sphere					1			16		0.5	2
76	24.4	Sphere					1		*Myrionecta*	16		0.5	2
76	34 x 37	Cylinder				1				16		0.5	2
76	27.3 x 44.3	Cone					1			16		0.5	2
76	35 x 37	Cylinder				1				16		0.5	2
76	15-20 x 25-30	Prolate spheroid			2					16		0.5	2
76	30.7 x 48.6	Cylinder				1				16		0.5	2
76	47 x 32	Cylinder				1				16		0.5	2
76	47 x 32	Cylinder				1				16		0.5	2
76	47 x 32	Cylinder				1				16		0.5	2
76	30	Cylinder				3			*Thalassiosira*	16		0.5	2
76	15-20 x 30-35	Cone			4					16		0.5	2
76	32.5 x 55.2	Cylinder				1				16		0.5	2
76	20-25	Sphere		2						16		0.5	2
76	30.5	Sphere					1		*Myrionecta*	16		0.5	2

76	30.5	Sphere					1		*Myrionecta*	16		0.5	2
76	61 x 32.5	Cone					1			16		0.5	2
76	25-30	Sphere			2					16		0.5	2
76	44.4 x 36.9	Cone					1		*Myrionecta*	16		0.5	2
76	36	Sphere					1		*Myrionecta*	16		0.5	2
76	36	Sphere					1		*Myrionecta*	16		0.5	2
76	36	Sphere					1			16		0.5	2
76	36	Sphere					1			16		0.5	2
76	5-10 x 35-40	Prolate spheroid			1				*Gyrodinium*	40	2		42.5
76	20-25	Sphere			5					16		0.5	2
76	26 x 248.67	Elliptic prism				1			*Pleurosigma*	16		0.5	2
76	25-30 x 40-45	Prolate spheroid			2					16		0.5	2
76	6 x 35.8	Elliptic prism				4			*Navicula*	25	2		27
76	42	Sphere			1					16		0.5	2
76	42	Sphere					1			16		0.5	2
76	42.7	Sphere					1			16		0.5	2
76	2-5 x 81	Elliptic prism				5			*Nitzschia/Pseudonitzschia*	25	2		27
76	15-20 x 20-25	Prolate spheroid			13					16		0.5	2
76	10-15 x 20-25	Prolate spheroid			2					25	2		27
76	2-5 x 44.7	Cylinder				11			*Thalassiosira*	25	2		27
76	10-15 x 20-25	Prolate spheroid			2					25	2		27
76	58.1 x 68.3	Cone					1			16		0.5	2
76	54.9	Sphere					1			16		0.5	2
76	23.4	Sphere		1					*Dictyocha*	25	2		27
76	20-25 x 30-35	Prolate spheroid			12					16		0.5	2
76	10-15 x 40-45	Prolate spheroid		4					*Euglena*	25	2		27
76	103 x 102	Cone					1			16		0.5	2
76	5 x 10	Sphere		2						40	2		42.5
76	2-5 x 2-5	Prolate spheroid		1					Choanoflagellates	40	2		42.5
76	2-5 x 2-5	Cylinder				16			*Chaetoceros*	16		0.5	2
76	2-5 x 5-10	Cone			1					40	2		42.5
76	2-5 x 5-10	Prolate spheroid		1					*Dinobryon*	40	2		42.5
76	2-5 x 5-10	Prolate spheroid			1					40	2		42.5
76	2-5 x 5-10	Cone		3						40	2		42.5
76	2-5 x 10-15	Prolate spheroid		1						40	2		42.5
76	2-5 x 5-10	Prolate spheroid			2					40	2		42.5
76	2-5 x 2-5	Prolate spheroid		6						40	2		42.5
76	18	Sphere					1			16		0.5	2
76	18	Sphere					1			16		0.5	2
76	18	Sphere					1			16		0.5	2
76	18	Sphere					1			16		0.5	2
76	18	Sphere					1			16		0.5	2
76	18	Sphere					1			16		0.5	2
76	18	Sphere					1			16		0.5	2
76	18	Sphere					1			16		0.5	2
76	18	Sphere					1			16		0.5	2
76	18	Sphere					1			16		0.5	2
76	18	Sphere					1			16		0.5	2
76	18	Sphere					1			16		0.5	2
76	18	Sphere					1			16		0.5	2
76	18	Sphere					1			16		0.5	2
76	18	Sphere					1			16		0.5	2
76	18	Sphere					1			16		0.5	2
76	2-5 x 5-10	Prolate spheroid		3					Choanoflagellates	40	2		42.5
76	18.9	Sphere					1		*Myrionecta*	16		0.5	2
76	5 x 10	Sphere		12					Choanoflagellates	40	2		42.5
76	5-10 x 5-10	Prolate spheroid		1						40	2		42.5
76	5-10 x 15-20	Cone		1						40	2		42.5
76	2-5 x 5-10	Prolate spheroid		7						40	2		42.5
76	5 x 10	Sphere		51						40	2		42.5
76	5-10 x 15-20	Prolate spheroid			1				*Gyrodinium*	40	2		42.5
76	5-10 x 15-20	Cone			2					40	2		42.5
76	15-20	Sphere		5						16		0.5	2
76	5-10	Sphere			3					40	2		42.5
76	10-15 x 10-15	Prolate spheroid			1					25	2		27
76	5-10 x 10-15	Prolate spheroid			2					40	2		42.5
76	5-10 x 15-20	Prolate spheroid		2						40	2		42.5
76	5-10 x 10-15	Prolate spheroid			3					40	2		42.5
76	5-10 x 5-10	Prolate spheroid			5					40	2		42.5
76	15.6	Sphere		1					*Dictyocha*	25	2		27
76	5-10 x 15-20	Prolate spheroid			3					40	2		42.5
76	15-20	Sphere			15					16		0.5	2

76	15-20 x 15-20	Prolate spheroid			16					16		0.5	2
76	5-10 x 15-20	Prolate spheroid			5					40	2		42.5
76	10 x 15	Sphere		4						25	2		27
76	10-15 x 15-20	Prolate spheroid		3						25	2		27
76	10-15 x 15-20	Prolate spheroid			3					25	2		27
76	2-5 x 2-5	Rectangular box				71				40	2		42.5
76	10-15 x 15-20	Prolate spheroid			4					25	2		27
76	10 x 15	Sphere			6					25	2		27
76	10-15 x 10-15	Prolate spheroid			6					25	2		27
76	10-15 x 10-15	Prolate spheroid		19						25	2		27
76	2 x 5	Sphere		7					Choanoflagellates	40	2		46
76	15	Sphere		6					*Dictyocha*	25	2		27
76	2 x 5	Sphere		4					*Pyramimonas*	40	2		46
76	1	Sphere	192							40	1		85
76	2 x 5	Sphere		33						40	2		42.5
76	2 x 5	Sphere		171						40	2		46
78	2-5 x 36	Elliptic prism				1			*Nitzschia/Pseudonitzschia*	16		0.5	2
78	2-5 x 62.5	Elliptic prism				4			*Nitzschia/Pseudonitzschia*	16		0.5	2
78	18.8 x 22.6	Cone					1			16		0.5	2
78	17.2 x 29.3	Cone					1			16		0.5	2
78	12.8 x 46.6	Elliptic prism				1			*Navicula*	16		0.5	2
78	21.1 x 22.8	Cone					1			16		0.5	2
78	22.4 x 26.2	Cone					1			16		0.5	2
78	15-20 x 20-25	Prolate spheroid			1					16		0.5	2
78	25.4 x 29.4	Cone					1			16		0.5	2
78	15-20 x 25-30	Prolate spheroid			1					16		0.5	2
78	15-20 x 30-35	Prolate spheroid			1					16		0.5	2
78	20-25	Sphere			1					16		0.5	2
78	15-20 x 30-35	Prolate spheroid			1					16		0.5	2
78	20-25 x 20-25	Prolate spheroid			1					16		0.5	2
78	24	Sphere					1			16		0.5	2
78	30.1 x 44	Cone					1			16		0.5	2
78	23.8 x 38	Prolate spheroid			1					16		0.5	2
78	20-25	Sphere			2				*Micracanthodinium claytonii*	16		0.5	2
78	12.5	Sphere					1			25	2		27
78	30	Sphere					1			16		0.5	2
78	37.2 x 39.6	Cone					1			16		0.5	2
78	15-20 x 20-25	Prolate spheroid		4						16		0.5	2
78	20-25 x 25-30	Prolate spheroid			2					16		0.5	2
78	35.6 x 45.1	Cone					1			16		0.5	2
78	5-10 x 20-25	Prolate spheroid			1					40	2		42.5
78	15-20 x 25-30	Prolate spheroid			5					16		0.5	2
78	39.6 x 54.3	Cone					1			16		0.5	2
78	33.7 x 42.9	Prolate spheroid			1					16		0.5	2
78	10-15 x 20-25	Prolate spheroid			1				*Amphidinium*	25	2		27
78	10-15 x 20-25	Prolate spheroid			1				*Gyrodinium*	25	2		27
78	15-20 x 20-25	Prolate spheroid			9					16		0.5	2
78	25-30	Sphere			3					16		0.5	2
78	42.5.1 x 40.2	Prolate spheroid			1					16		0.5	2
78	10-15 x 20-25	Prolate spheroid			3					25	2		27
78	9 - 50	Prolate spheroid		4					*Euglena*	25	2		27
78	2-5 x 2-5	Prolate spheroid		1					Choanoflagellates	40	2		42.5
78	2-5 x 5-10	Cone		1						40	2		42.5
78	2-5 x 16	Cylinder				7			*Cylindrotheca/nitzschia longissima*	16		0.5	2
78	2-5 x 2-5	Prolate spheroid			3					40	2		42.5
78	2-5 x 10-15	Prolate spheroid			1					40	2		42.5
78	17	Cylinder				2			*Thalassiosira*	16		0.5	2
78	18.7 x 19.6	Cone					1			16		0.5	2
78	15-20	Sphere			1							0.5	2
78	15-20 x 15-20	Prolate spheroid			1					16		0.5	2
78	18	Sphere					1			16		0.5	2
78	18	Sphere					1			16		0.5	2
78	18	Sphere					1			16		0.5	2
78	15-20	Sphere			1					16		0.5	2
78	5-10 x 5-10	Prolate spheroid		1						40	2		42.5
78	5-10 x 5-10	Prolate spheroid			1					40	2		42.5
78	18	Sphere					2			16		0.5	2
78	15-20 x 15-20	Prolate spheroid			2					16		0.5	2
78	2-5 x 5-10	Prolate spheroid			7					40	2		42.5
78	2-5 x 2-5	Prolate spheroid		17						40	2		42.5
78	30 x 40	Cone					1			16		0.5	2

78	2-5 x 5-10	Prolate spheroid		12						40	2		42.5
78	10-15	Sphere		1						25	2		27
78	2-5	Sphere		34						40	2		42.5
78	2-5 x 12.1	Elliptic prism				3				40	2		42.5
78	2-5 x 120	Elliptic prism				24			*Nitzschia/Pseudonitzschia*	16		0.5	2
78	5-10	Sphere			5					40	2		42.5
78	40 x 60	Cone					1			16		0.5	2
78	2-5 x 2-5	Rectangular box				34				40	2		42.5
78	10-15	Sphere			3					25	2		27
78	5-10	Sphere		14						40	2		42.5
78	2-5	Sphere		163						40	2		42.5
78	15	Sphere		5					*Dictyocha*	25	2		27
78	10-15 x 15-20	Prolate spheroid			7					25	2		27
78	5-10	Sphere		32						40	2		42.5
78	10-15 x 10-15	Prolate spheroid		17						25	2		27
78	1	Sphere	95							40	1		85
96	25	Sphere						1		16		0.5	2
96	5	Sphere						35		40	1		85
96	2-5 x 54	Elliptic prism				1			*Nitzschia/Pseudonitzschia*	16		0.5	2
96	6 x 40	Elliptic prism				1			*Nitzschia/Pseudonitzschia*	16		0.5	2
96	20 x 25	Cone			1					16		0.5	2
96	20 x 30	Cone					1			16		0.5	2
96	2-5 x 30	Elliptic prism				13				16		0.5	2
96	15-20 x 25-30	Prolate spheroid			1					16		0.5	2
96	23 x 49.7	Elliptic prism				1				16		0.5	2
96	20-25 x 20-25	Prolate spheroid			1					16		0.5	2
96	20 x 25	Sphere		1						16		0.5	2
96	15 x 35	Prolate spheroid			1					16		0.5	2
96	6 x 26	Elliptic prism				1				25	2		27
96	25	Cylinder				4				16		0.5	2
96	30 x 38	Cone					1			16		0.5	2
96	23.2 x 37.1	Prolate spheroid			1					16		0.5	2
96	36.3 x 42.5	Cone					1			16		0.5	2
96	44.5 x 50.42.5	Cylinder				1			*Bacterosira/Guinardia*	16		0.5	2
96	20-25 x 30-35	Prolate spheroid			2					16		0.5	2
96	40 x 50	Cone					1			16		0.5	2
96	35	Sphere					1			16		0.5	2
96	8.8 x 41.8	Prolate spheroid		1						25	2		27
96	30 x 50	Prolate spheroid			1					16		0.5	2
96	15-20 x 20-25	Cone			1					25	2		27
96	15-20 x 20-25	Cone			1					25	2		27
96	45.5 x 49.5	Cone					1			16		0.5	2
96	15-20 x 20-25	Cone			1					25	2		27
96	33.3 x 49.8	Prolate spheroid			1					16		0.5	2
96	20-25 x 25-30	Prolate spheroid			4					16		0.5	2
96	27.5 x 75	Prolate spheroid			1				*Gyrodinium*	16		0.5	2
96	15-20 x 25-30	Cone			1					25	2		27
96	25 x 30	Sphere			3					16		0.5	2
96	20 x 35	Cone					6			16		0.5	2
96	40	Sphere			1					16		0.5	2
96	40	Sphere					1			16		0.5	2
96	40	Sphere					1			16		0.5	2
96	40	Sphere					1			16		0.5	2
96	39.5 x 44.9	Prolate spheroid			1					16		0.5	2
96	20 x 25	Sphere			7					16		0.5	2
96	42	Cylinder				6			*Thalassiosira*	16		0.5	2
96	50	Sphere			1					16		0.5	2
96	15-20 x 20-25	Prolate spheroid			20					16		0.5	2
96	20-25 x 25-30	Prolate spheroid			1					25	2		27
96	15-20 x 25-30	Prolate spheroid			3					25	2		27
96	20-25 x 30-35	Prolate spheroid			2					25	2		27
96	2-5 x 2-5	Prolate spheroid		1					Choanoflagellates	40	1		85
96	2-5 x 2-5	Prolate spheroid		1					*Dinobryon*	40	1		85
96	2-5 x 10	Elliptic prism				16				16		0.5	2
96	17.5 x 20	Cone					1			16		0.5	2
96	2-5 x 5-10	Prolate spheroid		1					Choanoflagellates	40	1		85
96	2-5 x 5-10	Prolate spheroid		1						40	1		85
96	2-5 x 2-5	Cylinder				2			*Chaetoceros*	40	1		85
96	5-10 x 5-10	Cone			1					40	1		85
96	15 x 20	Sphere					2			16		0.5	2
96	8.6 x 13.2	Elliptic prism				1				25	2		27
96	2-5 x 2-5	Prolate spheroid		6						40	1		85

96	5-10 x 5-10	Elliptic prism				31				16		0.5	2
96	2-5 x 10-15	Prolate spheroid		2						40	1		85
96	2-5 x 12	Cylinder				69			*Chaetoceros*	16		0.5	2
96	5-10	Sphere			1					40	1		85
96	5-10 x 5-10	Prolate spheroid			2					40	1		85
96	5-10 x 15-20	Cone			2					40	1		85
96	5-10 x 10-15	Cone			3					40	1		85
96	15-20 x 15-20	Prolate spheroid			9					16		0.5	2
96	2-5	Sphere		42.5						40	1		85
96	10 x 15	Sphere		3						25	2		27
96	2-5 x 2-5	Rectangular box				31				40	1		85
96	5-10 x 5-10	Prolate spheroid		7						40	1		85
96	5-10	Sphere		9						40	1		85
96	10-15 x 10-15	Prolate spheroid			7					25	2		27
96	15 x 20	Sphere			39					16		0.5	2
96	2-5	Sphere		135						40	1		85
96	17.5	Sphere		48						16		0.5	2
96	10 x 15	Sphere			10					25	2		27
96	10-15 x 15-20	Prolate spheroid			10					25	2		27
96	10-15 x 15-20	Prolate spheroid		10						25	2		27
96	5-10	Sphere		27						40	1		85
96	1	Sphere	223							40	1		85
98	2-5 x 30	Prolate spheroid				2			*Cylindrotheca/nitzschia longissima*	16		0.5	2
98	50.1 x 7.2	Cone					1			16		0.5	2
98	2-5 x 60	Elliptic prism				3			*Nitzschia/Pseudonitzschia*	16		0.5	2
98	15-20 x 25-30	Cone			1					16		0.5	2
98	23.3 x 24.3	Cone					1			16		0.5	2
98	17.8 x 42.4	Cone					1			16		0.5	2
98	21.6 x 31.2	Cone					1			16		0.5	2
98	15-20 x 20-25	Prolate spheroid			1					16		0.5	2
98	15-20 x 25-30	Prolate spheroid		1						16		0.5	2
98	20-25 x 40-45	Cone			1					16		0.5	2
98	20-25 x 40-45	Cone			1				*Gyrodinium*	16		0.5	2
98	23.7 x 38.9	Cone					1			16		0.5	2
98	20-25 x 20-25	Prolate spheroid			1					16		0.5	2
98	26.6 x 35.6	Cone					1			16		0.5	2
98	24.4	Sphere					1			16		0.5	2
98	24.4	Sphere					1			16		0.5	2
98	30 x 36	Cone					1			16		0.5	2
98	20-25 x 30-35	Prolate spheroid			1					16		0.5	2
98	15-20 x 25-30	Prolate spheroid			2				*Amphidinium*	16		0.5	2
98	20-25 x 30-35	Prolate spheroid			1					16		0.5	2
98	32.8 x 42.4	Cone			1					16		0.5	2
98	5-10 x 20-25	Prolate spheroid			1					40	2		42.5
98	15-20 x 20-25	Prolate spheroid			4					16		0.5	2
98	24.4	Sphere		2					*Meringosphaera*	16		0.5	2
98	37.1 x 46.5	Cone					1			16		0.5	2
98	36.6	Sphere					1			16		0.5	2
98	35 x 42	Prolate spheroid			1					16		0.5	2
98	56.4 x 37.6	Cone					1			16		0.5	2
98	10 x 46	Prolate spheroid		1					Euglena	25	2		27
98	38 x 44	Prolate spheroid			1					16		0.5	2
98	20-25 x 25-30	Prolate spheroid			5					16		0.5	2
98	40 x 47.7	Prolate spheroid			1					16		0.5	2
98	10-15 x 30-35	Prolate spheroid			1				*Amphidinium*	25	2		27
98	25 x 30	Sphere			4					16		0.5	2
98	20 x 25	Sphere			8					16		0.5	2
98	15 x 39	Prolate spheroid			1				*Amphidinium*	25	2		27
98	10-15 x 20-25	Prolate spheroid			3					25	2		27
98	2-5 x 12	Elliptic prism				1			*Nitzschia/Pseudonitzschia*	16		0.5	2
98	5 x 10	Sphere		11						40	2		42.5
98	2-5 x 10	Cylinder				1			*Cylindrotheca/nitzschia longissima*	40	2		42.5
98	2-5 x 2-5	Prolate spheroid		4					Choanoflagellates	40	2		42.5
98	18.3	Sphere					1			16		0.5	2
98	18.3	Sphere					1			16		0.5	2
98	18.3	Sphere					1			16		0.5	2
98	2-5 x 10-15	Prolate spheroid			2					40	2		42.5
98	5-10 x 10-15	Cone			1					40	2		42.5
98	2-5 x 2-5	Rectangular box				5				40	2		42.5
98	2-5 x 5-10	Prolate spheroid			5					40	2		42.5
98	2-5 x 10-15	Prolate spheroid			3					40	2		42.5
98	7 x 12	Prolate spheroid					1			25	2		27

98	2-5 x 2-5	Prolate spheroid		18						40	2		42.5
98	5 x 10	Sphere		24						40	2		42.5
98	10-15 x 15-20	Cone			1					25	2		27
98	15	Sphere			1				*Dictyocha*	25	2		27
98	10-15 x 10-15	Prolate spheroid			2					25	2		27
98	15 x 20	Sphere			12					16		0.5	2
98	5-10 x 10-15	Prolate spheroid			5					40	2		42.5
98	5-10 x 5-10	Prolate spheroid		10						40	2		42.5
98	5-10 x 15-20	Prolate spheroid			5					40	2		42.5
98	5 x 10	Sphere			7					40	2		42.5
98	10 x 15	Sphere		5						25	2		27
98	10-15 x 15-20	Prolate spheroid			4					25	2		27
98	10-15 x 10-15	Prolate spheroid		6						25	2		27
98	10 x 15	Sphere			8					25	2		27
98	5	Sphere		28						40	2		42.5
98	2 x 5	Sphere		94						40	2		42.5
98	1	Sphere	147							40	1		85
98	2 x 5	Sphere		277						40	2		42.5
118	5	Sphere						33		40	1		85
118	2-5 x 30	Elliptic prism				1				16		0.5	2
118	15-20 x 20-25	Cone			1					16		0.5	2
118	24.4	Cylinder				1				16		0.5	2
118	18.3 x 24.4	Cone					1			16		0.5	2
118	15 x 35	Elliptic prism				1			*Thalassiosira*	16		0.5	2
118	18.8 x 27.4	Cone					1		*Stromtium*	16		0.5	2
118	19.9 x 27.8	Cone					1			16		0.5	2
118	20.1 x 29.1	Cone					1			16		0.5	2
118	20	Sphere					1			16		0.5	2
118	15-20 x 25-30	Prolate spheroid			1					16		0.5	2
118	15 x 37	Prolate spheroid			1					16		0.5	2
118	15 x 38	Prolate spheroid			1					16		0.5	2
118	15 x 39	Prolate spheroid			1					16		0.5	2
118	15 x 39.3	Prolate spheroid			1					16		0.5	2
118	16 x 38.8	Prolate spheroid			1				*Amphidinium*	16		0.5	2
118	15 x 41	Prolate spheroid			1					16		0.5	2
118	20-25 x 20-25	Prolate spheroid			1					16		0.5	2
118	26.7 x 36.3	Cone					1			16		0.5	2
118	23.2 x 49.2	Cone			1					16		0.5	2
118	24.4	Sphere					1			16		0.5	2
118	24.4	Sphere					1			16		0.5	2
118	24.4	Sphere					1			16		0.5	2
118	24.4	Sphere					1			16		0.5	2
118	24.4	Sphere					1			16		0.5	2
118	30 x 35.6	Cone					1			16		0.5	2
118	32.1 x 36.4	Cone					1			16		0.5	2
118	31.9 x 37.1	Cone					1			16		0.5	2
118	32.6 x 36.2	Cone					1			16		0.5	2
118	44.7 x 22.9	Cone					1			16		0.5	2
118	10-15 x 20-25	Cone			1					25	2		27
118	32.8 x 45.5	Cone			1					16		0.5	2
118	25-30 x 30-35	Prolate spheroid			1					16		0.5	2
118	15-20 x 20-25	Prolate spheroid			4					16		0.5	2
118	30.5	Sphere					1			16		0.5	2
118	27.8 x 42.1	Prolate spheroid			1					16		0.5	2
118	25 x 30	Sphere			2					16		0.5	2
118	34.1 x 39.6	Prolate spheroid			1					16		0.5	2
118	10-15 x 20-25	Prolate spheroid			1					25	2		27
118	20-25 x 30-35	Prolate spheroid			3					16		0.5	2
118	5-10 x 20-25	Prolate spheroid			1					40	1		85
118	20-25 x 25-30	Prolate spheroid			4					16		0.5	2
118	20 x 25	Sphere			5					16		0.5	2
118	13.4 x 33.7	Prolate spheroid			1					25	2		27
118	12.8 x 38.1	Prolate spheroid			1					25	2		27
118	68.9 x 44.5	Prolate spheroid			1					16		0.5	2
118	4 x 4	Cone		1					*Pyramimonas*	40	1		85
118	2-5 x 2-5	Prolate spheroid		1					Choanoflagellates	40	1		85
118	2-5 x 2-5	Prolate spheroid		1					*Pyramimonas*	40	1		85
118	15 x 20	Sphere		1					*Meringosphaera*	16		0.5	2
118	18.3	Sphere					1			16		0.5	2
118	18.3	Sphere					1			16		0.5	2
118	18.3	Sphere					1			16		0.5	2
118	18.3	Sphere					1			16		0.5	2
118	18.3	Sphere					1			16		0.5	2

118	18.3	Sphere					1			16		0.5	2
118	10-15 x 10-15	Cone		1						25	2		27
118	5 x 10	Sphere		7						40	1		85
118	2-5 x 5-10	Prolate spheroid		6						40	1		85
118	2-5 x 2-5	Prolate spheroid		17						40	1		85
118	5 x 10	Sphere		37						40	1		85
118	5-10 x 5-10	Prolate spheroid		2						40	1		85
118	5-10 x 15-20	Cone		2						40	1		85
118	5-10 x 10-15	Cone		3						40	1		85
118	5 x 10	Sphere			1					40	1		85
118	15	Sphere		21					*Dictyocha*	16		0.5	2
118	10-15 x 10-15	Prolate spheroid			3					25	2		27
118	10-15 x 10-15	Prolate spheroid		3						25	2		27
118	5-10 x 5-10	Prolate spheroid			5					40	1		85
118	15-20 x 15-20	Prolate spheroid			17					16		0.5	2
118	2-5 x 2-5	Rectangular box				31				40	1		85
118	10-15 x 15-20	Prolate spheroid		4						25	2		27
118	5-10 x 10-15	Prolate spheroid			5					40	1		85
118	10-15 x 15-20	Prolate spheroid			6					25	2		27
118	15 x 20	Sphere			49					16		0.5	2
118	10 x 15	Sphere		14						25	2		27
118	2 x 7	Elliptic prism				1				40	1		85
118	1	Sphere	473							40	1		85
118	2 x 5	Sphere		58						40	1		85
118	2 x 5	Sphere		194						40	1		85
120	5	Sphere						36		40	2		42.5
120	2-5 x 47.6	Prolate spheroid				1			*Cylindrotheca/nitzschia longissima*	16		0.5	2
120	18.3 x 24.4	Cone					1			16		0.5	2
120	20	Cylinder				1			*Thalassiosira*	16		0.5	2
120	18.5 x 37.2	Cone					1			16		0.5	2
120	24.2 x 27.4	Cone					1			16		0.5	2
120	15-20 x 25-30	Prolate spheroid			1					16		0.5	2
120	16.8 x 39.5	Prolate spheroid			1					16		0.5	2
120	20 x 25	Sphere			1					16		0.5	2
120	24.5 x 39.8	Cone					1			16		0.5	2
120	24.5 x 39.8	Cone					1			16		0.5	2
120	20-25 x 25-30	Prolate spheroid			1					16		0.5	2
120	30.1 x 31.6	Cone					1			16		0.5	2
120	24.4	Sphere					1			16		0.5	2
120	30.5 x 34.4	Cone					1			16		0.5	2
120	25.8 x 49.2	Cone					1			16		0.5	2
120	24 x 30	Prolate spheroid		1						16		0.5	2
120	27.3	Sphere					1			16		0.5	2
120	25 x 30	Sphere			1					16		0.5	2
120	25-30 x 30-35	Prolate spheroid			1					16		0.5	2
120	54.9 x 30.5	Cone					1			16		0.5	2
120	5-10 x 20-25	Prolate spheroid			1					40	2		42.5
120	39.0 x 47.9	Cone					1			16		0.5	2
120	15-20 x 20-25	Prolate spheroid			7					16		0.5	2
120	36.6	Sphere					1			16		0.5	2
120	36.6	Sphere					1			16		0.5	2
120	10-15 x 25-30	Prolate spheroid			1					25	2		27
120	42.7	Sphere					1			16		0.5	2
120	10-15 x 35-40	Prolate spheroid			1					25	2		27
120	10-15 x 20-25	Prolate spheroid			2					25	2		27
120	45.6 x 49.4	Prolate spheroid			1					16		0.5	2
120	48.9	Sphere					1		*Myrionecta*	16		0.5	2
120	48.9	Sphere					1			16		0.5	2
120	51.4 x 58.4	Prolate spheroid			1					16		0.5	2
120	60	Sphere			1					16		0.5	2
120	8.3 x 10.5	Cone					1		*Stromtium*	16		0.5	2
120	2-5 x 2-5	Cone		2						40	2		42.5
120	15	Sphere		1					Kinetoplasidea	16		0.5	2
120	5 x 10	Sphere		10						40	2		42.5
120	15 x 20	Sphere		1					*Meringosphaera*	16		0.5	2
120	18.3	Sphere					1			16		0.5	2
120	5-10 x 10-15	Cone		1						40	2		42.5
120	2-5 x 5-10	Prolate spheroid		7						40	2		42.5
120	2-5 x 2-5	Prolate spheroid		17						40	2		42.5
120	5 x 10	Sphere		35						40	2		42.5
120	15-20 x 15-20	Prolate spheroid			6					16		0.5	2
120	5-10 x 15-20	Prolate spheroid			2					40	2		42.5
120	15	Sphere		14					*Dictyocha*	16		0.5	2

120	15 x 20	Sphere			9					16		0.5	2
120	2-5 x 2-5	Rectangular box				33				40	2		42.5
120	5-10 x 10-15	Prolate spheroid		4						40	2		42.5
120	5-10 x 15-20	Prolate spheroid			4					40	2		42.5
120	5-10 x 5-10	Prolate spheroid		10						40	2		42.5
120	5-10 x 10-15	Prolate spheroid			7					40	2		42.5
120	10-15 x 10-15	Prolate spheroid			4					25	2		27
120	10-15 x 15-20	Prolate spheroid			5					25	2		27
120	10 x 15	Sphere			10					25	2		27
120	2 x 5	Sphere		63						40	2		42.5
120	1	Sphere	149							40	1		85
120	2 x 5	Sphere		217						40	2		42.5
130	6	Sphere						2		40	2		42.5
130	2-5 x 36	Elliptic prism				1				16		0.5	2
130	2-5 x 67.1	Elliptic prism				2				16		0.5	2
130	15-20 x 20-25	Prolate spheroid			1					16		0.5	2
130	9.4 x 40.1	Prolate spheroid		2					*Euglena*	16		0.5	2
130	24.4 x 24.4	Cone					1			16		0.5	2
130	15.8 x 41	Prolate spheroid					1			16		0.5	2
130	7.5 x 360	Prolate spheroid				1			*Rhizosolenia*	16		0.5	2
130	2-5 x 73.2	Elliptic prism				10			*Nitzschia/Pseudonitzschia*	16		0.5	2
130	18.3 x 36.6	Prolate spheroid					1			16		0.5	2
130	18.3 x 36.6	Prolate spheroid					1			16		0.5	2
130	26.6 x 36.6	Cone					1			16		0.5	2
130	20-25 x 25-30	Prolate spheroid			1					16		0.5	2
130	10-15 x 25-30	Prolate spheroid			1					25	4		6.8
130	24.4	Sphere					1			16		0.5	2
130	24.4	Sphere					1			16		0.5	2
130	24.4 x 30.5	Prolate spheroid					1		*Myrionecta*	16		0.5	2
130	25-30 x 30-35	Prolate spheroid			1					16		0.5	2
130	7.5 x 946.6	Prolate spheroid				1			*Rhizosolenia*	16		0.5	2
130	30.5	Sphere					1			16		0.5	2
130	7.5 x 984.1	Prolate spheroid				1			*Rhizosolenia*	16		0.5	2
130	28 x 38	Prolate spheroid			1					16		0.5	2
130	7.5 x 1037.9	Prolate spheroid				1			*Rhizosolenia*	16		0.5	2
130	25 x 53	Prolate spheroid			1					16		0.5	2
130	7.5 x 1168.4	Prolate spheroid				1			*Rhizosolenia*	16		0.5	2
130	20 x 25	Sphere			3				*Micracanthodinium claytonii*	16		0.5	2
130	26.7 x 49.7	Prolate spheroid			1					16		0.5	2
130	29.1 x 50.9	Prolate spheroid			1					16		0.5	2
130	36.6	Sphere					1			16		0.5	2
130	36.6	Sphere					1			16		0.5	2
130	36.6	Sphere					1			16		0.5	2
130	40 x 80	Cone					1			16		0.5	2
130	39 x 53	Prolate spheroid			1					16		0.5	2
130	49.9 x 67.6	Prolate spheroid			1					16		0.5	2
130	54.9 x 61	Prolate spheroid					1			16		0.5	2
130	61	Sphere			1					16		0.5	2
130	61	Sphere					1			16		0.5	2
130	12.2	Sphere					1			16		0.5	2
130	2-5 x 2-5	Prolate spheroid		4						40	2		42.5
130	5 x 10	Sphere		8						40	2		42.5
130	2-5 x 2-5	Prolate spheroid		5					Choanoflagellates	40	2		42.5
130	15-20	Sphere		1						16		0.5	2
130	2-5 x 12	Rectangular box				1				40	2		42.5
130	18.3	Sphere					1			16		0.5	2
130	18.3	Sphere					1			16		0.5	2
130	18.3	Sphere					1			16		0.5	2
130	18.3	Sphere					1			16		0.5	2
130	18.3	Sphere					1			16		0.5	2
130	10 x 10	Cylinder				12			*Chaetoceros*	16		0.5	2
130	15-20	Sphere			2					16		0.5	2
130	5-10 x 5-10	Prolate spheroid		2						40	2		42.5
130	2-5 x 5-10	Prolate spheroid		10						40	2		42.5
130	15-20	Sphere			4					16		0.5	2
130	18.3	Sphere					1			16		0.5	2
130	7 x 9	Prolate spheroid			3					40	2		42.5
130	10 x 15	Sphere		6						25	4		6.8
130	7.9 x 17.1	Prolate spheroid			2					40	2		42.5
130	2 x 5	Sphere		1					Choanoflagellates	40	2		42.5
130	2 x 5	Sphere		2					*Pyramimonas*	40	2		42.5
130	1	Sphere	90							40	1		85
130	2 x 5	Sphere		13						40	2		42.5

130	2 x 5	Sphere		89						40	2		42.5
132	18.3 x 24.4	Cone					1			16		0.5	2
132	18.3 x 24.4	Cone					1			16		0.5	2
132	18.3 x 24.4	Cone					1			16		0.5	2
132	18.3 x 30.5	Cone					1			16		0.5	2
132	15-20 x 20-25	Prolate spheroid		1						16		0.5	2
132	24.4 x 30.5	Cone					1			16		0.5	2
132	24.4 x 30.5	Cone					1			16		0.5	2
132	24.6 x 31.6	Cone					1			16		0.5	2
132	26.5 x 28.9	Cone					1			16		0.5	2
132	24.7 x 40.1	Cone					1			16		0.5	2
132	17.5 x 44.9	Prolate spheroid			1				*Gyrodinium*	16		0.5	2
132	15-20 x 20-25	Prolate spheroid			2					16		0.5	2
132	24.4	Sphere					1		*Myrionecta*	16		0.5	2
132	24.4	Sphere					1			16		0.5	2
132	24.4	Sphere					1			16		0.5	2
132	2-5 x 91	Elliptic prism				11			*Nitzschia/Pseudonitzschia*	16		0.5	2
132	15-20 x 25-30	Prolate spheroid			2					16		0.5	2
132	20-25 x 30-35	Prolate spheroid			1				*Protoperidinium*	16		0.5	2
132	25 x 30	Sphere			1				*Micracanthodinium claytonii*	16		0.5	2
132	25 x 30	Sphere			1					16		0.5	2
132	20-25 x 25-30	Prolate spheroid			2					16		0.5	2
132	30.5	Sphere					1			16		0.5	2
132	30.5	Sphere					1			16		0.5	2
132	32.2 x 37.2	Prolate spheroid			1					16		0.5	2
132	34.5 x 42.5.6	Prolate spheroid			1					16		0.5	2
132	20 x 25	Sphere			5					16		0.5	2
132	42.7	Sphere			1					16		0.5	2
132	42.7	Sphere					1			16		0.5	2
132	10-15 x 20-25	Prolate spheroid			2					25	2		27
132	2-5 x 2-5	Prolate spheroid		1					Choanoflagellates	40	2		42.5
132	12.2	Sphere					1			16		0.5	2
132	10 x 15	Sphere			1				*Meringosphaera*	16		0.5	2
132	5 x 10	Sphere		3						40	2		42.5
132	18.3	Sphere					1			16		0.5	2
132	18.3	Sphere					1			16		0.5	2
132	18.3	Sphere					1			16		0.5	2
132	18.3	Sphere					1			16		0.5	2
132	18.3	Sphere					1			16		0.5	2
132	2-5 x 2-5	Prolate spheroid		11						40	2		42.5
132	5 x 10	Sphere		24						40	2		42.5
132	5-10 x 5-10	Cylinder				25			*Chaetoceros*	16		0.5	2
132	10 x 15	Sphere			12					16		0.5	2
132	15	Sphere		8					*Dictyocha*	16		0.5	2
132	10-15 x 10-15	Prolate spheroid			1					25	2		27
132	5-10 x 5-10	Prolate spheroid			6					40	2		42.5
132	2-5 x 2-5	Rectangular box				38				40	2		42.5
132	5-10 x 5-10	Prolate spheroid		9						40	2		42.5
132	10-15 x 15-20	Prolate spheroid			4					25	2		27
132	10 x 15	Sphere			7					25	2		27
132	1	Sphere	138							40	1		85
132	2 x 5	Sphere		37						40	2		42.5
132	2 x 5	Sphere		60						40	2		42.5
151	5	Sphere						8		40	4		11
151	2-5 x 2-5	Prolate spheroid						12		40	4		11
151	2-5 x 36	Elliptic prism				1				16		0.5	2
151	2-5 x 46.8	Elliptic prism				1				16		0.5	2
151	2-5 x 101.3	Elliptic prism				1				16		0.5	2
151	16.6 x 27.7	Cylinder				1			*Chaetoceros*	16		0.5	2
151	5-10 x 73.6	Elliptic prism				1				16		0.5	2
151	17.1 x 22.5	Cone					1			16		0.5	2
151	10-15 x 20-25	Prolate spheroid		1						16		0.5	2
151	5-10 x 82.8	Elliptic prism				1				16		0.5	2
151	2-5 x 90	Elliptic prism				3			*Nitzschia/Pseudonitzschia*	16		0.5	2
151	18.1 x 40	Cone					1			16		0.5	2
151	20.1 x 27.1	Prolate spheroid			1					16		0.5	2
151	20-25 x 20-25	Prolate spheroid			1					16		0.5	2
151	24.4	Sphere					1			16		0.5	2
151	20-25 x 30-35	Prolate spheroid			1					16		0.5	2
151	20 x 25	Sphere			2					16		0.5	2
151	10-15 x 20-25	Prolate spheroid			8					16		0.5	2
151	24.4	Sphere					2			16		0.5	2
151	30	Sphere			1					16		0.5	2

151	30 x 40	Prolate spheroid			1					16		0.5	2
151	20 x 25	Sphere		5						16		0.5	2
151	51.5 x 71.8	Cone					1			16		0.5	2
151	79.3 x 48.8	Cone					1			16		0.5	2
151	20 x 15	Sphere		32						16		0.5	2
151	2-5 x 2-5	Prolate spheroid		2					Choanoflagellates	40	4		11
151	9.4 x 13.7	Cone					1			16		0.5	2
151	5 x 10	Sphere		2						40	4		11
151	2-5 x 2-5	Prolate spheroid		7						40	4		11
151	5 x 10	Sphere		9						40	4		11
151	10-15 x 10-15	Prolate spheroid			1					16		0.5	2
151	10-15 x 10-15	Cone		2						16		0.5	2
151	12.6	Sphere					1			16		0.5	2
151	2-5 x 2-5	Rectangular box				5				40	4		11
151	5-10 x 10-15	Prolate spheroid		1					Kinetoplasidea	40	4		11
151	5-10 x 15-20	Prolate spheroid			1					40	4		11
151	10-15 x 15-20	Prolate spheroid			2					16		0.5	2
151	10.7 x 16	Cylinder				1			*Chaetoceros*	40	4		11
151	10-15 x 15-20	Prolate spheroid		3						16		0.5	2
151	5-10 x 5-10	Prolate spheroid		5						40	4		11
151	15 x 20	Sphere			3					16		0.5	2
151	5-10 x 10-15	Prolate spheroid			6					40	4		11
151	1	Sphere	30							40	1		85
151	2 x 5	Sphere		16						40	4		11
151	2 x 5	Sphere		55						40	4		11
154	12.9 x 38.7	Cone					1			16		0.5	2
154	27.7 x 16.6	Elliptic prism				1				16		0.5	2
154	15-20 x 20-25	Prolate spheroid			1					16		0.5	2
154	18.6 x 35.1	Prolate spheroid			1					16		0.5	2
154	41.3	Cylinder				1				16		0.5	2
154	24.4	Sphere					1			16		0.5	2
154	28.4 x 39.4	Cone					1			16		0.5	2
154	15-20 x 25-30	Prolate spheroid			2					16		0.5	2
154	5-10 x 20-25	Prolate spheroid			1					40	2		42.5
154	30.5	Sphere					1			16		0.5	2
154	30.5	Sphere					1			16		0.5	2
154	28.7 x 35.9	Prolate spheroid			1					16		0.5	2
154	20 x 25	Sphere			3					16		0.5	2
154	2-5 x 90	Elliptic prism				31			*Nitzschia/Pseudonitzschia*	16		0.5	2
154	10-15 x 20-25	Prolate spheroid			1					25	2		27
154	67.1 x 42.7	Cone					1			16		0.5	2
154	24	Sphere		13					*Dictyocha*	16		0.5	2
154	2-5 x 2-5	Cone		1						40	2		42.5
154	2-5 x 2-5	Cylinder				1			*Chaetoceros*	25	2		27
154	2-5 x 2-5	Prolate spheroid		1					Choanoflagellates	40	2		42.5
154	2-5 x 2-5	Prolate spheroid				2				40	2		42.5
154	2-5 x 5-10	Prolate spheroid		1						40	2		42.5
154	18.3	Sphere					1			16		0.5	2
154	18.3	Sphere					1			16		0.5	2
154	18.3	Sphere					1			16		0.5	2
154	18.3	Sphere					1			16		0.5	2
154	18.3	Sphere					1			16		0.5	2
154	2-5 x 2-5	Prolate spheroid		11						40	2		42.5
154	5 x 10	Sphere		16						40	2		42.5
154	10 x 15	Sphere		6						16		0.5	2
154	10-15 x 10-15	Cone		1						25	2		27
154	2-5 x 2-5	Rectangular box				12				40	2		42.5
154	5-10 x 10-15	Prolate spheroid		2						40	2		42.5
154	5 x 10	Sphere		3						40	2		42.5
154	5-10 x 5-10	Prolate spheroid		6						40	2		42.5
154	18	Sphere		15					*Dictyocha*	16		0.5	2
154	10-15 x 15-20	Prolate spheroid			3					25	2		27
154	5-10 x 10-15	Prolate spheroid			10					40	2		42.5
154	10 x 15	Sphere		7						25	2		27
154	2 x 5	Sphere		82						40	2		42.5
154	1	Sphere	181							40	1		85
154	2 x 5	Sphere		42.5						40	2		42.5
163	5	Sphere						11		40	2		42.5
163	2-5 x 36.3	Elliptic prism				1				16		0.5	2
163	2-5 x 42	Elliptic prism				1				16		0.5	2
163	2-5 x 42.7	Elliptic prism				1				16		0.5	2
163	2-5 x 42.7	Elliptic prism				1				16		0.5	2
163	2-5 x 58.3	Elliptic prism				1				16		0.5	2

163	6 x 32.5	Elliptic prism				1				16		0.5	2
163	12.2 x 24.4	Elliptic prism				1				16		0.5	2
163	2-5 x 90	Elliptic prism				2			*Nitzschia/Pseudonitzschia*	16		0.5	2
163	6.9 x 79	Elliptic prism				1				16		0.5	2
163	8.8 x 62	Elliptic prism				1				16		0.5	2
163	18.3 x 24.4	Cone					1			16		0.5	2
163	7.5 x 100	Elliptic prism				1				16		0.5	2
163	24.2 x 29.3	Prolate spheroid				1			*Melosira arctica*	16		0.5	2
163	8.8 x 97.2	Elliptic prism				1				16		0.5	2
163	18.3 x 36.6	Cone					1		*Myrionecta*	16		0.5	2
163	33.7 x 28.9	Prolate spheroid				1			*Melosira arctica*	16		0.5	2
163	15-20 x 20-25	Prolate spheroid		1						16		0.5	2
163	29.1 x 31	Prolate spheroid				1			*Melosira arctica*	16		0.5	2
163	22.7 x 29.5	Cone					1		*Stromtium*	16		0.5	2
163	16.5 x 69.6	Elliptic prism				1				16		0.5	2
163	32 x 36	Prolate spheroid				1			*Melosira arctica*	16		0.5	2
163	15.4 x 86.78	Cone					1			16		0.5	2
163	24.4 x 36.6	Cone					1			16		0.5	2
163	15-20 x 35-40	Prolate spheroid			1					16		0.5	2
163	15-20 x 35-40	Cone			2					16		0.5	2
163	41.4 x 34.4	Cone					1			16		0.5	2
163	24	Sphere		1					*Dictyocha*	16		0.5	2
163	24.4	Sphere					1			16		0.5	2
163	26.9 x 41.9	Cone					1			16		0.5	2
163	30.9 x 34.4	Cone					1			16		0.5	2
163	30.5 x 36.6	Cone					1		*Myrionecta*	16		0.5	2
163	36.6 x 30.5	Cone					1			16		0.5	2
163	15.4 x 86.8	Prolate spheroid					1			16		0.5	2
163	38.1 x 30.1	Cone					1			16		0.5	2
163	30 x 56	Cone					1			16		0.5	2
163	15-20 x 20-25	Prolate spheroid			4					16		0.5	2
163	45.3 x 28.5	Cone					1		*Myrionecta*	16		0.5	2
163	35.7 x 52.2	Cone			1					16		0.5	2
163	42.7 x 36.6	Cone					1			16		0.5	2
163	25 x 30	Sphere			2					16		0.5	2
163	10-15 x 20-25	Prolate spheroid			1					25	2		27
163	36.6	Sphere					1		*Myrionecta*	16		0.5	2
163	15-20 x 25-30	Prolate spheroid			7					16		0.5	2
163	20 x 25	Sphere			6					16		0.5	2
163	44.1 x 83.2	Cone			1				*Gyrodinium*	16		0.5	2
163	48	Sphere			1					16		0.5	2
163	75.4 x 98.3	Cone					1			16		0.5	2
163	86.9 x 87	Cone					1			16		0.5	2
163	2-5 x 5-10	Cone		1						40	2		42.5
163	12	Sphere					1		*Myrionecta*	16		0.5	2
163	2-5 x 2-5	Rectangular box				1				40	2		42.5
163	2-5 x 2-5	Prolate spheroid		2					Choanoflagellates	40	2		42.5
163	2-5 x 2-5	Prolate spheroid		2					*Pyramimonas*	40	2		42.5
163	2-5 x 5-10	Prolate spheroid			1					40	2		42.5
163	7 x 14.7	Cylinder				3			*Chaetoceros*	16		0.5	2
163	2-5 x 10-15	Prolate spheroid			1					40	2		42.5
163	2-5 x 2-5	Rectangular box				2				40	2		42.5
163	5-10 x 5-10	Prolate spheroid			3					40	2		42.5
163	5-10 x 10-15	Cone		1						40	2		42.5
163	2-5 x 5-10	Prolate spheroid		6						40	2		42.5
163	5 x 10	Sphere		16						40	2		42.5
163	5-10 x 15-20	Prolate spheroid			1					40	2		42.5
163	5-10 x 15-20	Prolate spheroid		1						40	2		42.5
163	15-20 x 15-20	Prolate spheroid			4					16		0.5	2
163	2-5 x 2-5	Prolate spheroid		27						40	2		42.5
163	5-10 x 5-10	Prolate spheroid		4						40	2		42.5
163	5-10 x 10-15	Prolate spheroid			4					40	2		42.5
163	10-15 x 15-20	Prolate spheroid			2					25	2		27
163	5-10 x 10-15	Prolate spheroid		5						40	2		42.5
163	15 x 20	Sphere			18					16		0.5	2
163	10 x 15	Sphere		8						25	2		27
163	2 x 5	Sphere		4					Choanoflagellates	40	2		42.5
163	2 x 5	Sphere		6					*Pyramimonas*	40	2		42.5
163	1	Sphere	138							40	1		85
163	2 x 5	Sphere		31						40	2		42.5
163	2 x 5	Sphere		106						40	2		42.5
165	18.3	Sphere						1		16		0.5	2
165	19.8	Sphere						1		16		0.5	2

165	6	Sphere						6		40	2		42.5
165	2-5 x 36.6	Prolate spheroid				1			*Cylindrotheca/nitzschia longissima*	16		0.5	2
165	2-5 x 90	Elliptic prism				2			*Nitzschia/Pseudonitzschia*	16		0.5	2
165	15.8 x 26.5	Cone					1			16		0.5	2
165	18.3 x 30.5	Cone					1			16		0.5	2
165	18.3 x 30.5	Cone					1			16		0.5	2
165	10.2 x 76.5	Elliptic prism				1				16		0.5	2
165	10.3 x 82.2	Elliptic prism				1				16		0.5	2
165	21.8 x 25.1	Cone					1		*Stromtium*	16		0.5	2
165	19.1 x 34.7	Cone					1			16		0.5	2
165	15-20 x 20-25	Prolate spheroid			1					16		0.5	2
165	34.6 x 39	Prolate spheroid				1			*Melosira arctica*	16		0.5	2
165	15-20 x 30-35	Prolate spheroid			1					16		0.5	2
165	24.4	Sphere					1			16		0.5	2
165	24.4	Sphere					1			16		0.5	2
165	24.3 x 27.3	Prolate spheroid			1					16		0.5	2
165	25 x 30	Sphere			1					16		0.5	2
165	25-30 x 30-35	Prolate spheroid			1					16		0.5	2
165	15-20 x 40-45	Prolate spheroid			2					16		0.5	2
165	7.6 x 39.8	Prolate spheroid		1					*Euglena*	25	2		27
165	20 x 25	Sphere			3					16		0.5	2
165	9.7 x 18.9	Cone					1			16		0.5	2
165	2-5 x 5-10	Prolate spheroid			1					40	2		42.5
165	5 x 10	Sphere		3						40	2		42.5
165	2-5 x 2-5	Prolate spheroid		5						40	2		42.5
165	5 x 10	Sphere		8						40	2		42.5
165	18.3	Sphere					1			16		0.5	2
165	18.3	Sphere					1			16		0.5	2
165	15-20 x 15-20	Prolate spheroid			1				*Protoperidinium*	16		0.5	2
165	15-20 x 15-20	Prolate spheroid			1				*Protoperidinium*	16		0.5	2
165	2-5 x 5-10	Prolate spheroid		4						40	2		42.5
165	5-10 x 5-10	Prolate spheroid		1						40	2		42.5
165	2-5 x 5-10	Cylinder				3			*Chaetoceros*	40	2		42.5
165	10-15 x 10-15	Prolate spheroid		1						25	2		27
165	15 x 20	Sphere			6					16		0.5	2
165	2-5 x 2-5	Rectangular box				25				40	2		42.5
165	10-15 x 15-20	Prolate spheroid		1						25	2		27
165	5-10 x 10-15	Prolate spheroid			7					40	2		42.5
165	10 x 15	Sphere		6						25	2		27
165	1	Sphere	62							40	1		85
165	2 x 5	Sphere		45						40	2		42.5
165	2 x 5	Sphere		81						40	2		42.5
179	5	Sphere						7		40	2		42.5
179	2-5 x 24.4	Prolate spheroid				1			*Cylindrotheca/nitzschia longissima*	16		0.5	2
179	24.4	Cylinder				1				16		0.5	2
179	18.3 x 24.4	Cone					1		*Myrionecta*	16		0.5	2
179	28.0 x 16.9	Cylinder				1				16		0.5	2
179	15-20 x 20-25	Prolate spheroid			1				*Amphidinium*	16		0.5	2
179	2-5 x 25-30	Prolate spheroid		1					*Euglena*	40	2		42.5
179	18.3 x 48.8	Cone					1			16		0.5	2
179	15-20 x 30-35	Prolate spheroid			1					16		0.5	2
179	15-20 x 35-40	Prolate spheroid			1					16		0.5	2
179	9.8 x 62.5	Elliptic prism				3				16		0.5	2
179	20-25 x 25-30	Prolate spheroid			1					16		0.5	2
179	2-5 x 25	Rectangular box				8				40	2		42.5
179	5-10 x 25-30	Cone		1						40	2		42.5
179	15-20 x 25-30	Prolate spheroid			2					16		0.5	2
179	30.5 x 36.6	Cone					1		*Stromtium*	16		0.5	2
179	25 x 30	Sphere			1					16		0.5	2
179	20-25 x 20-25	Prolate spheroid			2					16		0.5	2
179	25 x 30	Sphere			1					16		0.5	2
179	54.9	Cylinder				1				16		0.5	2
179	30.5	Sphere					1		*Myrionecta*	16		0.5	2
179	30.5	Sphere					1		*Myrionecta*	16		0.5	2
179	5-10 x 35-40	Prolate spheroid		1						40	2		42.5
179	20 x 25	Sphere			4					16		0.5	2
179	10-15 x 20-25	Prolate spheroid			1					25	2		27
179	36.6	Sphere			1					16		0.5	2
179	36.6	Sphere					1			16		0.5	2
179	10-15 x 20-25	Prolate spheroid			1				*Protoperidinium*	25	2		27
179	24.4	Sphere		4					*Dictyocha*	16		0.5	2
179	42.7	Sphere					1			16		0.5	2
179	48.8	Sphere					1			16		0.5	2

179	48.8	Sphere					1			16		0.5	2
179	54.9	Sphere					1			16		0.5	2
179	2-5 x 2-5	Prolate spheroid		1					Choanoflagellates	40	2		42.5
179	12.2	Sphere					1		*Myrionecta*	16		0.5	2
179	12.2	Sphere					1		*Myrionecta*	16		0.5	2
179	2-5 x 2-5	Prolate spheroid		2					*Pyramimonas*	40	2		42.5
179	5-10 x 5-10	Cylinder				6			*Chaetoceros*	16		0.5	2
179	2-5 x 10-15	Prolate spheroid		1						40	2		42.5
179	15-20 x 15-20	Prolate spheroid			1					16		0.5	2
179	18.3	Sphere					1		*Myrionecta*	16		0.5	2
179	18.3	Sphere					1		*Myrionecta*	16		0.5	2
179	18.3	Sphere					1		*Myrionecta*	16		0.5	2
179	18.3	Sphere					1		*Myrionecta*	16		0.5	2
179	18.3	Sphere					1		*Myrionecta*	16		0.5	2
179	2-5 x 2-5	Prolate spheroid		13						40	2		42.5
179	5 x 10	Sphere		25						40	2		42.5
179	5 x 10	Sphere		2						40	2		42.5
179	10 x 15	Sphere		1						25	2		27
179	5-10 x 5-10	Prolate spheroid		3						40	2		42.5
179	10-15 x 15-20	Prolate spheroid			1					25	2		27
179	10-15 x 15-20	Prolate spheroid		1						25	2		27
179	5-10 x 15-20	Prolate spheroid			2					40	2		42.5
179	15 x 20	Sphere			8					16		0.5	2
179	10 x 15	Sphere			2					25	2		27
179	10-15 x 10-15	Prolate spheroid			2					25	2		27
179	2 x 5	Sphere		1					*Dinobryon*	40	2		42.5
179	1	Sphere	310							40	1		85
179	2 x 5	Sphere		36						40	2		42.5
179	2 x 5	Sphere		97						40	2		42.5
181	20	Sphere						1		16		0.5	2
181	5	Sphere						3		40	2		42.5
181	2-5 x 60	Elliptic prism				1				16		0.5	2
181	2-5 x 30.6	Cylinder				4			*Cylindrotheca/nitzschia longissima*	16		0.5	2
181	2-5 x 61.8	Elliptic prism				2			*Nitzschia/Pseudonitzschia*	16		0.5	2
181	15-20 x 20-25	Prolate spheroid				1			*Melosira arctica*	16		0.5	2
181	18.3 x 30.5	Cone					1			16		0.5	2
181	22.8 x 25.8	Cone					1			16		0.5	2
181	15-20 x 25-30	Prolate spheroid			1					16		0.5	2
181	15-20 x 25-30	Prolate spheroid			1					16		0.5	2
181	19.5 x 23.4	Cylinder				2			*Thalassiosira*	16		0.5	2
181	25.3 x 33.9	Cone					1			16		0.5	2
181	24.4	Cylinder				3			*Thalassiosira*	16		0.5	2
181	24.4 x 42.7	Cone					1			16		0.5	2
181	15-20 x 20-25	Prolate spheroid			2					16		0.5	2
181	25-30 x 45-50	Cone			1					16		0.5	2
181	20 x 25	Sphere			2					16		0.5	2
181	25-30 x 30-35	Prolate spheroid			1					16		0.5	2
181	30.5	Sphere					1			16		0.5	2
181	24.4	Sphere		2					*Dictyocha*	16		0.5	2
181	5-10 x 40-45	Prolate spheroid		1					*Euglena*	25	2		27
181	20-25 x 25-30	Prolate spheroid			2					16		0.5	2
181	20-25 x 30-35	Prolate spheroid			2					16		0.5	2
181	10-15 x 20-25	Prolate spheroid			2					25	2		27
181	10-15 x 25-30	Prolate spheroid			2					25	2		27
181	12.2	Sphere					1		*Myrionecta*	16		0.5	2
181	16.3 x 19.3	Cone					1			16		0.5	2
181	2-5 x 2-5	Rectangular box				2				40	2		42.5
181	2-5 x 2-5	Prolate spheroid		5						40	2		42.5
181	15-20 x 15-20	Prolate spheroid			1					16		0.5	2
181	5 x 10	Sphere		2						40	2		42.5
181	18.3	Sphere					1		*Myrionecta*	16		0.5	2
181	18.3	Sphere					1		*Myrionecta*	16		0.5	2
181	18.3	Sphere					1		*Myrionecta*	16		0.5	2
181	18.3	Sphere					1			16		0.5	2
181	18.3	Sphere					1			16		0.5	2
181	18.3	Sphere					1			16		0.5	2
181	15 x 20	Sphere			1				*Micracanthodinium claytonii*	16		0.5	2
181	15 x 20	Sphere			2					16		0.5	2
181	2-5 x 5-10	Prolate spheroid		9						40	2		42.5
181	10-15 x 15-20	Cone		1						25	2		27
181	15 x 20	Sphere			7					16		0.5	2
181	10-15 x 10-15	Prolate spheroid			2					25	2		27
181	5-10 x 10-15	Prolate spheroid		4						40	2		42.5

181	10-15 x 15-20	Prolate spheroid			2					25	2		27
181	5-10 x 5-10	Prolate spheroid		10						40	2		42.5
181	5 x 10	Sphere		18						40	2		42.5
181	10-15 x 15-20	Prolate spheroid		3						40	2		42.5
181	10 x 15	Sphere		7						25	2		27
181	1	Sphere	144							40	1		85
181	2 x 5	Sphere		22						40	2		42.5
181	2 x 5	Sphere		74						40	2		42.5
195	23.8	Sphere						1		16		0.5	2
195	36.6	Sphere						1		16		0.5	2
195	10-15 x 15-20	Prolate spheroid						1		25	2		27
195	6	Sphere						7		40	2		42.5
195	2-5 x 30	Prolate spheroid				2			*Cylindrotheca/nitzschia longissima*	16		0.5	2
195	2-5 x 42.7	Elliptic prism				1			*Cylindrotheca/nitzschia longissima*	16		0.5	2
195	2-5 x 60	Prolate spheroid				3			*Cylindrotheca/nitzschia longissima*	16		0.5	2
195	12.2 x 30.5	Cone					1		*Myrionecta*	16		0.5	2
195	12.2 x 30.5	Cone					1		*Myrionecta*	16		0.5	2
195	18.3 x 24.4	Cone					1		*Myrionecta*	16		0.5	2
195	18.3 x 24.4	Cone					1		*Myrionecta*	16		0.5	2
195	18.3 x 30.5	Cone					1		*Myrionecta*	16		0.5	2
195	18.3 x 30.5	Cone					1		*Myrionecta*	16		0.5	2
195	18.3 x 30.5	Cone					1		*Myrionecta*	16		0.5	2
195	18.3 x 36.6	Cone			1					16		0.5	2
195	18.3 x 42.7	Cone					1			16		0.5	2
195	21.9 x 30.2	Cone					1			16		0.5	2
195	15-20 x 25-30	Prolate spheroid			1					16		0.5	2
195	24.9 x 33.4	Cone					1		*Myrionecta*	16		0.5	2
195	24.4 x 36.6	Cone					1		*Myrionecta*	16		0.5	2
195	24.4 x 36.6	Cone					1			16		0.5	2
195	20 x 25	Sphere			1					16		0.5	2
195	30.5 x 30.5	Cone					1		*Stromtium*	16		0.5	2
195	24.4	Sphere					1		*Myrionecta*	16		0.5	2
195	24.4	Sphere					1		*Myrionecta*	16		0.5	2
195	24.4	Sphere					1		*Myrionecta*	16		0.5	2
195	24.4	Sphere					1		*Myrionecta*	16		0.5	2
195	24.4	Sphere					1		*Myrionecta*	16		0.5	2
195	24.4	Sphere					1		*Myrionecta*	16		0.5	2
195	24.4	Sphere					1		*Myrionecta*	16		0.5	2
195	24.4	Sphere					1		*Myrionecta*	16		0.5	2
195	24.4	Sphere					1			16		0.5	2
195	24.4 x 48.8	Cone					1			16		0.5	2
195	15-20 x 40-45	Prolate spheroid			1				*Amphidinium*	16		0.5	2
195	24.4 x 54.9	Cone			1					16		0.5	2
195	20-25 x 30-35	Prolate spheroid			1					16		0.5	2
195	20-25 x 35-40	Prolate spheroid			1					16		0.5	2
195	2-5 x 60	Elliptic prism				1				40	2		42.5
195	7.8 x 22.9	Cylinder				1				40	2		42.5
195	25 x 30	Sphere			1					16		0.5	2
195	30.5	Sphere					1			16		0.5	2
195	30.5	Sphere					1			16		0.5	2
195	30.5	Sphere					1			16		0.5	2
195	9 x 46.8	Elliptic prism				11			*Eucampia groenlandica*	16		0.5	2
195	25 x 30	Sphere			2					16		0.5	2
195	24.4 x 48.8	Cone			3					16		0.5	2
195	10-15 x 20-25	Prolate spheroid			1					25	2		27
195	36.6	Sphere			1					16		0.5	2
195	36.6	Sphere					1			16		0.5	2
195	15-20 x 20-25	Prolate spheroid			8					16		0.5	2
195	10 x 42	Prolate spheroid		1					*Euglena*	25	2		27
195	7.5 x 32.7	Cylinder				2				40	2		42.5
195	20-25 x 25-30	Prolate spheroid			5					16		0.5	2
195	81.1 x 97.6	Cone					1			16		0.5	2
195	24.4	Sphere		25					*Dictyocha*	16		0.5	2
195	71.7 x 145.9	Cone			1					16		0.5	2
195	79.3	Sphere			1					16		0.5	2
195	2-5 x 2-5	Prolate spheroid		1					Choanoflagellates	40	2		42.5
195	5-10 x 5-10	Cylinder				4			*Chaetoceros*	16		0.5	2
195	12.2	Sphere					1			16		0.5	2
195	2-5 x 2-5	Prolate spheroid		2						40	2		42.5
195	2-5 x 15.6	Prolate spheroid				1			*Cylindrotheca/nitzschia longissima*	25	2		27
195	5 x 10	Sphere		6						40	2		42.5
195	10 x 15	Sphere			2					16		0.5	2
195	18.3	Sphere					1		*Myrionecta*	16		0.5	2

195	18.3	Sphere					1		*Myrionecta*	16		0.5	2
195	18.3	Sphere					1		*Myrionecta*	16		0.5	2
195	18.3	Sphere					1		*Myrionecta*	16		0.5	2
195	18.3	Sphere					1		*Myrionecta*	16		0.5	2
195	18.3	Sphere					1		*Myrionecta*	16		0.5	2
195	18.3	Sphere					1		*Myrionecta*	16		0.5	2
195	18.3	Sphere					1		*Myrionecta*	16		0.5	2
195	18.3	Sphere					1		*Myrionecta*	16		0.5	2
195	18.3	Sphere					1		*Myrionecta*	16		0.5	2
195	18.3	Sphere					1		*Myrionecta*	16		0.5	2
195	18.3	Sphere					1			16		0.5	2
195	18.3	Sphere					1			16		0.5	2
195	18.3	Sphere					1			16		0.5	2
195	18.3	Sphere					1			16		0.5	2
195	18.3	Sphere					1			16		0.5	2
195	18.3	Sphere					1			16		0.5	2
195	10-15 x 10-15	Cone		1						25	2		27
195	5-10 x 10-15	Prolate spheroid			1					40	2		42.5
195	5-10 x 10-15	Prolate spheroid		1						40	2		42.5
195	10 x 15	Sphere			13					16		0.5	2
195	5-10 x 5-10	Prolate spheroid		3						40	2		42.5
195	9.7 x 19.5	Cylinder				1				40	2		42.5
195	15-20 x 15-20	Prolate spheroid			6					16		0.5	2
195	2-5 x 2-5	Rectangular box				22				40	2		42.5
195	10-15 x 10-15	Prolate spheroid		2						25	2		27
195	10-15 x 15-20	Prolate spheroid			2					25	2		27
195	18.3	Sphere		21					*Dictyocha*	16		0.5	2
195	10 x 15	Sphere		10						25	2		27
195	5 x 10	Sphere		22						40	2		42.5
195	12.2	Sphere					15		*Myrionecta*	25	2		27
195	1	Sphere	83							40	1		85
195	2 x 5	Sphere		21						40	2		42.5
195	2 x 5	Sphere		60						40	2		42.5
197	6	Sphere						2		40	2		42.5
197	2-5 x 30.5	Prolate spheroid				1			*Cylindrotheca/nitzschia longissima*	16		0.5	2
197	2-5 x 42.7	Prolate spheroid				1			*Cylindrotheca/nitzschia longissima*	16		0.5	2
197	2-5 x 36.6	Prolate spheroid				1			*Cylindrotheca/nitzschia longissima*	16		0.5	2
197	2-5 x 24.4	Prolate spheroid				2			*Cylindrotheca/nitzschia longissima*	16		0.5	2
197	2.8 x 45.1	Elliptic prism				2				16		0.5	2
197	2-5 x 73.2	Elliptic prism				1			*Nitzschia/Pseudonitzschia*	16		0.5	2
197	9.3 x 24.4	Cylinder				2				16		0.5	2
197	12.2 x 24.4	Prolate spheroid					1		*Myrionecta*	16		0.5	2
197	12.2 x 24.4	Prolate spheroid					1		*Myrionecta*	16		0.5	2
197	12.2 x 24.4	Prolate spheroid					1		*Myrionecta*	16		0.5	2
197	12.0 x 54.9	Elliptic prism				1				16		0.5	2
197	11.9 x 89.5	Elliptic prism				1				16		0.5	2
197	15.4 x 37.8	Prolate spheroid			1				*Gyrodinium*	16		0.5	2
197	10.5 x 121.4	Elliptic prism				1				16		0.5	2
197	16.3 x 34.2	Prolate spheroid					1			16		0.5	2
197	20 x 25	Sphere		1						16		0.5	2
197	15-20 x 20-25	Prolate spheroid			2					16		0.5	2
197	42.7	Cylinder				1				16		0.5	2
197	21.8 x 34.2	Prolate spheroid					1			16		0.5	2
197	36.6	Cylinder				1				16		0.5	2
197	18.4 x 27.4	Prolate spheroid					1			16		0.5	2
197	30.5	Sphere					1			16		0.5	2
197	8.7 x 32	Prolate spheroid			1				*Euglena*	25	2		27
197	20 x 25	Sphere			3					16		0.5	2
197	9.6 x 24	Prolate spheroid			1				*Amphidinium*	40	2		42.5
197	36.6	Sphere					1		*Myrionecta*	16		0.5	2
197	31.7 x 49.7	Prolate spheroid					1			16		0.5	2
197	20 x 40	Cylinder				2				16		0.5	2
197	26 x 32.6	Cylinder				7			*Thalassiosira*	16		0.5	2
197	24.4	Sphere		18					*Dictyocha*	16		0.5	2
197	12.2	Cylinder				1				16		0.5	2
197	2-5 x 5-10	Prolate spheroid		1						40	2		42.5
197	2-5 x 2-5	Cylinder				2			*Chaetoceros*	40	2		42.5
197	12.2 x 12.2	Cylinder				4				16		0.5	2
197	15 x 20	Sphere			1				*Micracanthodinium claytonii*	16		0.5	2
197	2-5 x 2-5	Prolate spheroid		6						40	2		42.5
197	5 x 10	Sphere		8						40	2		42.5
197	9.3 x 16.6	Cylinder				5				16		0.5	2
197	2-5 x 15-20	Cylinder				1			*Attheya*	40	2		42.5

197	18.3	Sphere					1		*Myrionecta*	16		0.5	2
197	18.3	Sphere					1			16		0.5	2
197	18.3	Sphere					1			16		0.5	2
197	18.3	Sphere					1			16		0.5	2
197	18.3	Sphere					1			16		0.5	2
197	18.3	Sphere					1			16		0.5	2
197	15 x 20	Sphere			1					16		0.5	2
197	15 x 20	Sphere			3					16		0.5	2
197	5-10 x 15-20	Prolate spheroid		1						40	2		42.5
197	11.7	Sphere					1		*Myrionecta*	25	2		27
197	11.7	Sphere					1		*Myrionecta*	25	2		27
197	11.7	Sphere					1		*Myrionecta*	25	2		27
197	2-5 x 2-5	Rectangular box				14				40	2		42.5
197	10-15 x 10-15	Prolate spheroid			1					25	2		27
197	5-10 x 10-15	Prolate spheroid		2						40	2		42.5
197	10 x 15	Sphere			1					25	2		27
197	18.3	Sphere		8					*Dictyocha*	16		0.5	2
197	10 x 15	Sphere			2					25	2		27
197	5-10 x 5-10	Prolate spheroid		7						40	2		42.5
197	2 x 5	Sphere		1					Choanoflagellates	40	2		42.5
197	1	Sphere	65							40	1		85
197	2 x 5	Sphere		60						40	2		42.5

Annex IV Light Microscopy: abundance, biomass and taxonomic divisions

Table IV a: Abundance (amount of cells per litre * 1,000) of taxa of phytoplankton and other protists identified at the different stations at **(A)** a depth of 2 m and **(B)** the fluorescence maximum for the different water masses.

Divisions / Stations (A)	**209**	**212**	**218**	**222**	**227**	**230**	**235**	**239**	**245**	**250**
Unidentified flagellates	367.5	1055.8	232.8	692.9	1259.7	253.3	69.1	380.9	648	222.9
Pyramimonas spp.	0.85	0.85	3.64	0	3.4	1.7	0	6.8	1.7	0
Euglena spp.	0	0	2.16	0	0	0.08	0	0	0.85	0.54
Dictyocha spp.	0	0	4.32	0	0.84	0	0	0.04	0.16	1.84
Meringosphaera tenerrima	0	0	0	0	0.04	0	0	0	0	0
Dinobryon spp.	0	0	0.85	0	0	0	0	0	0.8	0
Choanoflagellates	0	0	19.97	3.4	1.7	5.1	0.43	5.1	0.85	0.85
Total flagellates	377.4	1056.6	293.5	784.7	1376.2	267.8	73.1	419.2	684.6	249.1
Unidentified dinoflagellates	32.7	31.6	38.9	39	31.3	5	2.3	12	5.9	4.5
Amphidinium spp.	0	0	0	0	0.04	0	0	0	0	0.04
Gyrodinium spp.	0	0	1.7	0.04	0	0	0	0.04	0	0
Protoperidinium spp.	0	0.04	0.04	0	0	0	0	0	0.54	0
Micracanthodinium claytonii	0	0	0	0	0	0.12	0	0	0	0
Total dinoflagellates	32.6	31.6	40.7	39.1	31.4	5.2	2.3	12	6.4	4.5
Unidentified Pennate diatoms	3.4	4.4	60.4	56.2	54.4	0.9	1.3	3	7	20
Unidentified Centric diatoms	0	9.5	0.4	0.2	0	0	0	0	0.1	3.4
Navicula spp.	0	0	2.2	0	0	0	0	0	0	0
Thalassiosira spp.	0	0.08	6.1	0.24	0.04	0	0	0	0	0
Cylindrotheca spp./*Nitzschia longissima*	0.62	1.08	0.2	0	0	0	0	0	0.04	0.78
Pleurosigma spp.	0	0	0.04	0	0	0	0	0	0	0
Chaetoceros spp.	0	0	0.64	6.16	0	0.48	0.25	0.12	0.24	0.16
Eucampia groenlandica	0	0	0	0	0	0	0	0	0	0.44
Rhizosolenia spp.	0	0	0	0	0	0.2	0	0	0	0
Melosira arctica	0	0	0	0	0	0	0	0.16	0	0
Attheya spp.	0	0.85	0	0	0	0	0	0	0	0
Nitzschia spp./*Pseudonitzschia* spp.	0.04	0.4	2.78	0.08	0	0.44	0.12	0.08	0	0
Guinardia spp.	0.04	0.04	0	0.04	0	0	0	0	0	0
Total diatoms	4.1	16.3	72.7	62.9	54.5	2.1	1.6	3.4	7.3	24.3
Unidentified ciliates	0.1	0.1	1.7	0.7	0.9	0.8	0.3	0.6	0.2	0.7
Myrionecta rubra	0	0	0.32	0	0	0.04	0	0.2	0.4	9.22
Stromtium spp.	0	0	0.04	0	0.04	0	0	0.04	0.04	0.04
Total ciliates	0.1	0.1	2.1	0.7	0.9	0.9	0.3	0.8	0.7	9.9
Total upo's	0	0.9	18.7	59.5	56.1	1.7	5.3	9.4	6	6

Divisions / Stations (B)	209	212	218	222	227	230	235	239	245	250
Unidentified flagellates	771	932.3	253.79	558.8	497.4	-323	380.3	193.9	353.7	61.6
Pyramimonas spp.	2.55	0.85	0	0	0	0	0	0	0	0
Euglena spp.	0	0.08	2.16	0.54	0	0	0	0.54	0.54	0.54
Dictyocha spp.	0	0	2.7	0.54	5.6	0.32	1.12	0	0.08	1.04
Meringosphaera tenerrima	0	0	0	0.08	0.04	0.04	0	0	0	0
Dinobryon spp.	0	0	0	0	0	0	0	0	0	0
Choanoflagellates	0	0	0.85	3.4	0	0.85	0.85	0	0	0.85
Total flagellates	773.5	933.2	410	652.6	565.1	358.2	454.5	235.2	374.7	75.9
Unidentified dinoflagellates	41.2	8.9	23.6	36.6	25.5	13.7	11.8	7.4	5.2	3.16
Amphidinium spp.	0	0	0.54	1.16	0	0	0	0.04	0	0.85
Gyrodinium spp.	0	0	0.54	0.04	0	0.04	0	0	0	0
Protoperidinium spp.	0	0	0	0	0	0.04	0	0.08	0	0
Micracanthodinium claytonii	0	0	0.08	0	0	0.04	0	0	0.04	0.04
Total dinoflagellates	412	8.9	24.8	37.8	25.5	13.8	11.8	7.5	5.2	4
Unidentified Pennate diatoms	0.9	9.4	31.5	4.3	28	32.2	12	21.3	1.7	12.1
Unidentified Centric diatoms	3.4	0.9	0	0	0	0	0.1	0	0	0.5
Navicula spp.	0.04	0	0.04	0	0	0	0	0	0	0
Thalassiosira spp.	0	0.08	0.08	0	0.04	0	0	0	0.02	0.28
Cylindrotheca spp./*Nitzschia longissima*	0	0.16	0.28	0.93	0.04	0	0	0.04	0.16	0.2
Pleurosigma spp.	0	0	0	0	0	0	0	0	0	0
Chaetoceros spp.	0.76	0	0	0	0	1	0.54	2.55	0	1.7
Eucampia groenlandica	0	0	0	0	0	0	0	0	0	0
Rhizosolenia spp.	0	0	0	0	0	0	0	0	0	0
Melosira arctica	0	0	0	0	0	0	0	0.04	0.04	0
Attheya spp.	0	0	0	0	0	0	0	0	0	0.85
Nitzschia spp./*Pseudonitzschia* spp.	0.08	1.08	1.16	0.16	0	0.44	1.24	0.08	0.08	0.04
Guinardia spp.	0.04	0	0	0	0	0	0	0	0	0
Total diatoms	5.2	11.4	33	5.3	28.1	33.7	13.8	24	2.2	15.7
Unidentified ciliates	0.1	0	0.6	1.1	0.7	0.8	0.4	0.4	0.4	0.4
Myrionecta rubra	0	0	0	0	0.04	0.04	0	0	0.16	1.82
Stromtium spp.	0	0	0	0	0.04	0	0	0.04	0	0
Total ciliates	0.1	0	0.6	1.1	0.8	0.8	0.4	0.4	0.5	2.2
Total upo's	0	0.9	0	0	30.6	0	0	5.2	2.6	1.7

Table IV b: Biomass (µg C L^{-1}) of taxa of phytoplankton and other protists identified at the different stations at (A) a depth of 2 m and (B) the fluorescence maximum for the different water masses.

Taxa / Stations (A)	209	212	218	222	227	230	235	239	245	250
Unidentified flagellates	2.392	1.309	3.403	3.81	4.201	0.58	1.118	1.476	1.135	1.449
Pyramimonas spp.	0.005	0.005	0.009	0	0.007	0.004	0	0.017	0.004	0
Euglena spp.	0	0	0.826	0	0	0.016	0	0	0.017	0.131
Dictyocha spp.	0	0	1.146	0	0.163	0	0	0.032	0.134	1.133
Meringosphaera tenerrima	0	0	0	0	0.012	0	0	0	0	0
Dinobryon spp.	0	0	0.005	0.004	0	0	0	0	0.002	0
Choanoflagellates	0	0	0.279	0.013	0.004	0.013	0.001	0.01	0	0
Total flagellates	2.397	1.314	5.779	4.379	4.920	0.64	1.133	1.6	1.409	2.881
Unidentified dinoflagellates	8.076	5.887	4.481	7.350	4.286	0.802	0.407	1.647	1.083	3.301
Amphidinium spp.	0	0	0	0	0.025	0	0	0	0.016	0.035
Gyrodinium spp.	0	0	0.179	0.131	0	0	0	0.186	0	0
Protoperidinium spp.	0	0.089	0.009	0	0	0	0	0	0.129	0
Micracanthodinium claytonii	0	0	0	0	0	0.079	0	0	0	0
Total dinoflagellates	8.076	5.976	4.66	7.481	4.311	1.881	0.407	1.833	1.228	3.336
Unidentified Pennate diatoms	0.132	0.056	0.336	0.376	0.254	0.02	0.028	0.087	0.06	0.134
Unidentified Centric diatoms	0	0.355	0.321	0.039	0.009	0	0	0	0.083	0.269
Navicula spp.	0	0	0.158	0	0	0	0	0	0	0
Thalassiosira spp.	0	0.049	0.305	0.201	0.001	0	0	0	0	0
Cylindrotheca spp./ *Nitzschia longissima*	0.008	0.024	0.005	0	0	0	0	0	0.001	0.012
Pleurosigma spp.	0	0	0.139	0	0	0	0	0	0	0
Chaetoceros spp.	0	0	0.002	0.042	0	0	0.024	0.001	0.006	0.004
Eucampia groenlandica	0	0	0	0	0	0	0	0	0	0.069
Rhizosolenia spp.	0	0	0	0	0	0.302	0	0	0	0
Melosira arctica	0	0	0	0	0	0	0	0.064	0	0
Attheya spp.	0	0.003	0	0	0	0	0	0	0	0
Nitzschia spp./*Pseudonitzschia* spp.	0.004	0.02	0.209	0.005	0	0.026	0.01	0.006	0	0
Guinardia spp.	0.101	0.068	0	0.072	0	0	0	0	0	0
Total diatoms	0.245	0.574	1.475	0.734	0.273	0.369	0.06	0.162	0.149	0.488
Unidentified ciliates	0.186	0.03	3.128	1.047	0.622	1.82	0.668	1.959	1.225	1.268
Myrionecta rubra	0	0	0.52	0	0	0.04	0	0.24	0.22	1.38
Stromtium spp.	0	0	0.01	0	0.011	0	0	0.018	0.04	0.033
Total ciliates	0.186	0.030	3.658	1.047	0.633	1.860	0.668	2.127	1.485	2.678
Total upo's	0	0.07	0.454	0.464	0.404	0.021	0.019	0.067	0.043	0.105

Taxa / Stations (B)	209	212	218	222	227	230	235	239	245	250
Unidentified flagellates	2.479	0.867	1.977	2.091	1.67	0.854	1.142	0.934	1.867	0.494
Pyramimonas spp.	0.062	0.005	0	0	0	0	0	0	0	0
Euglena spp.	0	0.01	0.504	0.143	0	0	0	0.072	0.074	0.075
Dictyocha spp.	0	0	0.525	0.105	0.109	0.062	0.615	0	0.006	0.715
Meringosphaera tenerrima	0	0	0	0.067	0.012	0.005	0	0	0	0
Dinobryon spp.	0	0	0	0	0	0	0	0	0	0
Choanoflagellates	0	0	0.02	0.008	0	0.002	0.002	0	0	0
Total flagellates	2.541	0.882	3.657	2.838	2.13	1.06	1.99	1.162	2.034	1.313
Unidentified dinoflagellates	12.236	1.110	2.328	3.613	3.602	1.96	1.014	0.617	1.277	0.605
Amphidinium spp.	0	0	0.129	0.548	0	0	0	0	0	0.108
Gyrodinium spp.	0	0	0.129	0.025	0	0.032	0	0	0	0.018
Protoperidinium spp.	0	0	0	0	0	0.045	0	0.029	0	0
Micracanthodinium claytonii	0	0	0.053	0	0	0.048	0	0	0.015	0.012
Total dinoflagellates	12.236	1.11	2.639	4.186	3.602	2.085	1.014	0.646	1.292	0.743
Unidentified Pennate diatoms	0.01	0.109	0.219	0.019	0.132	0.152	0.052	0.125	0.01	0.106
Unidentified Centric diatoms	0.031	0.012	0	0	0	0	0.042	0	0	0.068
Navicula spp.	0.055	0	0.01	0	0	0	0	0	0	0
Thalassiosira spp.	0	0	0.001	0	0.018	0	0	0	0.048	0.309
Cylindrotheca spp./ *Nitzschia longissima*	0	0.004	0.004	0.009	0.001	0	0	0.001	0.004	0.003
Pleurosigma spp.	0	0	0	0	0	0	0	0	0	0
Chaetoceros spp.	0.018	0	0	0	0	0.022	0.023	0.005	0	0.006
Eucampia groenlandica	0	0	0	0	0	0	0	0	0	0
Rhizosolenia spp.	0	0	0	0	0	0	0	0	0	0
Melosira arctica	0	0	0	0	0	0	0	0.026	0.006	0
Attheya spp.	0	0	0	0	0	0	0	0	0	0.013
Nitzschia spp./*Pseudonitzschia* spp.	0.009	0.031	0.112	0.007	0	0.036	0.01	0.006	0.004	0.003
Guinardia spp.	0.066	0	0	0	0	0	0	0	0	0
Total diatoms	0.189	0.156	0.353	0.035	0.152	0.211	0.194	0.192	0.073	0.508
Unidentified ciliates	0.097	0	0.5	0.603	1.116	0.61	0.5	0.143	0.192	0.374
Myrionecta rubra	0	0	0	0	0.27	0.03	0	0	0.05	0.3
Stromtium spp.	0	0	0	0	0.001	0	0	0.014	0	0
Total ciliates	0.097	0	0.5	0.603	1.39	0.64	0.5	0.157	0.242	0.674
Total upo's	0	0	0	0	0.22	0	0	0.133	0.037	0.0211

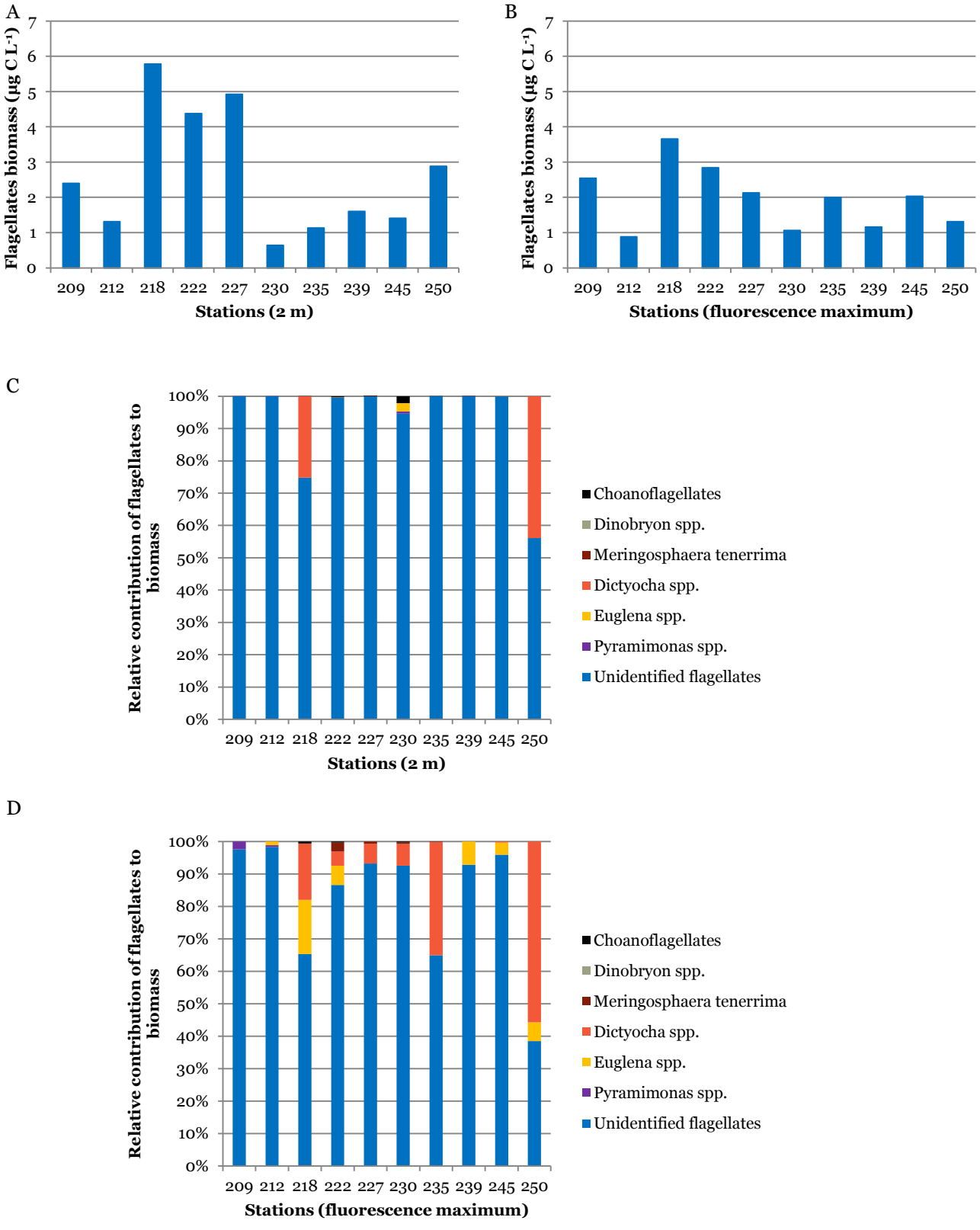

Figure IV a: Biomass (µg C L^{-1}) of flagellates for (A) a depth of 2 m and (B) the depth of the fluorescence maximum and the relative biomass of flagellates of a (C) depth of 2 m and (D) the depth of the fluorescence maximum.

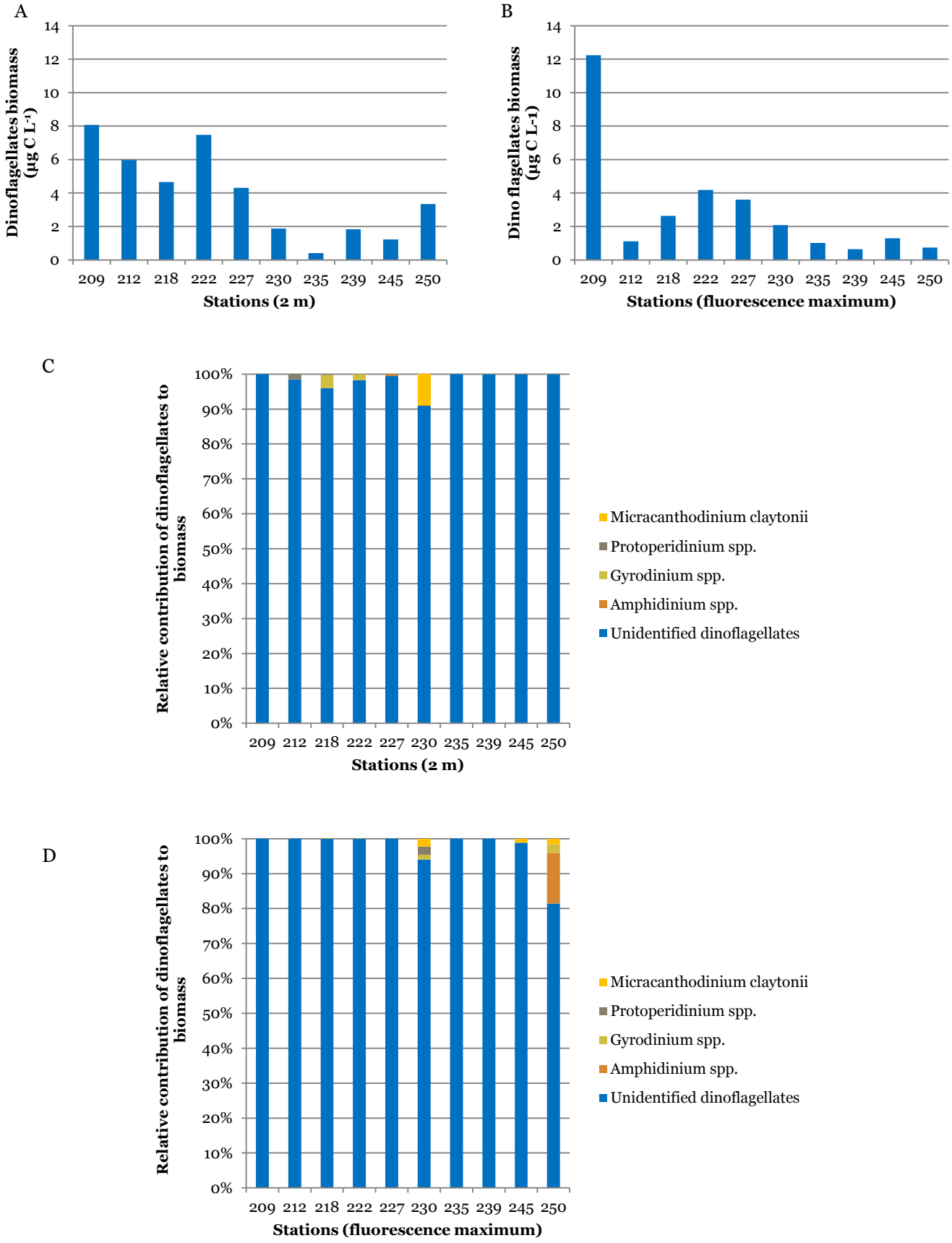

Figure IV b: Biomass (µg C L^{-1}) of dinoflagellates for (A) a depth of 2 m and (B) the depth of the fluorescence maximum and the relative biomass of dinoflagellates of a (C) depth of 2 m and (D) the depth of the fluorescence maximum.

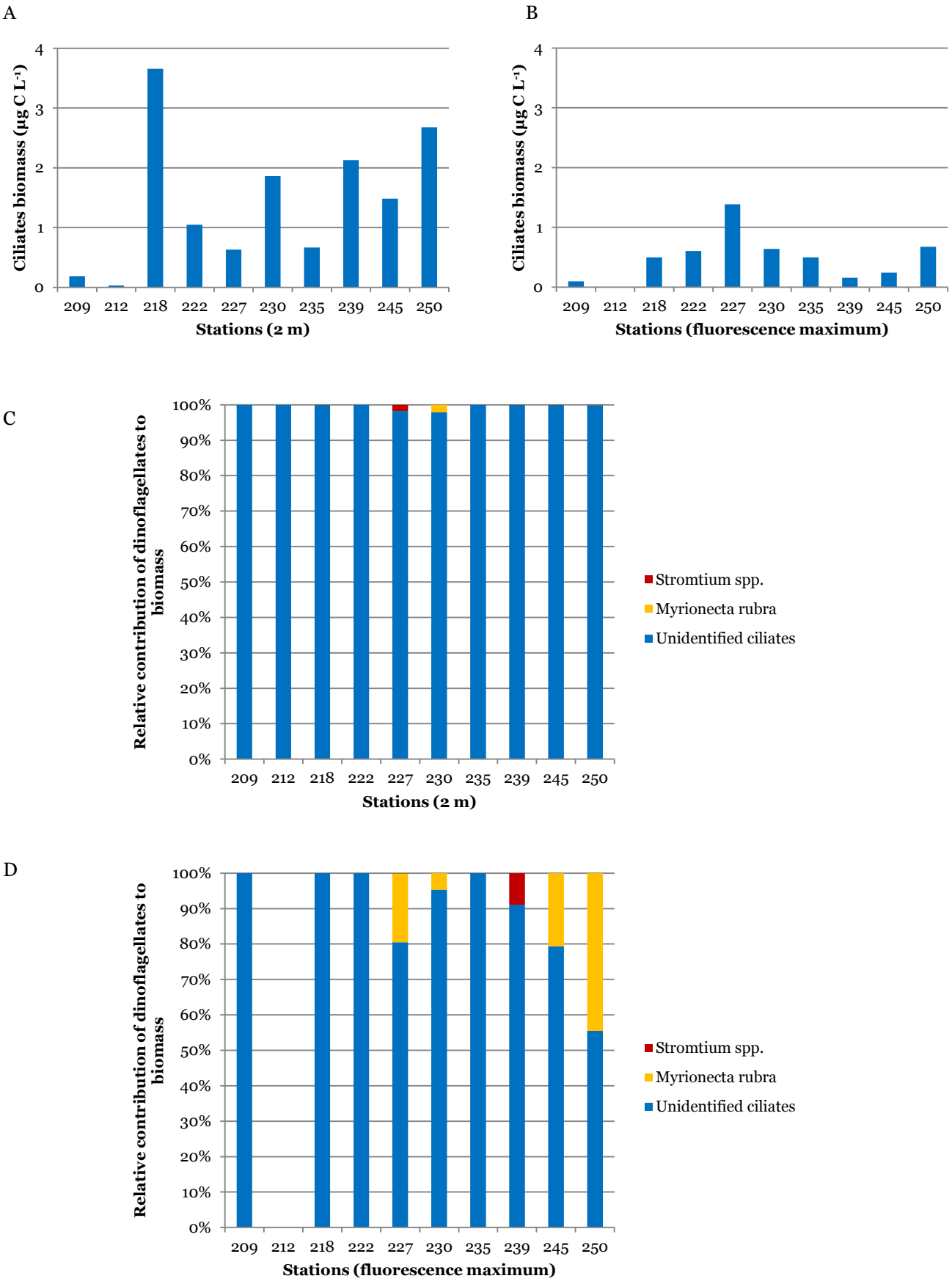

Figure IV c: Biomass (µg C L^{-1}) of ciliates for (A) a depth of 2 m and (B) the depth of the fluorescence maximum and the relative biomass of ciliates of a (C) depth of 2 m and (D) the depth of the fluorescence maximum.

Annex V Flow cytometry: abundance and biomass

Table V a: Abundance (amount of cells per ml) for both picoplankton and nanoplankton and biomass (µg C L^{-1}) for both picoplankton and nanoplankton until the depth of the fluorescence maximum at the selected stations.

Stations	Depth	Picoplankton abundance ml	Nanoplankton abundance ml	Picoplankton Biomass µg	Nanoplankton Biomass µg
250-2	24	1199.7987	138.9597	0.6716	0.9898
250-2	10	3876.7677	204.0404	2.1537	1.7638
250-2	2	3982.3826	159.2953	2.1097	1.3496
245-2	18	678.4343	20.4040	0.3950	0.4099
245-2	10	1785.3535	61.2121	0.0996	0.5271
245-2	2	2397.4747	147.9293	0.1212	2.3802
239-2	28	530.5051	85.0168	0.3103	0.5307
239-2	10	3538.3893	98.2886	0.1277	1.0373
239-2	2	3650.2349	166.0738	0.1242	2.6977
235-2	52	1148.9597	338.9262	0.7943	2.3325
235-2	25	2094.5638	183.0201	0.0788	1.0092
235-2	10	2935.1007	213.5235	0.0731	2.1684
235-2	2	3057.1141	196.5772	0.0750	1.4729
230-1	50	938.5859	278.8552	0.4708	1.0389
230-1	35	3640.0671	376.2081	1.7273	1.7429
230-1	10	4733.7374	431.8855	0.0995	3.0409
230-1	2	4585.6711	332.1477	0.0972	1.7388
227-2	25	663.1313	370.6734	0.5781	3.5067
227-2	10	4363.0640	1033.8047	2.3373	7.2834
227-2	2	4849.3603	945.3872	2.4014	7.2946
222-2	25	642.7273	459.0909	0.4595	3.6902
222-2	10	3631.9192	795.7576	2.4659	8.7350
222-2	2	4730.3367	1095.0168	2.7277	12.4798
218-2	50	37.2819	111.8456	0.0834	0.8862
218-2	20	404.6801	394.4781	0.4297	2.8963
218-2	10	1741.1448	850.1684	1.0119	7.7910
218-2	2	1931.8792	806.6443	1.1822	7.8700
212-2	25	996.3973	23.8047	0.6249	0.2368
212-2	10	2336.2626	47.6094	1.4379	0.5074
212-2	2	4179.4276	68.0135	2.9428	0.7626
209-2	50	422.3636	146.9091	0.3313	0.8256
209-2	14	489.6970	277.4949	0.3033	5.3338
209-2	10	328.5051	65.2929	0.1949	1.3893
209-2	2	697.8182	153.0303	0.3922	2.6174
203-1	25	5555.000	2009.8322	2.6607	21.6179
203-1	2	14419.1457	2639.1960	0.6706	40.4977